GEOLOGICAL SURVEY OF CANADA

OPEN FILE 2656

A suite of type temperature-depth profiles in permafrost for areas of Holocene shoreline regression and marine transgression, Arctic Canada

Jennifer Adams

1993

Energy, Mines and Resources Canada

Énergie, Mines et Ressources Canada

Canada

TABLE OF CONTENTS

PREFACE

Permafrost exists today in response to present and past climatic and environmental conditions. In Arctic Canada, permafrost is currently aggrading along some coastlines and degrading along others in dynamic response to changes in relative sea level. In areas of Holocene emergence, such as the central Queen Elizabeth Islands and the land surrounding Hudson Bay, permafrost is growing as seabed becomes land exposed to severe arctic air temperatures; permafrost thickness increases inland from the shoreline. In contrast, in areas of Holocene marine transgression such as the Mackenzie-Beaufort region, permafrost is melting as sea water inundates a permafrost landscape; several hundred meters of permafrost on the Beaufort Shelf is melting from the top and bottom.

In these particular coastal areas, the questions are asked, "How thick is the permafrost?", "How long does it take to grow permafrost?", "What is the nature of the thermal regime?" or "Can the time of emergence or transgression be estimated from the shape of a measured temperature profile?". Given a knowledge of the geology, these questions may be answered through use of appropriate geothermal models. In this report, Ms. Adams has used such a model to prepare a suite of example temperature-depth profiles for areas of shoreline emergence and marine transgression. Sands and sandstones, clays and shales are realistic lithologies in these areas and the calculations are undertaken for these as bracketing lithologies.

This project was conducted under the direction of Al Taylor of GSC's Terrain Sciences Division as a contribution to GSC project 920042, "Geothermal investigations and reconstruction of past environments from ground temperatures".

ABSTRACT

The effects of coastal emergence in the Arctic Islands and of marine transgression in the Beaufort Sea during the Holocene can be observed today in the permafrost growth or decay in these areas. In this project, Outcalt's (1985) program, which incorporates the effects of latent heat in its analysis, was used to create a suite of temperature profiles that should be observed today, assuming that the emergence or transgression occurred at selected times before present. This report can be used as a guide to types of temperature profiles and permafrost thicknesses that could be anticipated today for geologic parameters typical of these areas. The suite of temperature profiles shows that permafrost growth varies directly with time since emergence and that permafrost melting occurs at both the top and bottom of the frozen interval since transgression.

1.0 INTRODUCTION

During the Holocene, large changes in ground surface temperatures accompanied marine regression caused by glacioisostatic uplift in some regions and marine transgression attributed to subsidence and eustatically rising sea levels in others. As offshore areas emerged from submarine to arctic subaerial conditions, or as arctic terrestrial areas were inundated, strong thermal transients propagated in the ground, resulting in pronounced anomalies in subsurface temperatures.

Previously, temperature profiles from the Beaufort Sea and the Arctic Islands have been analyzed using an analytic method (e.g. Taylor, 1991). This technique does not take fully into account the phase changes that occur in permafrost regions. The latent heat of ice-water phase change may affect estimates of permafrost growth or decay.

In this project, a finite difference numerical model was used to develop a suite of temperature profiles distinctive to emergent coastal areas in the Arctic Islands and to the transgressive environment in the Beaufort Sea (Fig. 1). The physical property parameters that were chosen are considered to be geologically reasonable estimates of the physical properties of rocks and sediments of the regions studied. The profiles were calculated at several times between 0.5 Ka and 10 Ka B.P., to simulate various times of Holocene emergence or transgression.

This report will be a guide to types of temperature profiles and permafrost thicknesses that might be measured today, given coastal emergence or marine transgression, at a specific time in the past.

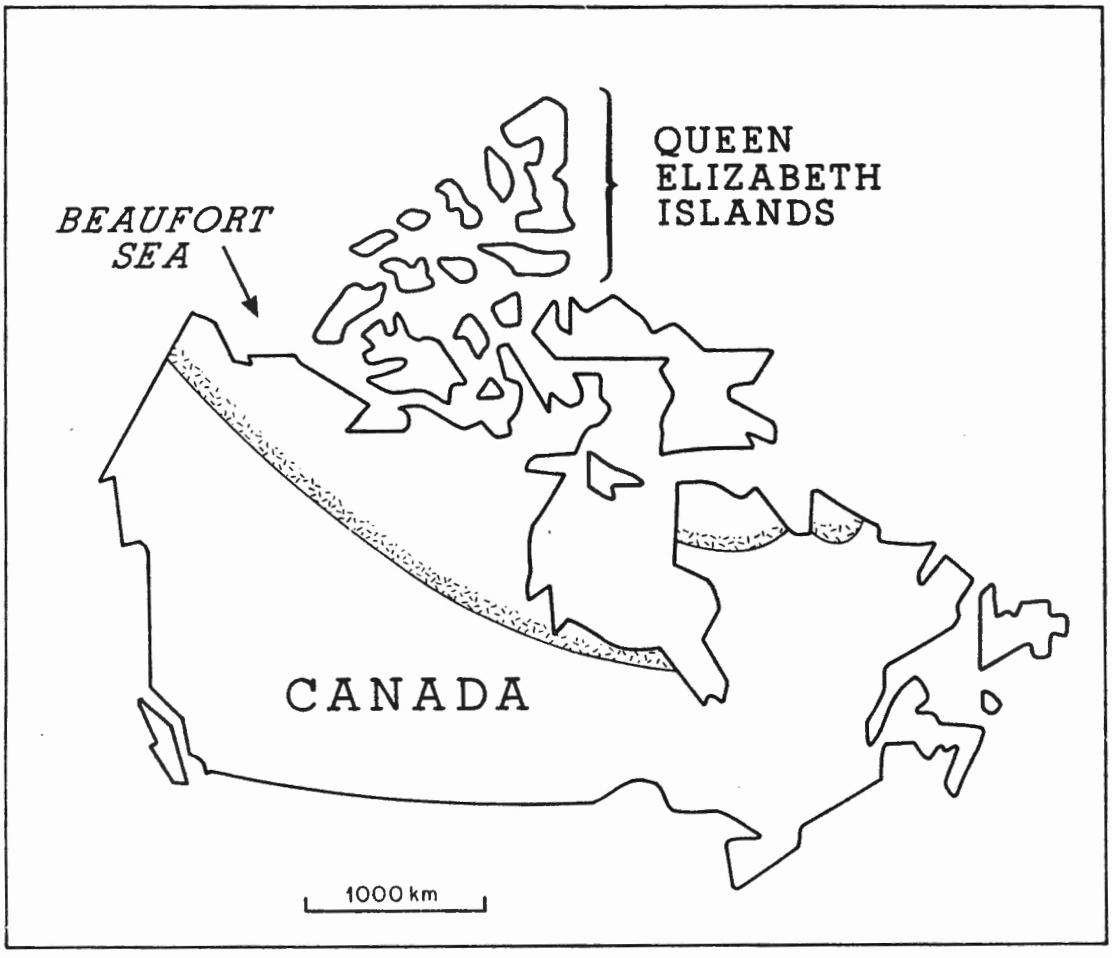

Fig. 1 Location of study areas. Hachured line is southern limit of continuous permafrost.

2.0 REGIONAL GEOLOGY

2.1 Recent Emergence in the Arctic Islands

In the Queen Elizabeth Islands, over forty onshore wells have been used to obtain precise temperature logs and permafrost thicknesses (Fig. 2) (Taylor et al., 1982). The results of the logs suggest that substantial changes in permafrost thicknesses in the Queen Elizabeth Islands have resulted from both recent emergence and Late Quaternary paleoclimatic history. Along the island coastlines, the permafrost can be as thin as 140m. On the other hand, thicknesses over 700m have been recorded inland on the islands. Much of this disparity is a result of uplift and shoreline regression, occurring predominantly during the Holocene (e.g. Dyke et al., 1991; Fig 3). Permafrost grew, as offshore areas became exposed to severe air temperatures; nearshore seabed, for instance, would experience a temperature change from about 0°C to perhaps -15°C to -20°C as it became exposed land (Taylor, 1991).

In an inter-island channel, several tens of meters of permafrost has been found using an accurate temperature log from a well drilled in 244m of water (Taylor et al., 1989). This phenomenon results from the slightly negative mean annual water temperature on the ocean floor. Generally, it is assumed that permafrost is thin or absent in the inter-island channels and may not be ice-bonded. The seabed in the inter-island channels seems to have reached an equilibrium with the marine environment, except near shorelines (Taylor, 1988).

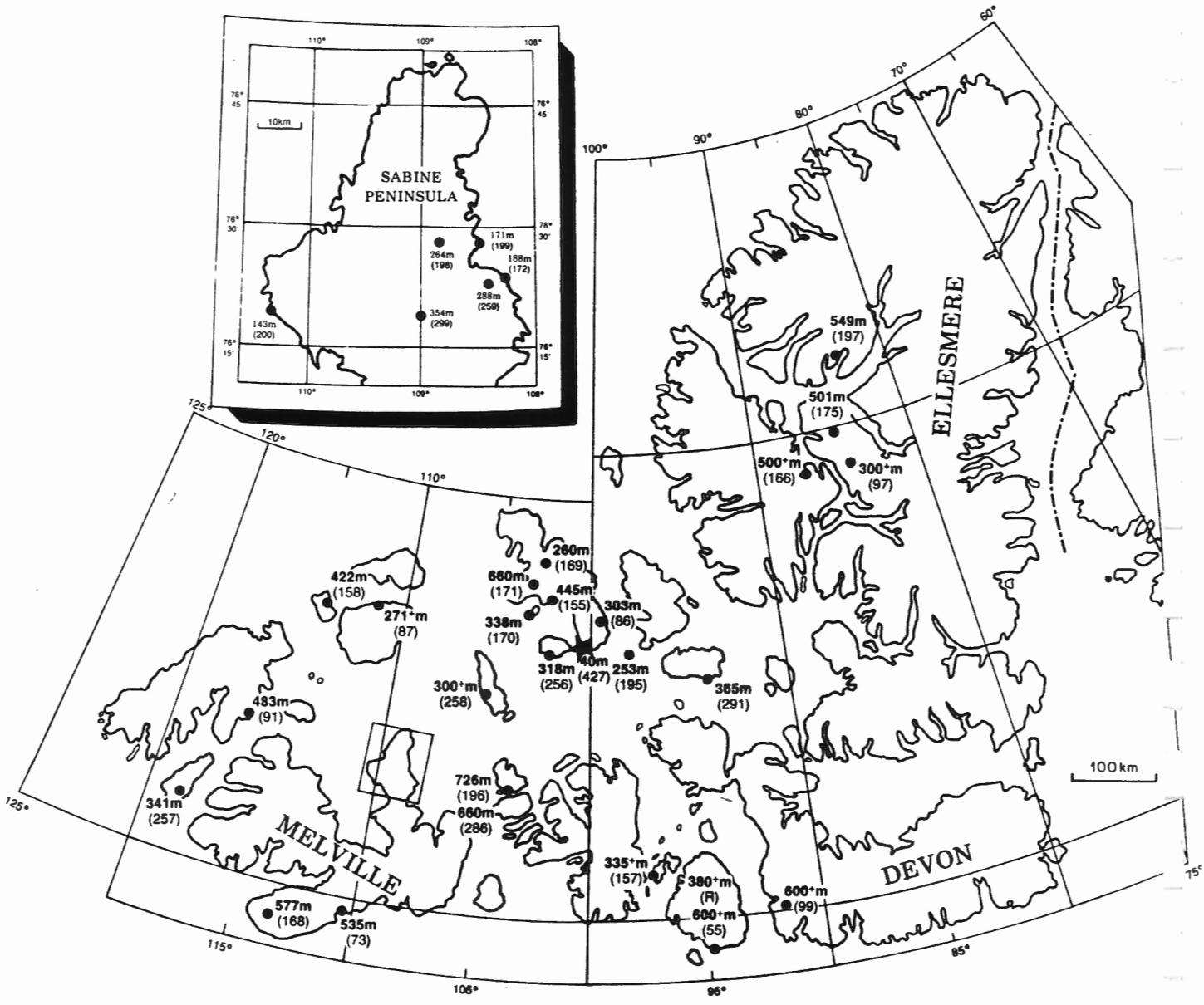

Fig 2. Locations in the Queen Elizabeth Islands of the Canadian Arctic Archipelago, where precise well temperatures have been measured by the GSC (Taylor et al., 1982). Permafrost thicknesses are given in meters; numbers in parentheses are GSC site numbers. The solid circles are terrestrial sites and the star is an offshore location.

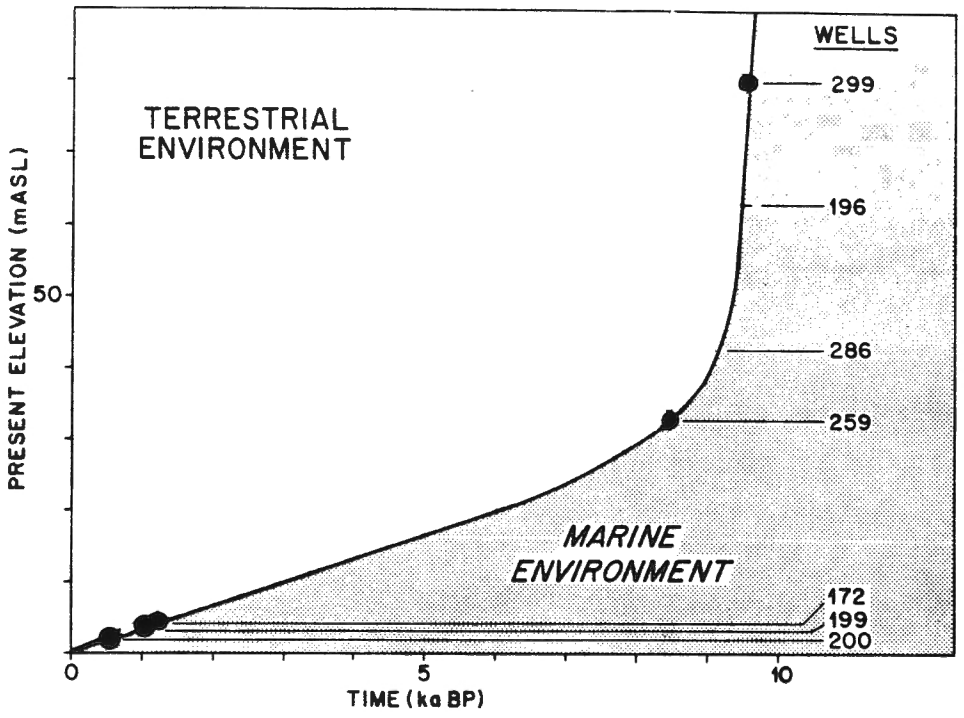

Fig. 3 Emergence curve published for Sabine Peninsula of Melville Island (McLaren and Barnett, 1978). Solid symbols, position on the appropriate emergence curve of the geothermal sites according to their present elevation. The marine environment is shown screened for Sabine peninsula curve. Site #200 is the Hecla I-69 well considered in Fig. 7a,b.

2.2 Marine Transgression in the Beaufort Sea

The Beaufort Shelf developed its form in the Quaternary through delta formation, glaciation and sea-level fluctuations. Today, the evidence of thick permafrost must indicate that the offshore experienced much colder temperatures than the present for a long time. Ice-bonded permafrost exists out to a water depth of 90m, and is up to 700m thick (Fig. 4) (Judge and Taylor, 1986). Hill et al.(1985) reconstructed the sea-level curve of the late Quaternary using radio-carbon dated peat and peaty clay taken from boreholes (Fig. 5). They reached the conclusion that the shelf was subaerial for a minimum of 16 Ka before the marine transgression. Others have suggested that the Beaufort Shelf was subaerial for most of the Wisconsinan (Allen et al., 1988; Brigham and Miller, 1986; Smith, 1986; Blasco et al., 1989). In any case, the marine transgression caused the mean surface temperature to rise 8° to 16° or more. In response to the dramatic change in temperature, the permafrost has been gradually degrading.

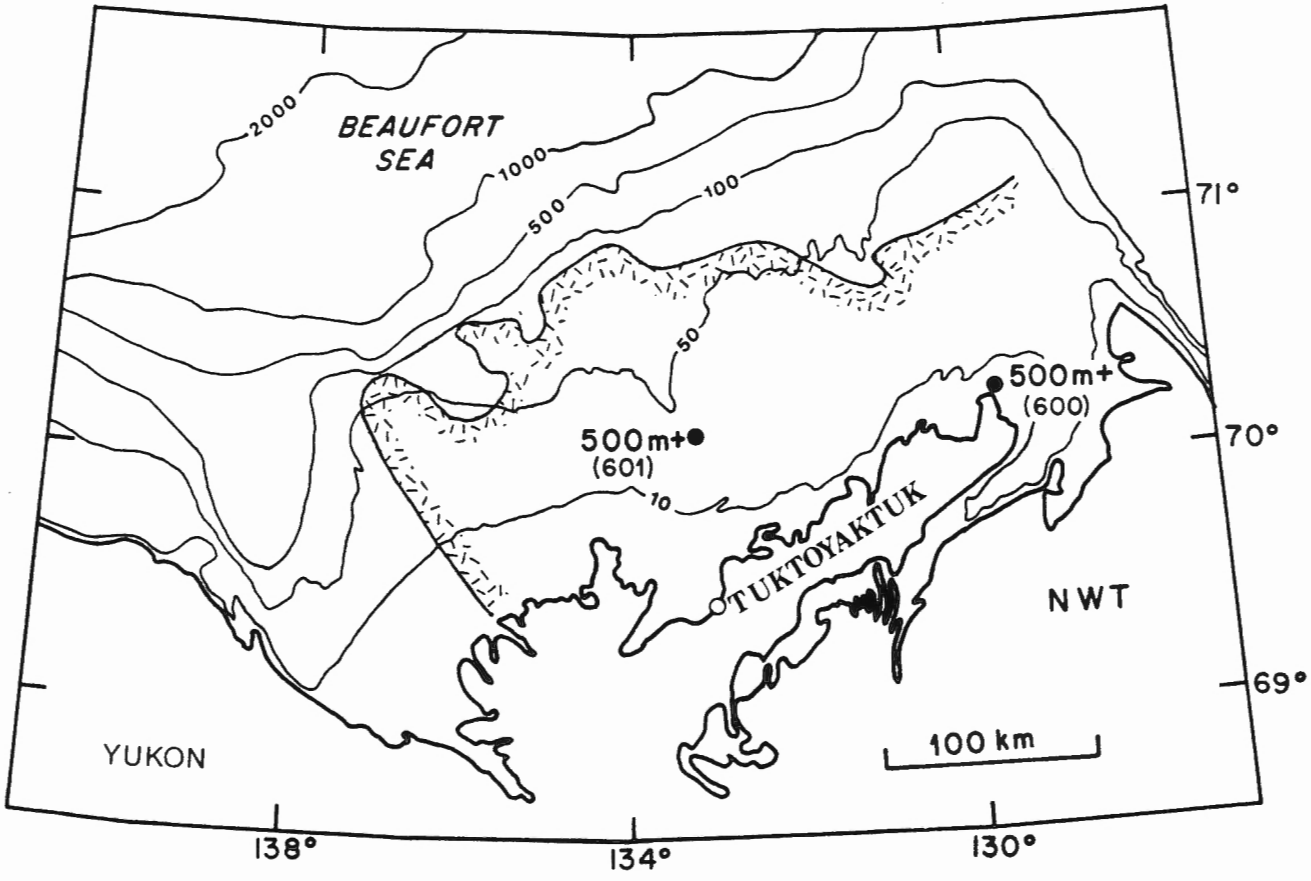

Fig. 4 The Beaufort Sea-Mackenzie Delta region, with permafrost thicknesses and site numbers as in Figure 2. The hachured line is the seaward limit of offshore ice-bonded permafrost. Water depths are contoured in metres.

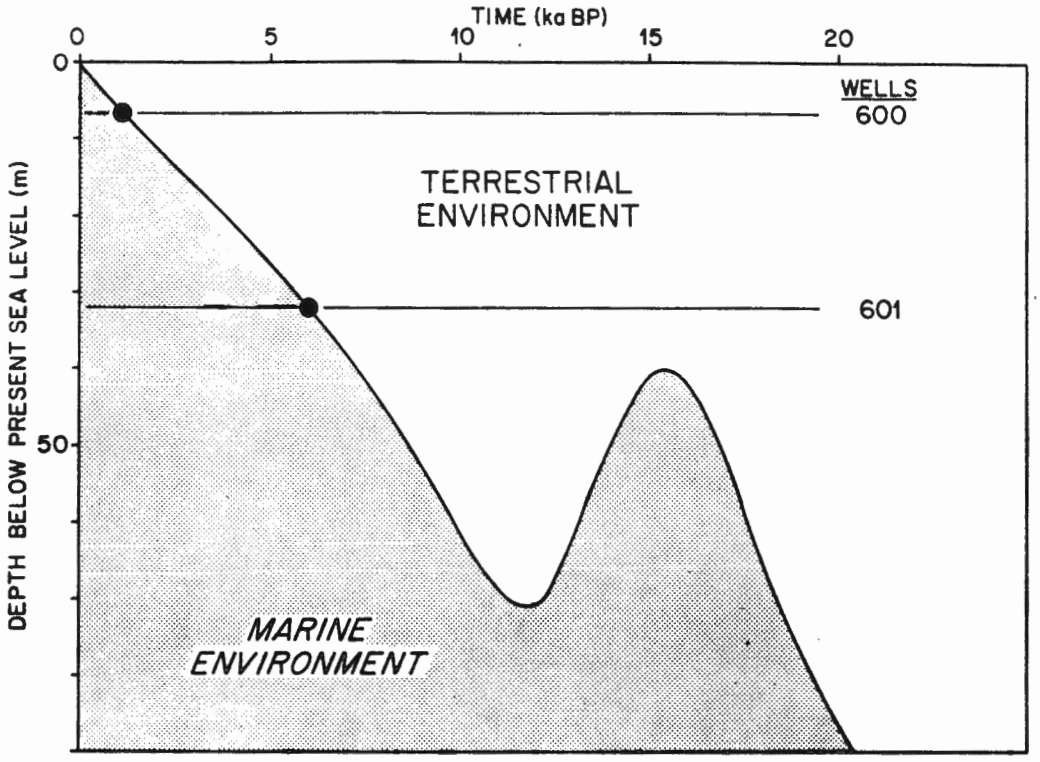

Fig. 5 Relative sea level curve for the Canadian Beaufort Shelf, based on radiocarbon ages and seismic evidence (Hill et al., 1985). Solid symbols, position of the wells on the sea level curve according to their water depth; horizontal lines illustrate how wells progressed from a subaerial to a marine environment over the past 20,000 yrs. From Taylor, 1991.

3.0 METHOD

3.1 Description of Outcalt's quantitative analysis

Outcalt's (1985) thermal modelling program simulates the offshore temperature and ice content profiles observed in the degrading permafrost of the Beaufort Shelf region. The program can also generate similar models for emergence as found in the Arctic Islands. Outcalt's calculations take into account the volumetric latent heat that is needed as frozen or unfrozen ground changes phase. Frozen soils, particularly fine-grained soils such as clays and silts, may have an appreciable unfrozen water content at temperatures a few degrees below freezing. This property is also accommodated in Outcalt's program. The recently modified program (Wawrow, 1993) enables the user to input values for terrestrial heat flow (Q), thermal conductivity of the solid (K_s), salinity (s), porosity (n), freezing point (T_f), the initial long-term equilibrium temperature (T_o), and the temperature and time step increments for the surface temperature history being applied (T_{step}, t_{step}). In addition, the program determines the shape of the unfrozen water content vs. the negative temperature through a user-supplied exponential parameter (A_x). (See Appendix E for a more detailed discussion of Outcalt's program.)

3.2 Modelling Procedure

Typical values for each parameter were chosen to input into Outcalt's modified program (Table 1). These values are representative of measured values for the Arctic Islands and the Beaufort Shelf (Taylor, 1991). For the Arctic Islands, the initial temperature was set at 0°C as the seabed temperature and the step temperatures were taken to be -15°C and -20°C, similar to the mean annual temperature today. In the Beaufort Sea area during the late Wisconsinan and early Holocene the land was subaerial and had a mean annual temperature between -10°C to -15°C (Brigham and Miller, 1983; Smith, 1986; Allen et al., 1988). The step

temperature is the temperature of the sea water which is about 0°C.

The terrestrial heat flow in the Arctic Islands ranges from 40-60 mWm^{-2}. Whereas, in the Beaufort Shelf, it is close to 60 mWm^{-2} although both values were used in the model (see discussion in Taylor, 1991). The thermal conductivity of the solid depends solely on the lithology. In both the Arctic Islands and the Beaufort Shelf the lithology can range from sands and silty sands (K_s = 4.0 W/mK) to clays, silty clays and shale (K_s = 2.0 W/mK). In calculating the bulk thermal conductivity, a porosity n = 0.2 is paired with K_s = 2.0, giving an unfrozen K_b = 1.57 as the clay or shale case, and an n = 0.4 is paired with K_s = 4.0, giving an unfrozen K_b = 1.87, as the sand or sandstone case. A frozen K_b will be somewhat higher and will depend on A_x (See Appendix E).

Table 1. Range of parameters

Parameters	Arctic Islands	Beaufort Sea
t_{step}	0.5, 1.0, 2.0, 3.0, 5.0, 10.0 Ka	
T_{step}	-15°C -20°C	0°C 0°C
T_o (initial temp)	0°C 0°C	-10°C -15°C
Q (heat flow) (mWm^{-2})	40 60	40 60
K_s ($Wm^{-1}K^{-1}$)	2.0 4.0	2.0 4.0
n (porosity)	0.2 0.4	0.2 0.4

Thus, there are two options for each of T_{step}, T_o, Q and (K_s, n). The other variable, time, has six options. When all combinations were taken, 48 models for each region were

created ready to be inputed into Outcalt's program. The output files from the program were entered into a graphing program which plotted the temperature and ice content profiles. Next, some of the profiles were compared to create derived plots to help interpret the results.

4.0 RESULTS

The results of Outcalt's program were plotted on graphs that show six temperature and ice content profiles versus the depth for a given lithology. An example of one of the graphs can be seen in Fig. 6. The ice content section shows the ice fraction of the total percent porosity of the solid on the horizontal axis versus the depth on the vertical axis. Below the graph there are six sections, each one pertaining to one profile. The line above each section indicates the profile on the graph to which the section applies. The phrase below the line indicates the number of thousands of years that the ground has been at the given step temperature. For example, -20°C for .50 Ka means that the surface temperature dropped to -20°C from 0°C, 500 years ago and has remained constant at -20°C ever since. The temperature profiles show the effect of this time step on the permafrost depth and temperature. The next several lines list the parameters that were entered in Outcalt's program to calculate the particular model. The last line in each of the six sections is the input file name. The full suite of temperature profiles can be found in Appendices A & B and the derived graphs in Appendices C and D.

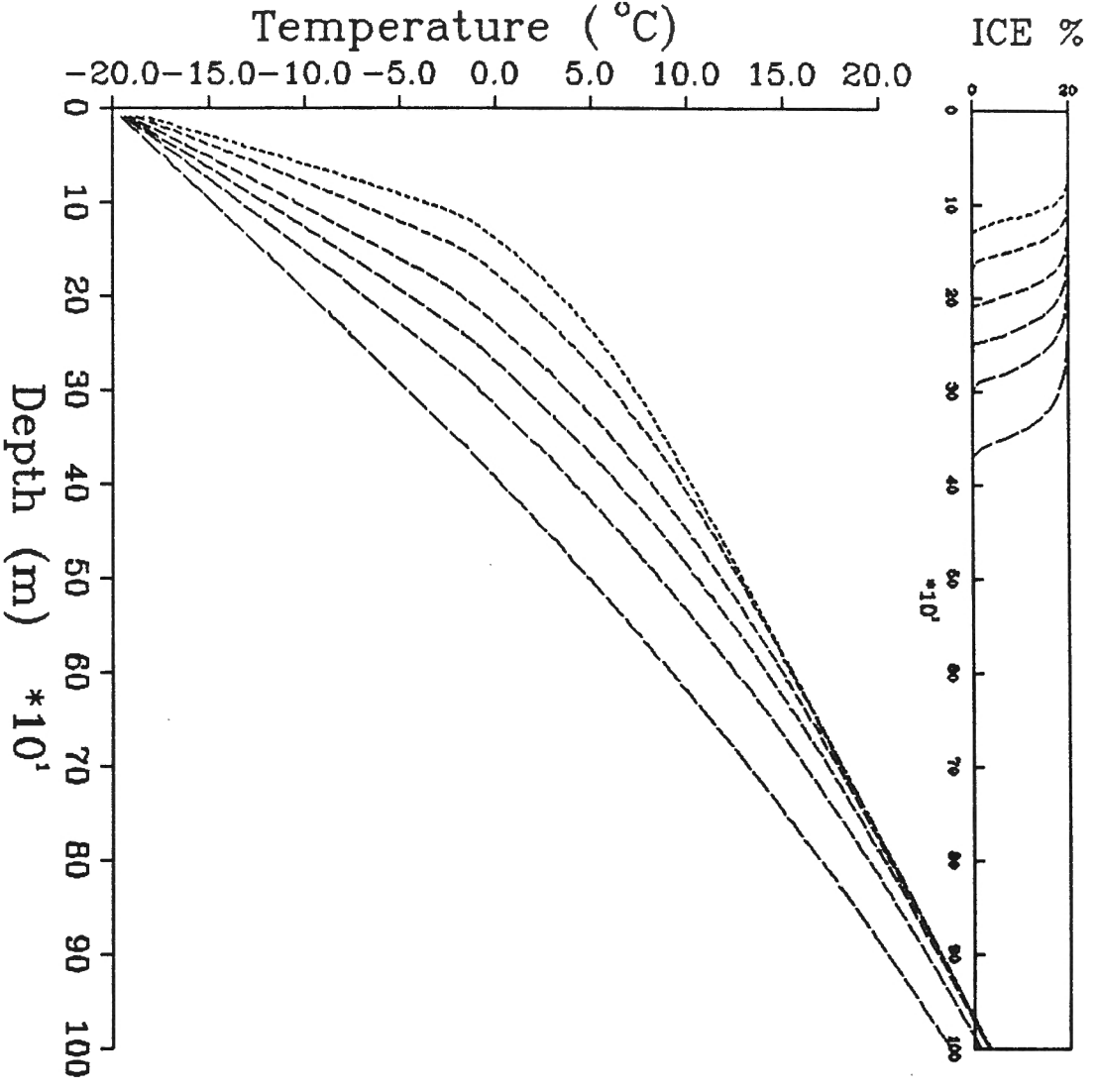

MEASURED DATA

\TC\TDUM.DAT
\LITH\LITH.DUM

-20.00 C FOR 0.500 Ka	-20.00 C FOR 1.000 Ka	-20.00 C FOR 2.000 Ka
To= 0.0 C Tf= -0.27 C n= 0.20 S= 5 ppt Ks= 2.00 W/mK Q= 40 W/m2 Ax= 0.7 DZ= 10 m	To= 0.0 C Tf= -0.27 C n= 0.20 S= 5 ppt Ks= 2.00 W/mK Q= 40 W/m2 Ax= 0.7 DZ= 10 m	To= 0.0 C Tf= -0.27 C n= 0.20 S= 5 ppt Ks= 2.00 W/mK Q= 40 W/m2 Ax= 0.7 DZ= 10 m
OF1.1	OF2.1	OF3.1

-20.00 C FOR 3.000 Ka	-20.00 C FOR 5.000 Ka	-20.00 C FOR 10.000 Ka
To= 0.0 C Tf= -0.27 C n= 0.20 S= 5 ppt Ks= 2.00 W/mK Q= 40 W/m2 Ax= 0.7 DZ= 10 m	To= 0.0 C Tf= -0.27 C n= 0.20 S= 5 ppt Ks= 2.00 W/mK Q= 40 W/m2 Ax= 0.7 DZ= 10 m	To= 0.0 C Tf= -0.27 C n= 0.20 S= 5 ppt Ks= 2.00 W/mK Q= 40 W/m2 Ax= 0.7 DZ= 10 m
OF4.1	OF5.1	OF6.1

Fig. 6 An example of type temperature profiles for the Arctic Islands

5.0 DISCUSSION

The temperature profiles in Appendix A and B are typical of those measured today in the Arctic Islands following Holocene emergence and in the Beaufort Sea after marine transgression.

In the emergence case, the profiles show the growth of permafrost with time since the beginning of the emergence. The intersection of the temperature profile with 0°C shows the depth of the permafrost. The depth of the ice-bonded permafrost is slightly less than the depth at 0°C due to freezing point depression; this result is seen in the ice-content profile. The transition from the bonded to unbonded permafrost is gradual due to the unfrozen water content present in the permafrost.

In the transgression case, the profiles show the melting of permafrost with time following marine transgression on a permafrost landscape. It is clear from the ice-content profiles that melting occurs predominantly at the upper surface of the permafrost initially, whereas after several thousands of years the melting is greater at the base of the permafrost. This is more evident in the derived curves of permafrost degradation over time (see section 5.1, below).

As an example of the use of these profiles (Fig. 7), we take temperature data recorded at site #200, Hecla I-69 (See Judge et al., 1981). The data, on an acetate overlay, may be compared to suites of temperature profiles of the Holocene emergence, Appendix A. Two profiles fit the data very well. Placing the overlay on file "F" shows a very good fit for emergence of 1000 years ago (Fig. 7a); these profiles represent the case of shale, with a porosity of 0.2 and a solid conductivity of 2.0 $Wm^{-1}K^{-1}$, where Q is equal to 40 mWm^{-2}. Placing the overlay on file "LL" is somewhat less close to the modelled temperature profile (Fig. 7b) for the case of sandstone, porosity of 0.4 and a conductivity of 4.0 $Wm^{-1}K^{-1}$, with a Q of 60 mWm^{-2}. This poorer fit is to be

expected, since the dominant lithology at Hecla is shale (see overlay). As the surface temperature intercept for the Hecla measurements is -17.5°C, the type curves are shifted slightly so that they intersect the surface at approximately -17.5°C instead of -20°C. To apply the temperature profiles to other areas, the user can select parameters that are most representative of the regional geology. The parameters were chosen as reasonably typical values which bracket the possible parameters for the Arctic Islands and the Beaufort-Mackenzie region.

5.1 Derived curves of permafrost growth following emergence.

To plot the derived curves, permafrost thicknesses were extracted from the temperature profiles in Appendix A. The values were then entered into the spreadsheet with the physical parameters. A suite of profiles show how the depths of ice-bonded permafrost vary as time for various combinations of parameters (Appendix C). Fig. 8 demonstrates that permafrost grows with time and somewhat faster in a higher conductivity lithology. The derived curves also indicate permafrost growth for a lower porosity and a lower step temperature.

5.2 Derived curves of permafrost degradation following marine transgression.

The same process as described in 5.1 was used to plot the derived curves for marine transgression. The distinct difference between the two cases is that the permafrost is degrading from both the top and the bottom in marine transgression (Fig 9). On inspection of all the derived transgression curves, it is evident that permafrost degrades more quickly for lower porosity and the higher initial subaerial temperatures.

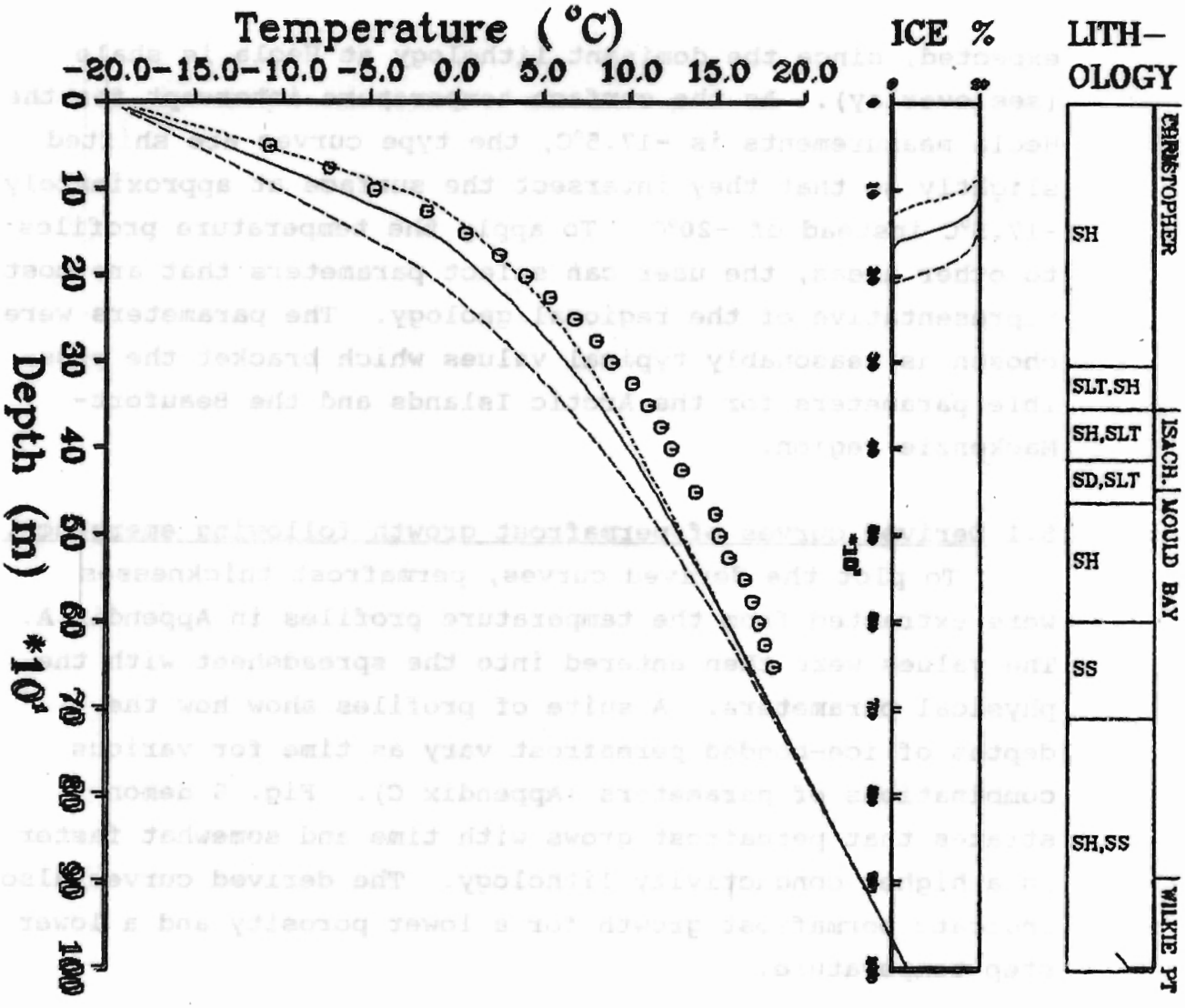

Fig. 7a Suite of curves for shale case and T_o = -20°C (File F, Appendix A). Overlay is shifted about 2.5 degrees to match surface temperatures of data with type curves available.

OL for Fig. 7a

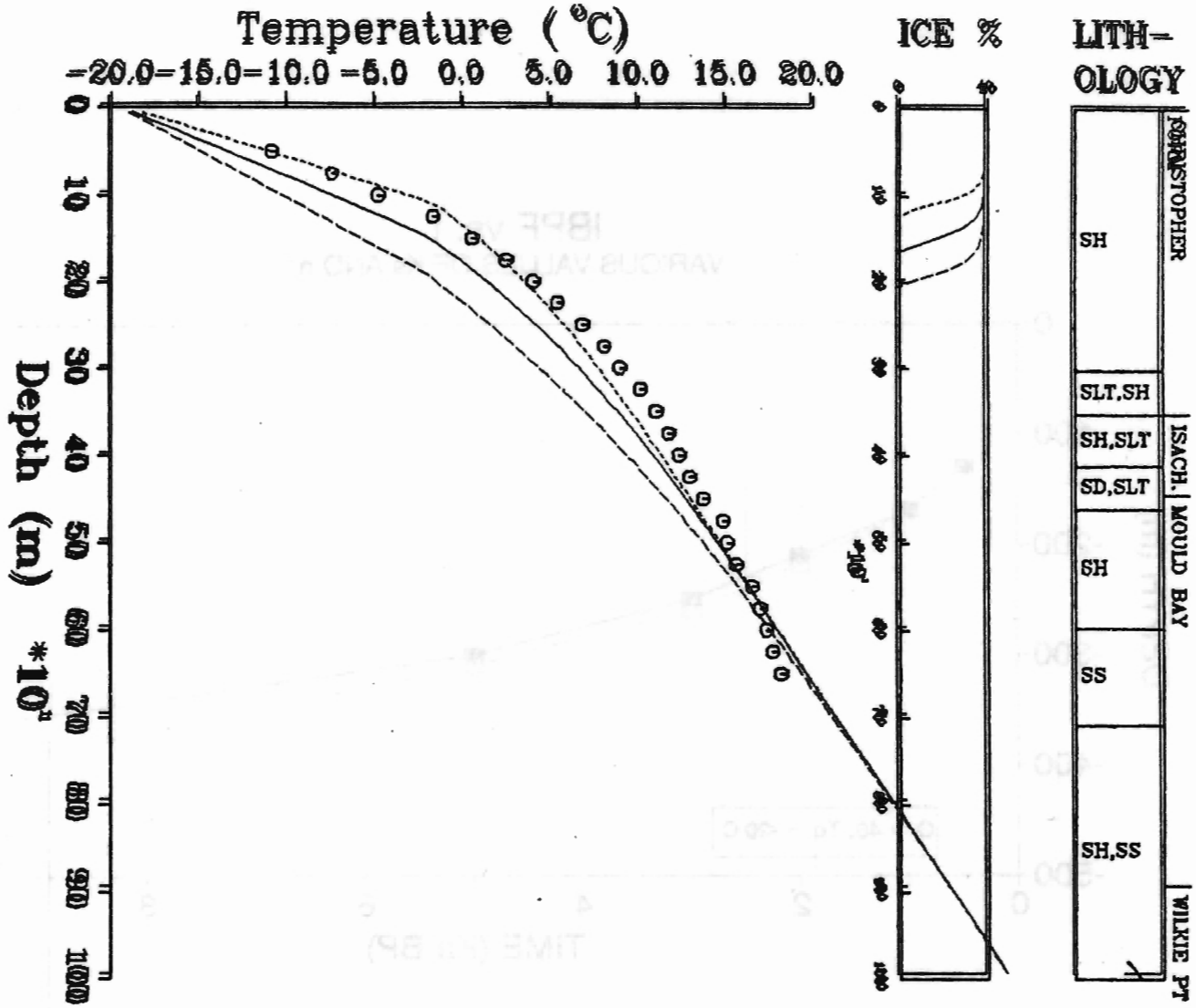

Fig. 7b Suite of curves for sandstone case and T_o = -15°C (File LL, Appendix A). Overlay is shifted about 2.5 degrees to match surface temperature of data with type curves available.

OL for Fig. 7b

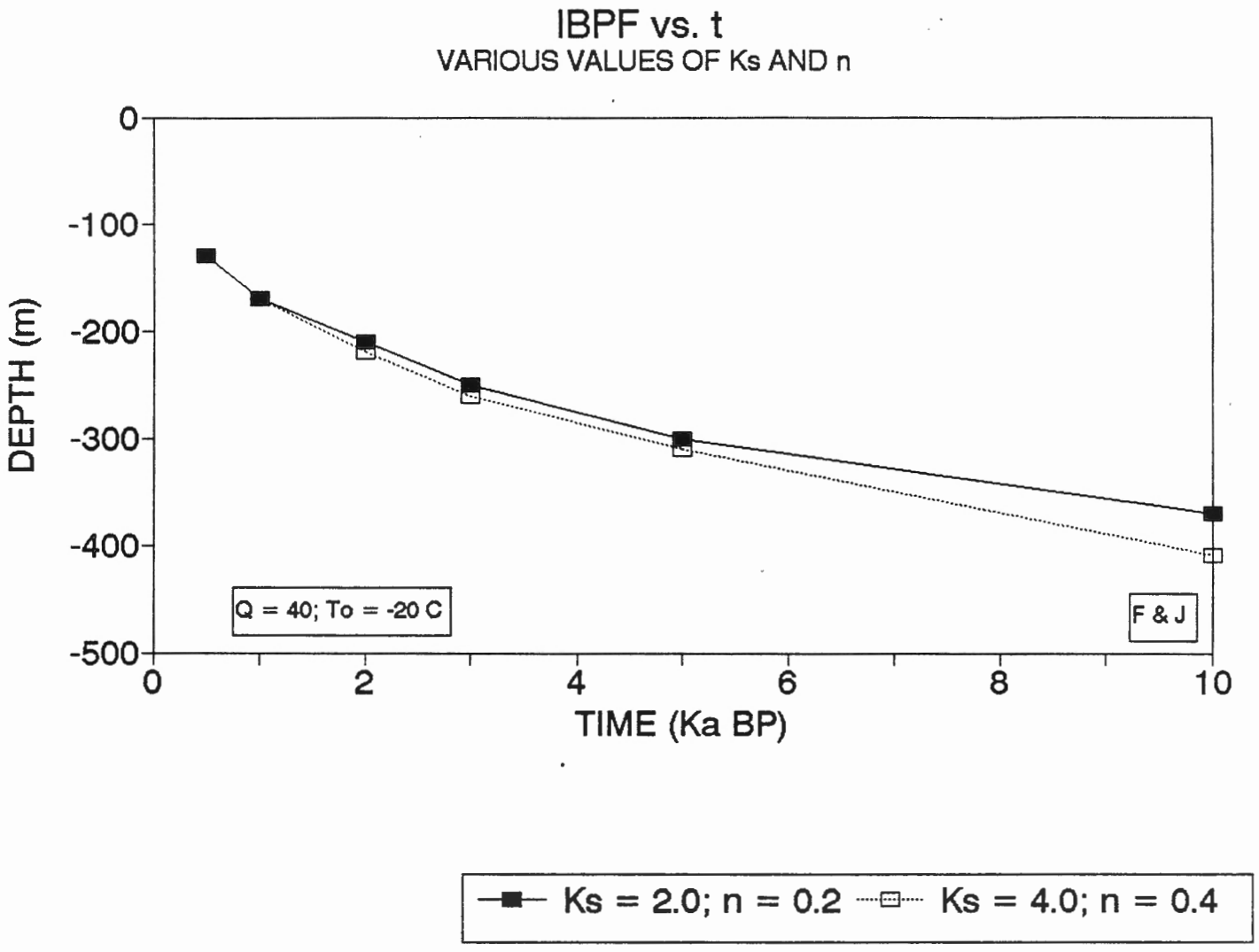

Fig. 8 Example of a derived curve for the Arctic Islands. It shows that permafrost grows with time and somewhat faster in a higher conductivity lithology.

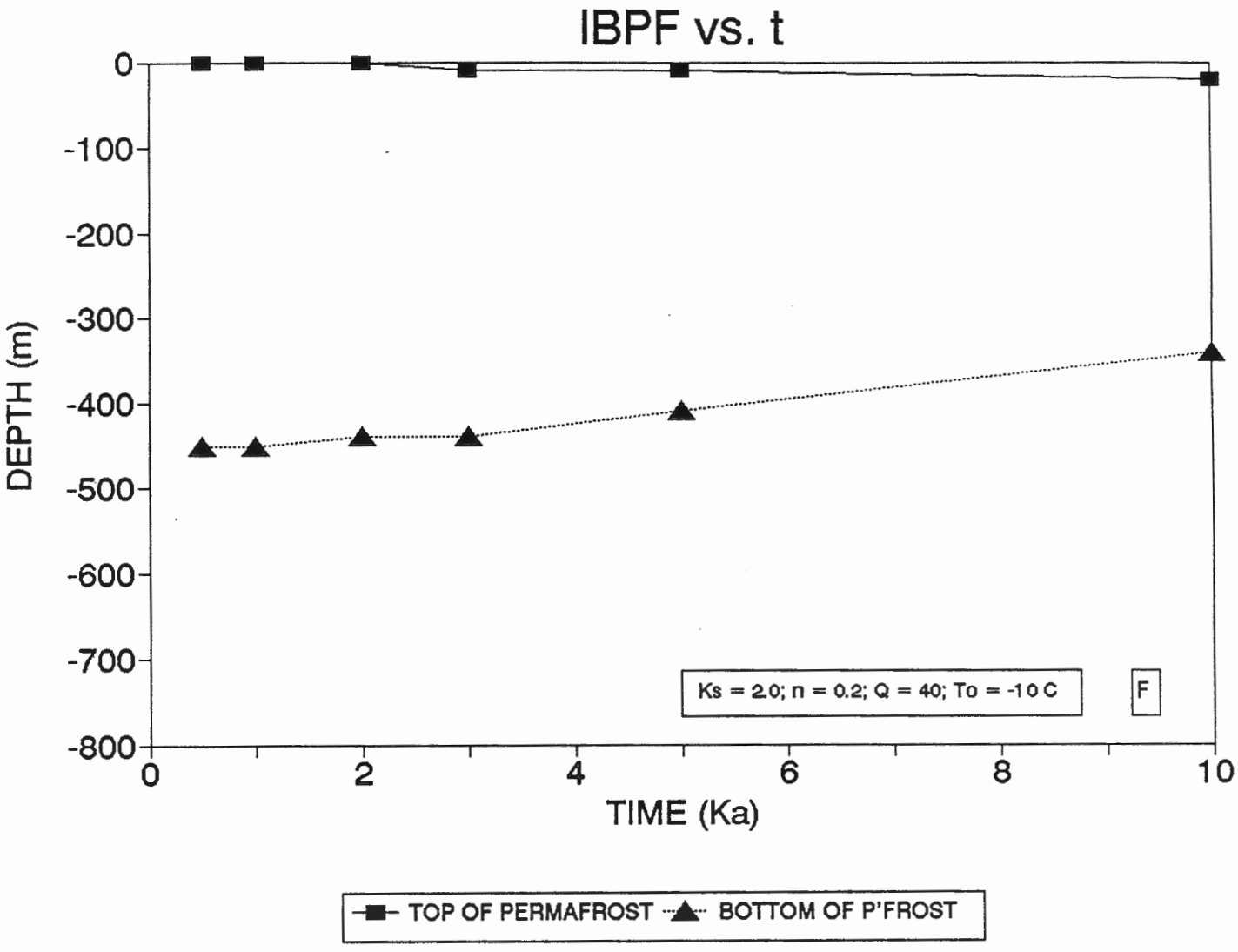

Fig. 9 Example of a derived curve for the Beaufort Sea. Here, it is evident that the permafrost is degrading from the top and the bottom.

6.0 CONCLUSION

The numerical model used to predict the temperature versus permafrost depth profiles fits very well with a set of observed data in the Arctic Islands. During emergence in the Arctic Islands, deeper permafrost will be associated with a higher conductivity lithology, a lower porosity and a lower step temperature for a given time. Similarly for the marine transgression in the Beaufort Sea, permafrost degrades most rapidly in a higher conductivity lithology, with a lower porosity and higher initial temperature.

ACKNOWLEDGMENTS

Under the direction of Mr. Alan Taylor, the author undertook this project as part of the recently developed "GSC Volunteers Program". Dr. S. I. Outcalt kindly permitted the use of his program in this work. Funding was provided by the Panel on Energy Research and Development, EMR Canada.

REFERENCES

Allen, D.M., Michel, F.A. and Judge, A.S., 1988, The permafrost regime in the Mackenzie Delta, Beaufort Sea region, N.W.T. and its significance to the reconstruction of the palaeoclimatic history: J. Quaternary Sci. 3, 3-13.

Blasco, S.M., Fortin, G., Hill, P.R., O'Connor, M.J. and Brigham-Grette, J., 1990, The late Neogene and Quaternary stratigraphy of the Canadian Beaufort continental shelf. in, Grantz, A., Johnson, L. and Sweeney, J.F., ed. The Arctic Ocean region. Geological Society of America, Boulder. The Geology of North America, v. L.

Brigham, J.K. and G.H. Miller, 1983, Paleotemperature estimates of the Alaskan Arctic coastal plain during the last 125,000 years, in, Permafrost, Fourth International Conference Proceedings, National Academy Press, Washington, D.C., p. 80-85.

Dyke, A.S., T.F. Morris and D.G.C. Green, 1991, Postglacial tectonic and sea level history of the central Canadian Arctic, Geological Survey of Canada, Bull. 397.

Geo-engineering Ltd., 1990, Geothermal modelling, offshore temperature profiles at Angasak and Amauligak, Beaufort Shelf, Geological Survey of Canada, Open File 2226, 56 pages.

Hill, P.R., Mudie, P.J., Moran, K. and Blasco, S.M., 1985, A sea-level curve for the Canadian Beaufort Shelf: Can. J. Earth Sci. 22, 1383-1393.

Ingersoll, L.R., Zobel, O.J. and Ingersoll, A.C., 1954, Heat Conduction with engineering, geological, and other applications: University of Wisconsin Press, Madison, WI, 325 pages.

Judge, A.S., Taylor, A.E., Burgess, M. and V.S. Allen, 1981, Canadian Geothermal Data Collection - Northern Wells, 1978-80, Geothermal Series #12, Earth Physics Branch, EMR Canada, 190 pages, 1982.

Judge, A.S. and Taylor, A.E., 1985, Permafrost distribution in Northern Canada - interpretation of well-logs: in, Brown, J., Metz, M.C. and Hoekstra, P., ed. Workshop on permafrost geophysics. U.S. Army cold Regions Research and Engineering Laboratory, Hanover, NH. Special Report 85-5.

Nixon, J.F., 1986, Thermal simulation of subsea permafrost: Can. J. Earth Sci. 23, p. 2039-2046.

Outcalt, S., 1985, A numerical model of subsea permafrost: In, D.M. Anderson and P.J. Williams, ed., Freezing and thawing of soil-water systems. Am. Soc. of Civil Eng., New York, p. 58-65.

Smith, P.A., 1986, The late Pleistocene-Holocene stratigraphic records, Canning River Delta region, northern Alaska: Geological Survey of Canada, Open file report 1237, p. 51-54.

Taylor, Alan, A constraint to the Wisconsinan glacial history, Canadian Arctic Archipelago, J. Quat. Sci., 3, 15-18, 1988.

Taylor, A.E., 1991, Marine transgression, shoreline emergence - evidence in seabed and terrestrial ground temperatures of changing relative sea levels, Arctic Canada: J. Geophysical Res. 96, 6893-6909.

Taylor, A.E., M. Burgess, A.S. Judge and V.S. Allen, Canadian Geothermal Data Collection - Northern Wells, 1981, Geothermal Series #13, Earth Physics Branch, EMR Canada, 153 pages, 1982.

Taylor, A., A. Judge and V. Allen, 1989, The automatic well temperature measuring system installed at Cape Allison C-47, offshore well, Arctic Islands of Canada. Part 2: Data retrieval and analysis of the thermal regime, J. Can. Petrol. Technol., 28, 95-101.

Wawrow, B., 1993, Modelling the depth to the upper surface of offshore permafrost, Canadian Beaufort Shelf. Internal Report, Terrain Sciences Div., Geological Survey of Canada.

APPENDIX A. Shoreline emergence.

Curves of permafrost temperatures versus depth for various times following emergence. Temperatures are shown for times 0.5, 1.0, 2.0, 3.0, 5.0 and 10.0 Ka after emergence to subaerial temperatures of -15° and -20°C. Degree of ice-bonding versus depth is shown in "ICE" column.

Parameters are listed at lower edge of each graph.

T_{step} °C for t_{step} Ka = surface temperature history step model applied to equilibrium profile; T_{step} = new temperature in °C established at t_{step} = time in past in Ka

T_o = equilibrium surface temperature before emergence (i.e. sea bottom temperature) (°C)

T_f = Freezing point temperature of rock, function of salinity (°C)

n = the volumetric water content of the rock (percentage of total volume)

S = the salinity of the water in the rock (ppt)

K_s = Thermal conductivity of the solid component of the rock (W/mK)

Q = terrestrial heat flux (mWm^{-2})

A_x = exponential parameter in the relationship between unfrozen water content and temperature (see Appendix E)

DZ = depth increment in numerical model (m)

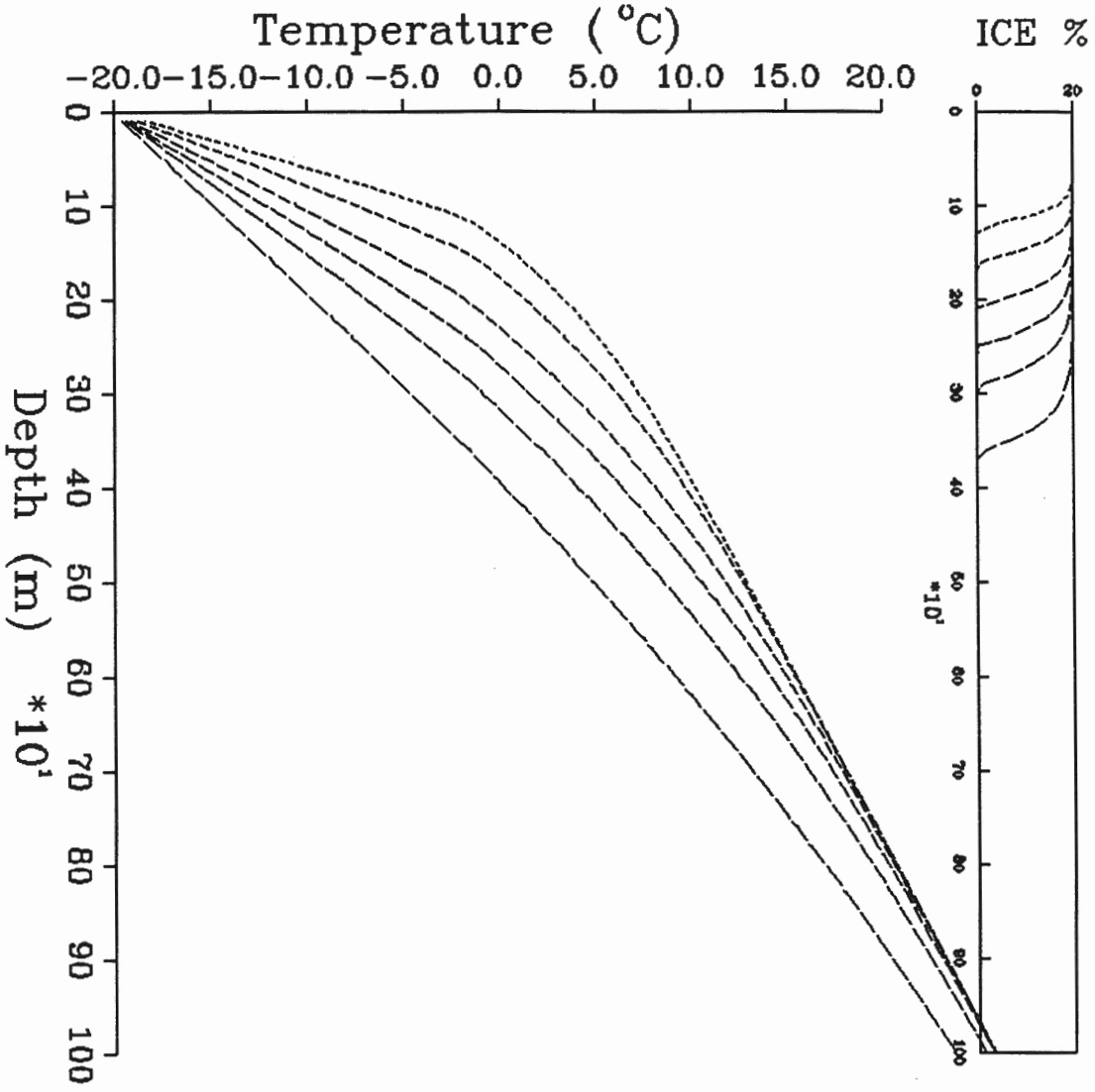

MEASURED DATA

\TC\TDUM.DAT
\LITH\LITH.DUM

-20.00 C FOR 0.500 Ka	-20.00 C FOR 1.000 Ka	-20.00 C FOR 2.000 Ka
To= 0.0 C Tf= -0.27 C n= 0.20 S= 5 ppt Ks= 2.00 W/mK Q= 40 W/m2 Ax= 0.7 DZ= 10 m	To= 0.0 C Tf= -0.27 C n= 0.20 S= 5 ppt Ks= 2.00 W/mK Q= 40 W/m2 Ax= 0.7 DZ= 10 m	To= 0.0 C Tf= -0.27 C n= 0.20 S= 5 ppt Ks= 2.00 W/mK Q= 40 W/m2 Ax= 0.7 DZ= 10 m
OF1.1	OF2.1	OF3.1

-20.00 C FOR 3.000 Ka	-20.00 C FOR 5.000 Ka	-20.00 C FOR 10.000 Ka
To= 0.0 C Tf= -0.27 C n= 0.20 S= 5 ppt Ks= 2.00 W/mK Q= 40 W/m2 Ax= 0.7 DZ= 10 m	To= 0.0 C Tf= -0.27 C n= 0.20 S= 5 ppt Ks= 2.00 W/mK Q= 40 W/m2 Ax= 0.7 DZ= 10 m	To= 0.0 C Tf= -0.27 C n= 0.20 S= 5 ppt Ks= 2.00 W/mK Q= 40 W/m2 Ax= 0.7 DZ= 10 m
OF4.1	OF5.1	OF6.1

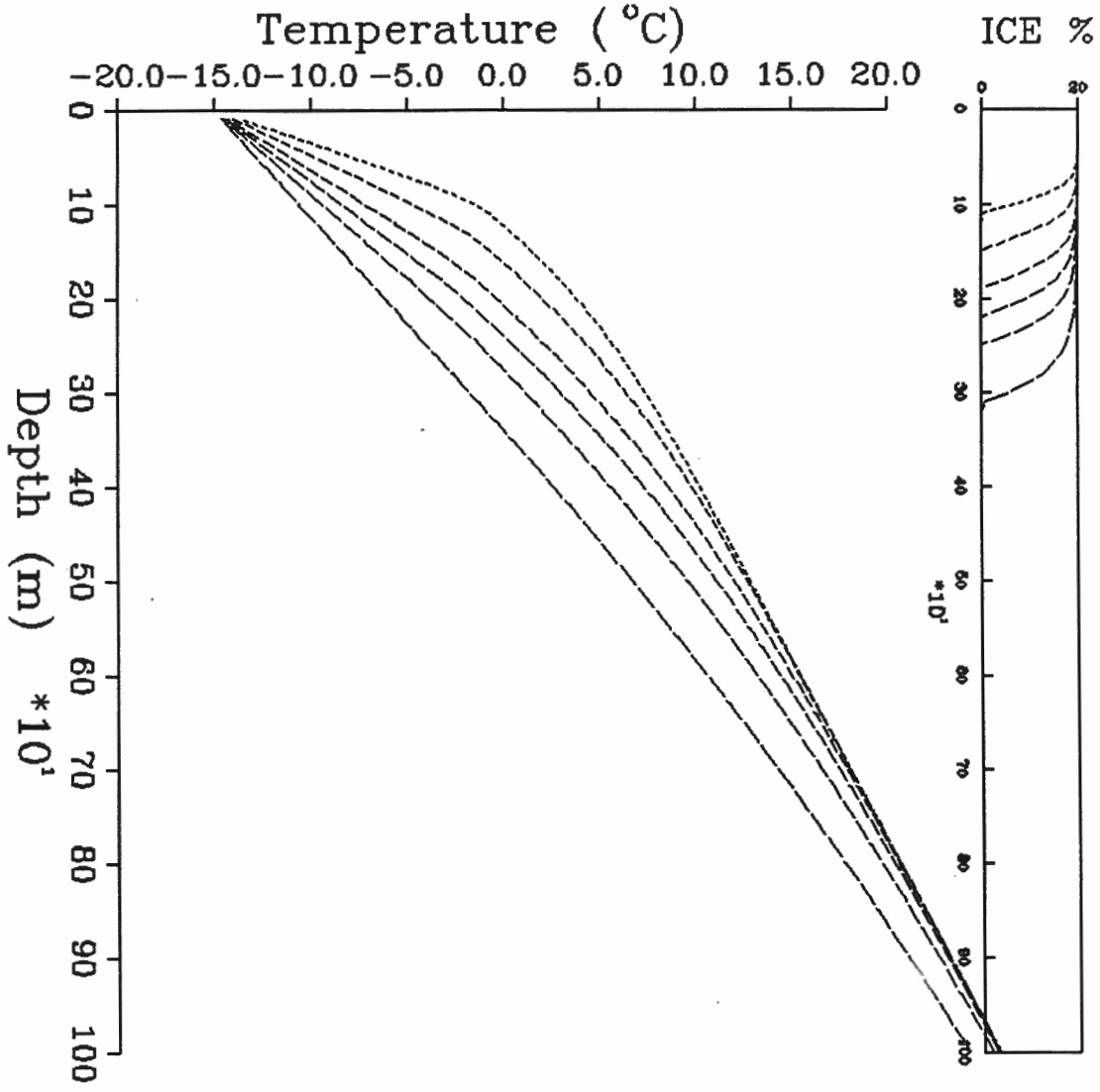

MEASURED DATA

\TC\TDUM.DAT
\LITH\LITH.DUM

-15.00 C FOR 0.500 Ka	-15.00 C FOR 1.000 Ka	-15.00 C FOR 2.000 Ka
To= 0.0 C Tf= -0.27 C n= 0.20 S= 5 ppt Ks= 2.00 W/mK Q= 40 W/m2 Ax= 0.7 DZ= 10 m	To= 0.0 C Tf= -0.27 C n= 0.20 S= 5 ppt Ks= 2.00 W/mK Q= 40 W/m2 Ax= 0.7 DZ= 10 m	To= 0.0 C Tf= -0.27 C n= 0.20 S= 5 ppt Ks= 2.00 W/mK Q= 40 W/m2 Ax= 0.7 DZ= 10 m
OG1.1	OG2.1	OG3.1

-15.00 C FOR 3.000 Ka	-15.00 C FOR 5.000 Ka	-15.00 C FOR 10.000 Ka
To= 0.0 C Tf= -0.27 C n= 0.20 S= 5 ppt Ks= 2.00 W/mK Q= 40 W/m2 Ax= 0.7 DZ= 10 m	To= 0.0 C Tf= -0.27 C n= 0.20 S= 5 ppt Ks= 2.00 W/mK Q= 40 W/m2 Ax= 0.7 DZ= 10 m	To= 0.0 C Tf= -0.27 C n= 0.20 S= 5 ppt Ks= 2.00 W/mK Q= 40 W/m2 Ax= 0.7 DZ= 10 m
OG4.1	OG5.1	OG6.1

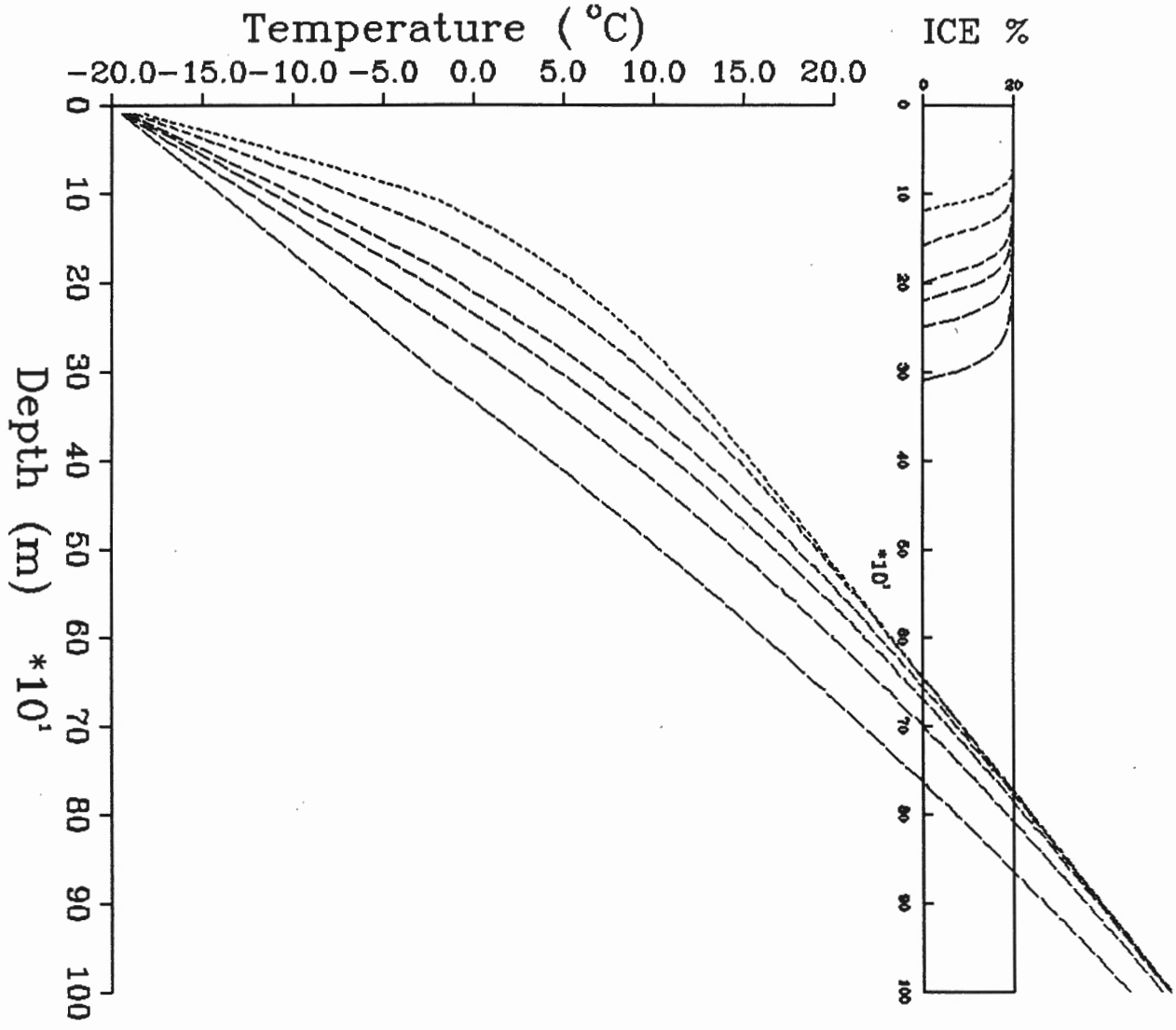

MEASURED DATA

\TC\TDUM.DAT
\LITH\LITH.DUM

-20.00 C FOR 0.500 Ka	-20.00 C FOR 1.000 Ka	-20.00 C FOR 2.000 Ka
To= 0.0 C Tf= -0.27 C n= 0.20 S= 5 ppt Ks= 2.00 W/mK Q= 60 W/m2 Ax= 0.7 DZ= 10 m	To= 0.0 C Tf= -0.27 C n= 0.20 S= 5 ppt Ks= 2.00 W/mK Q= 60 W/m2 Ax= 0.7 DZ= 10 m	To= 0.0 C Tf= -0.27 C n= 0.20 S= 5 ppt Ks= 2.00 W/mK Q= 60 W/m2 Ax= 0.7 DZ= 10 m
OH1.1	OH2.1	OH3.1

-20.00 C FOR 3.000 Ka	-20.00 C FOR 5.000 Ka	-20.00 C FOR 10.000 Ka
To= 0.0 C Tf= -0.27 C n= 0.20 S= 5 ppt Ks= 2.00 W/mK Q= 60 W/m2 Ax= 0.7 DZ= 10 m	To= 0.0 C Tf= -0.27 C n= 0.20 S= 5 ppt Ks= 2.00 W/mK Q= 60 W/m2 Ax= 0.7 DZ= 10 m	To= 0.0 C Tf= -0.27 C n= 0.20 S= 5 ppt Ks= 2.00 W/mK Q= 60 W/m2 Ax= 0.7 DZ= 10 m
OH4.1	OH5.1	OH6.1

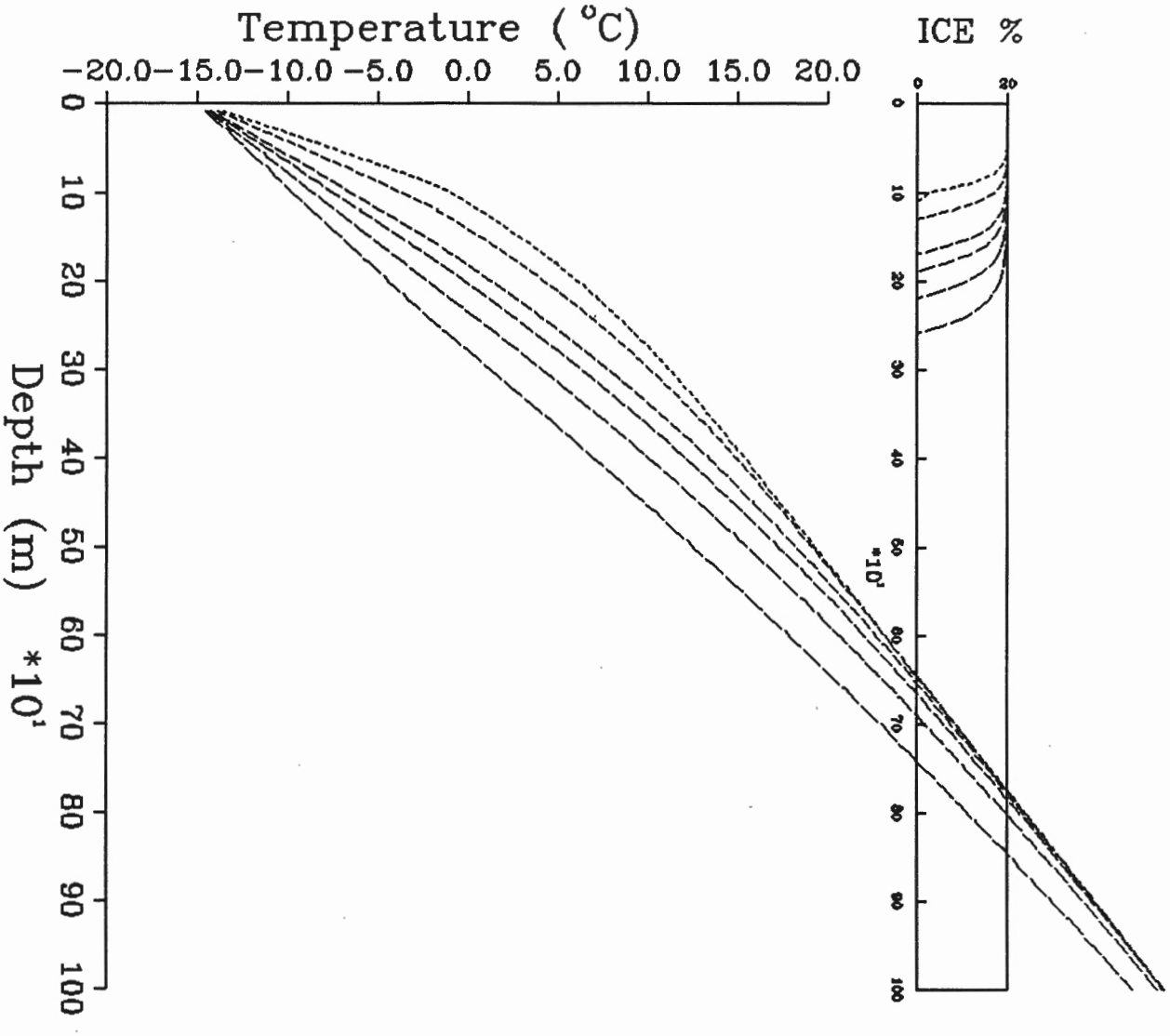

MEASURED DATA

\TC\TDUM.DAT
\LITH\LITH.DUM

-15.00 C FOR 0.500 Ka	-15.00 C FOR 1.000 Ka	-15.00 C FOR 2.000 Ka
To= 0.0 C Tf= -0.27 C n= 0.20 S= 5 ppt Ks= 2.00 W/mK Q= 60 W/m2 Ax= 0.7 DZ= 10 m	To= 0.0 C Tf= -0.27 C n= 0.20 S= 5 ppt Ks= 2.00 W/mK Q= 60 W/m2 Ax= 0.7 DZ= 10 m	To= 0.0 C Tf= -0.27 C n= 0.20 S= 5 ppt Ks= 2.00 W/mK Q= 60 W/m2 Ax= 0.7 DZ= 10 m
OI1.1	OI2.1	OI3.1

-15.00 C FOR 3.000 Ka	-15.00 C FOR 5.000 Ka	-15.00 C FOR 10.000 Ka
To= 0.0 C Tf= -0.27 C n= 0.20 S= 5 ppt Ks= 2.00 W/mK Q= 60 W/m2 Ax= 0.7 DZ= 10 m	To= 0.0 C Tf= -0.27 C n= 0.20 S= 5 ppt Ks= 2.00 W/mK Q= 60 W/m2 Ax= 0.7 DZ= 10 m	To= 0.0 C Tf= -0.27 C n= 0.20 S= 5 ppt Ks= 2.00 W/mK Q= 60 W/m2 Ax= 0.7 DZ= 10 m
OI4.1	OI5.1	OI6.1

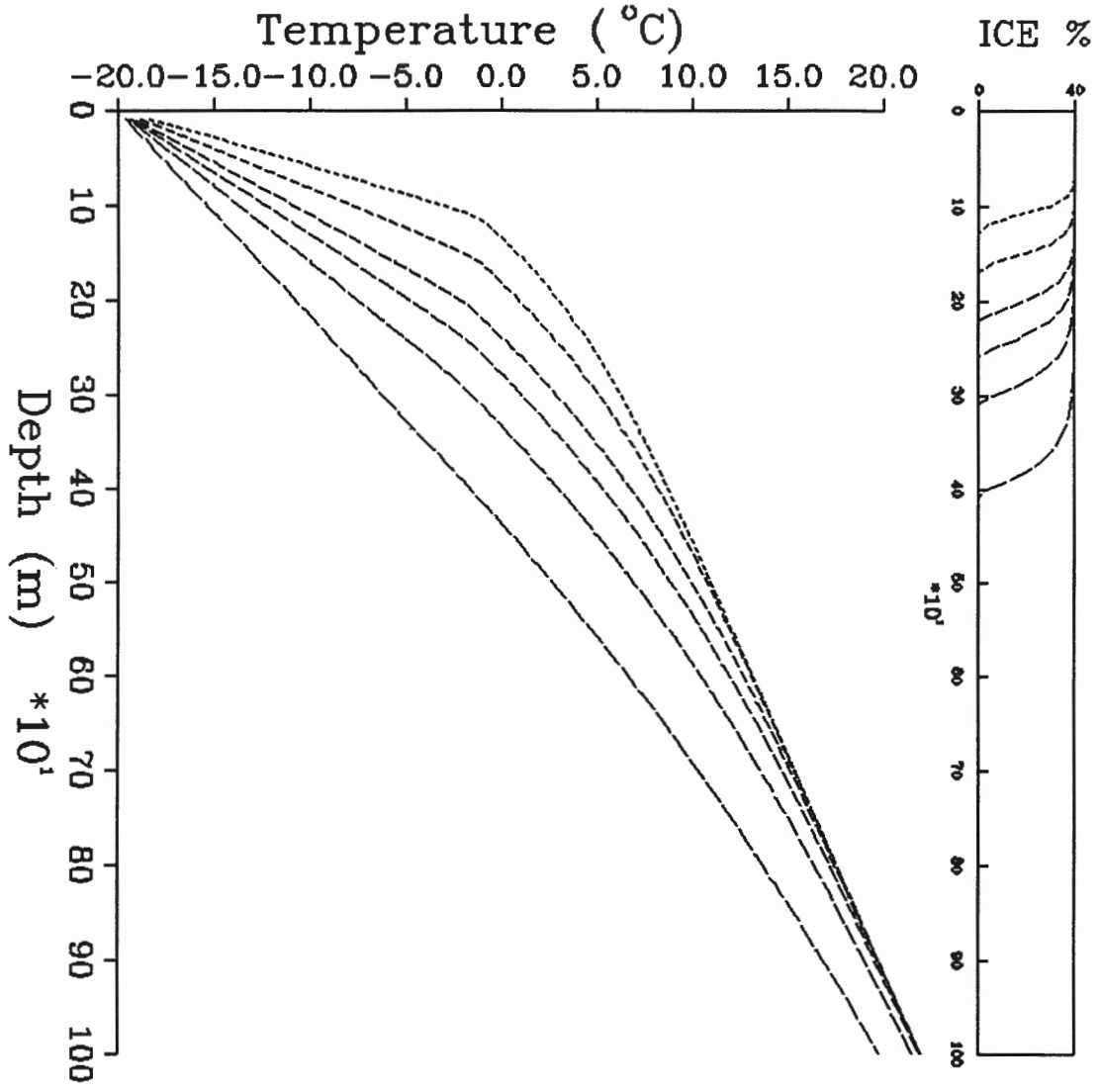

MEASURED DATA

\TC\TDUM.DAT
\LITH\LITH.DUM

-20.00 C FOR 0.500 Ka	-20.00 C FOR 1.000 Ka	-20.00 C FOR 2.000 Ka
To= 0.0 C Tf= -0.27 C n= 0.40 S= 5 ppt Ks= 4.00 W/mK Q= 40 W/m2 Ax= 0.7 DZ= 10 m	To= 0.0 C Tf= -0.27 C n= 0.40 S= 5 ppt Ks= 4.00 W/mK Q= 40 W/m2 Ax= 0.7 DZ= 10 m	To= 0.0 C Tf= -0.27 C n= 0.40 S= 5 ppt Ks= 4.00 W/mK Q= 40 W/m2 Ax= 0.7 DZ= 10 m
OJ1.1	OJ2.1	OJ3.1

-20.00 C FOR 3.000 Ka	-20.00 C FOR 5.000 Ka	-20.00 C FOR 10.000 Ka
To= 0.0 C Tf= -0.27 C n= 0.40 S= 5 ppt Ks= 4.00 W/mK Q= 40 W/m2 Ax= 0.7 DZ= 10 m	To= 0.0 C Tf= -0.27 C n= 0.40 S= 5 ppt Ks= 4.00 W/mK Q= 40 W/m2 Ax= 0.7 DZ= 10 m	To= 0.0 C Tf= -0.27 C n= 0.40 S= 5 ppt Ks= 4.00 W/mK Q= 40 W/m2 Ax= 0.7 DZ= 10 m
OJ4.1	OJ5.1	OJ6.1

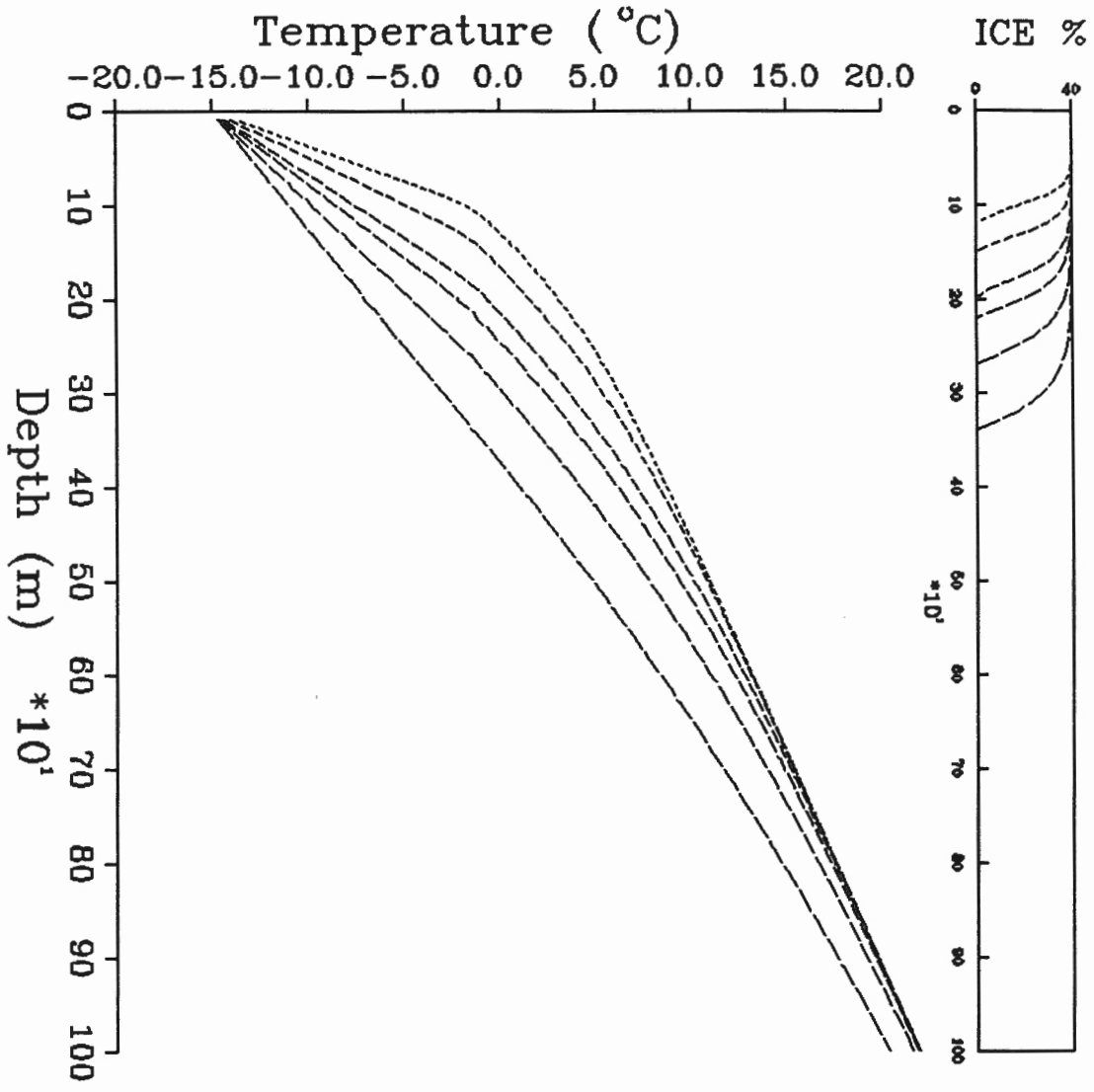

MEASURED DATA

\TC\TDUM.DAT
\LITH\LITH.DUM

−15.00 C FOR 0.500 Ka	−15.00 C FOR 1.000 Ka	−15.00 C FOR 2.000 Ka
To= 0.0 C Tf= −0.27 C n= 0.40 S= 5 ppt Ks= 4.00 W/mK Q= 40 W/m2 Ax= 0.7 DZ= 10 m	To= 0.0 C Tf= −0.27 C n= 0.40 S= 5 ppt Ks= 4.00 W/mK Q= 40 W/m2 Ax= 0.7 DZ= 10 m	To= 0.0 C Tf= −0.27 C n= 0.40 S= 5 ppt Ks= 4.00 W/mK Q= 40 W/m2 Ax= 0.7 DZ= 10 m
OK1.1	OK2.1	OK3.1

−15.00 C FOR 3.000 Ka	−15.00 C FOR 5.000 Ka	−15.00 C FOR 10.000 Ka
To= 0.0 C Tf= −0.27 C n= 0.40 S= 5 ppt Ks= 4.00 W/mK Q= 40 W/m2 Ax= 0.7 DZ= 10 m	To= 0.0 C Tf= −0.27 C n= 0.40 S= 5 ppt Ks= 4.00 W/mK Q= 40 W/m2 Ax= 0.7 DZ= 10 m	To= 0.0 C Tf= −0.27 C n= 0.40 S= 5 ppt Ks= 4.00 W/mK Q= 40 W/m2 Ax= 0.7 DZ= 10 m
OK4.1	OK5.1	OK6.1

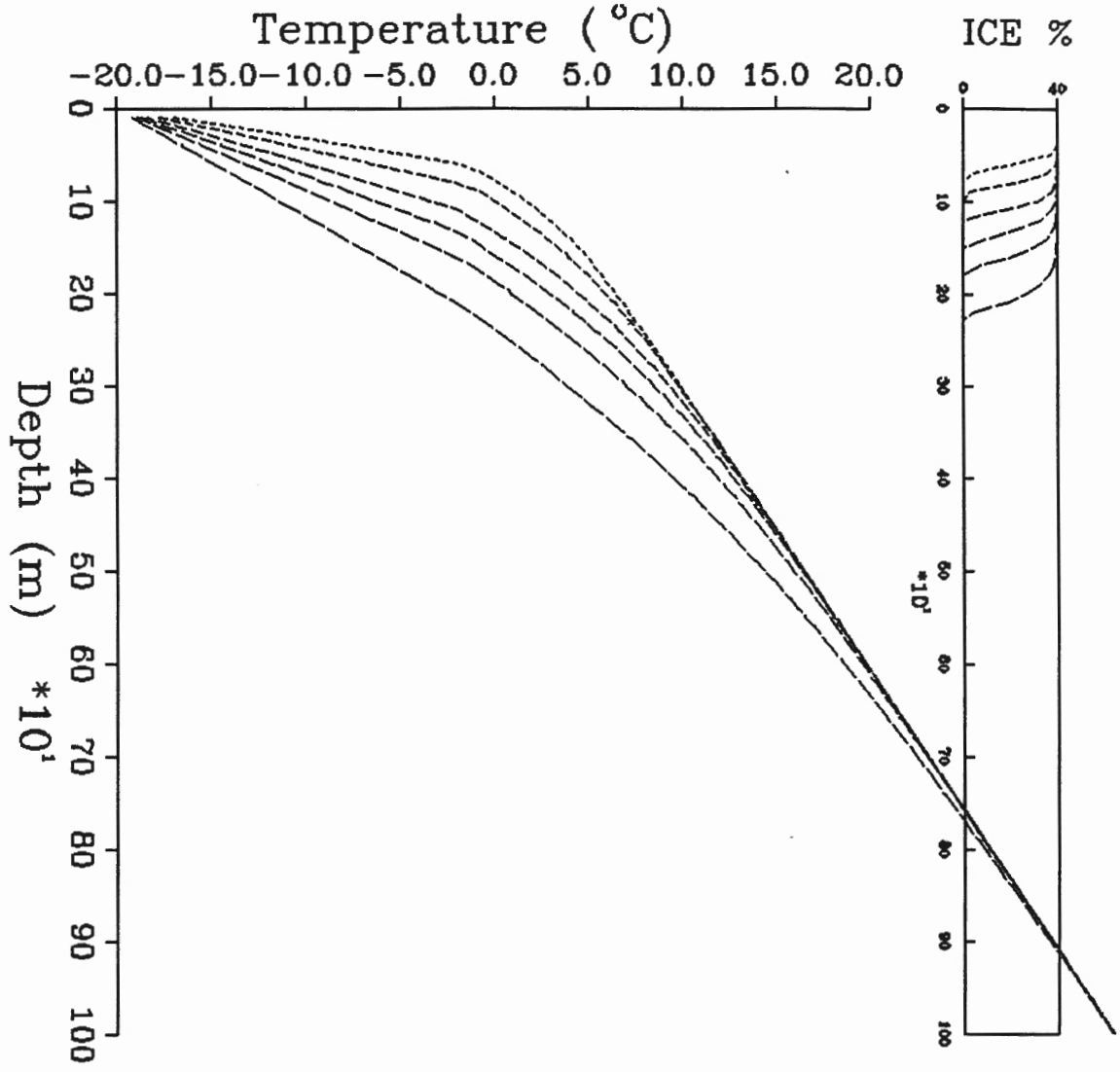

MEASURED DATA

\TC\TDUM.DAT
\LITH\LITH.DUM

-20.00 C FOR 0.500 Ka	-20.00 C FOR 1.000 Ka	-20.00 C FOR 2.000 Ka
To= 0.0 C Tf= -0.27 C n= 0.40 S= 5 ppt Ks= 4.00 W/mK Q= 60 W/m2 Ax= 0.7 DZ= 10 m	To= 0.0 C Tf= -0.27 C n= 0.40 S= 5 ppt Ks= 4.00 W/mK Q= 60 W/m2 Ax= 0.7 DZ= 10 m	To= 0.0 C Tf= -0.27 C n= 0.40 S= 5 ppt Ks= 4.00 W/mK Q= 60 W/m2 Ax= 0.7 DZ= 10 m
OL1.1	OL2.1	OL3.1

-20.00 C FOR 3.000 Ka	-20.00 C FOR 5.000 Ka	-20.00 C FOR 10.000 Ka
To= 0.0 C Tf= -0.27 C n= 0.40 S= 5 ppt Ks= 4.00 W/mK Q= 60 W/m2 Ax= 0.7 DZ= 10 m	To= 0.0 C Tf= -0.27 C n= 0.40 S= 5 ppt Ks= 4.00 W/mK Q= 60 W/m2 Ax= 0.7 DZ= 10 m	To= 0.0 C Tf= -0.27 C n= 0.40 S= 5 ppt Ks= 4.00 W/mK Q= 60 W/m2 Ax= 0.7 DZ= 10 m
OL4.1	OL5.1	OL6.1

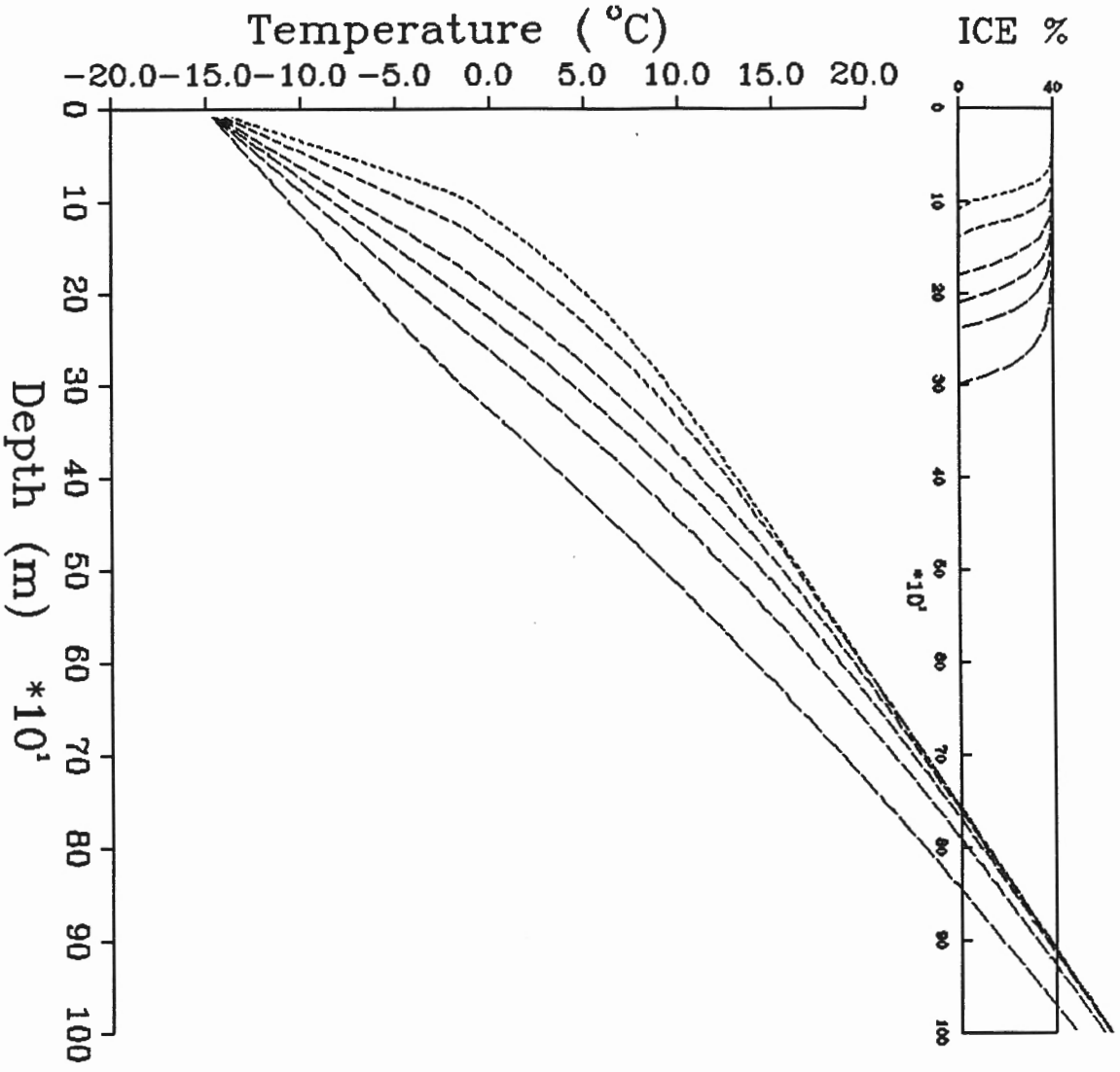

MEASURED DATA

\TC\TDUM.DAT
\LITH\LITH.DUM

-15.00 C FOR 0.500 Ka	-15.00 C FOR 1.000 Ka	-15.00 C FOR 2.000 Ka
To= 0.0 C Tf= -0.27 C n= 0.40 S= 5 ppt Ks= 4.00 W/mK Q= 60 W/m2 Ax= 0.7 DZ= 10 m	To= 0.0 C Tf= -0.27 C n= 0.40 S= 5 ppt Ks= 4.00 W/mK Q= 60 W/m2 Ax= 0.7 DZ= 10 m	To= 0.0 C Tf= -0.27 C n= 0.40 S= 5 ppt Ks= 4.00 W/mK Q= 60 W/m2 Ax= 0.7 DZ= 10 m
OM1.1	OM2.1	OM3.1

-15.00 C FOR 3.000 Ka	-15.00 C FOR 5.000 Ka	-15.00 C FOR 10.000 Ka
To= 0.0 C Tf= -0.27 C n= 0.40 S= 5 ppt Ks= 4.00 W/mK Q= 60 W/m2 Ax= 0.7 DZ= 10 m	To= 0.0 C Tf= -0.27 C n= 0.40 S= 5 ppt Ks= 4.00 W/mK Q= 60 W/m2 Ax= 0.7 DZ= 10 m	To= 0.0 C Tf= -0.27 C n= 0.40 S= 5 ppt Ks= 4.00 W/mK Q= 60 W/m2 Ax= 0.7 DZ= 10 m
OM4.1	OM5.1	OM6.1

APPENDIX B. Marine transgression

Curves of permafrost temperatures versus depth for various times following marine transgression. Temperatures are shown for times 0.5, 1.0, 2.0, 3.0, 5.0 and 10 Ka after transgression, from subaerial temperatures of -10°C and -15°C. Degree of ice-bonding versus depth is shown in "ICE" column.

Parameters are listed at lower edge of each graph.

T_{step} °C for t_{step} Ka = surface temperature history step model applied to equilibrium profile; T_{step} = new temperature in °C established at t_{step} = time in past in Ka

T_o = equilibrium surface temperature (ie. subaerial surface temperature) for the late Wisconsinan/early Holocene

T_f = Freezing point temperature of sediments, function of salinity (°C)

n = the volumetric water content of the rock (percentage of total volume)

S = the salinity of the water in the rock (ppt)

K_s = Thermal conductivity of the solid component of the rock

Q = terrestrial heat flux (mWm^{-2})

A_x = exponential parameter in the relationship between unfrozen water content and temperature (see Appendix E)

DZ = depth increment in numerical model (See Appendix E)

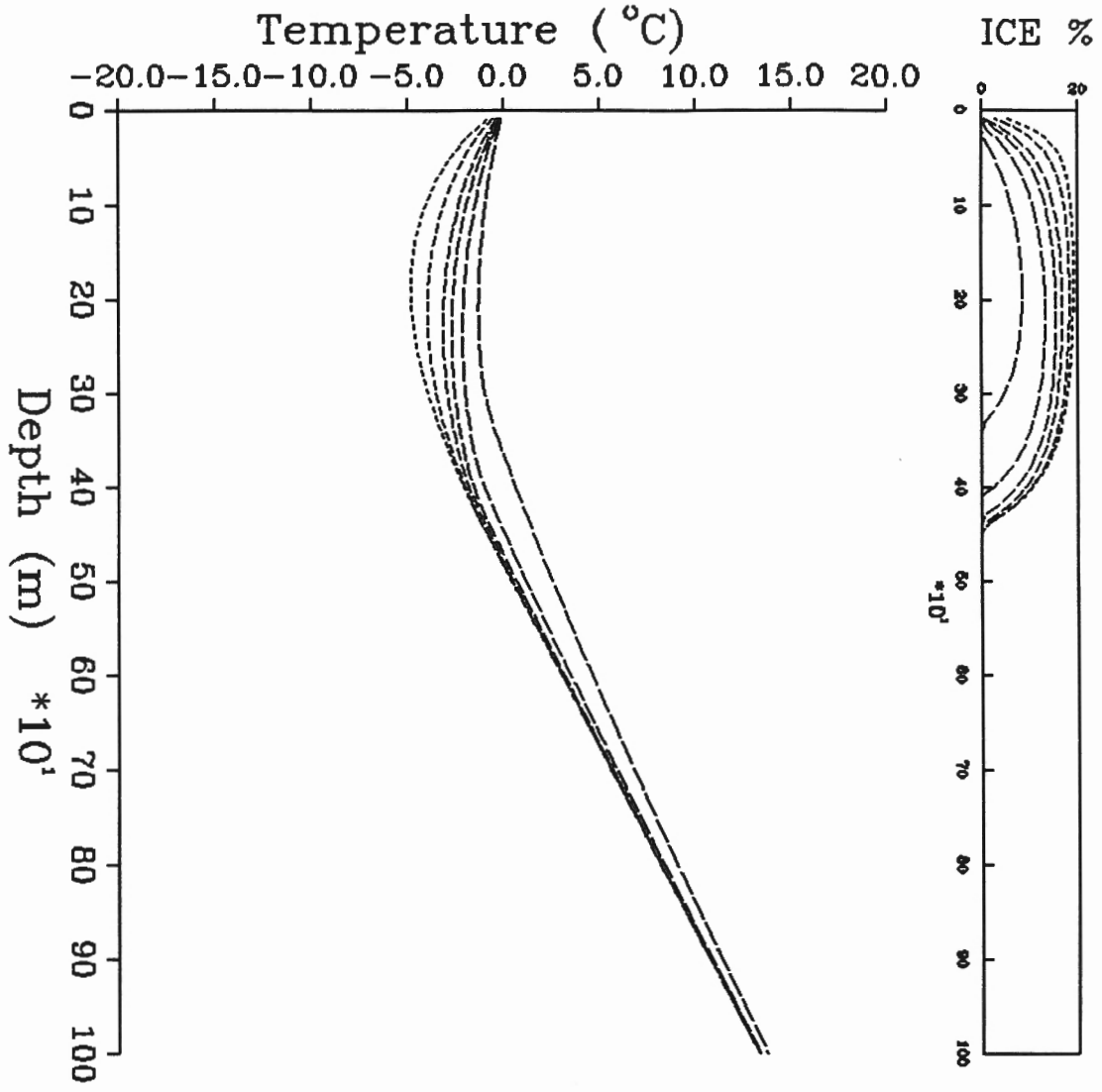

MEASURED DATA

\TC\TDUM.DAT
\LITH\LITH.DUM

0.00 C FOR 0.500 Ka

To= -10.0 C
Tf= -0.27 C
n= 0.20
S= 5 ppt
Ks= 2.00 W/mK
Q= 40 W/m2
Ax= 0.7
DZ= 10 m

OF1.DAT

0.00 C FOR 1.000 Ka

To= -10.0 C
Tf= -0.27 C
n= 0.20
S= 5 ppt
Ks= 2.00 W/mK
Q= 40 W/m2
Ax= 0.7
DZ= 10 m

OF2.DAT

0.00 C FOR 2.000 Ka

To= -10.0 C
Tf= -0.27 C
n= 0.20
S= 5 ppt
Ks= 2.00 W/mK
Q= 40 W/m2
Ax= 0.7
DZ= 10 m

OF3.DAT

0.00 C FOR 3.000 Ka

To= -10.0 C
Tf= -0.27 C
n= 0.20
S= 5 ppt
Ks= 2.00 W/mK
Q= 40 W/m2
Ax= 0.7
DZ= 10 m

OF4.DAT

0.00 C FOR 5.000 Ka

To= -10.0 C
Tf= -0.27 C
n= 0.20
S= 5 ppt
Ks= 2.00 W/mK
Q= 40 W/m2
Ax= 0.7
DZ= 10 m

OF5.DAT

0.00 C FOR 10.000 Ka

To= -10.0 C
Tf= -0.27 C
n= 0.20
S= 5 ppt
Ks= 2.00 W/mK
Q= 40 W/m2
Ax= 0.7
DZ= 10 m

OF6.DAT

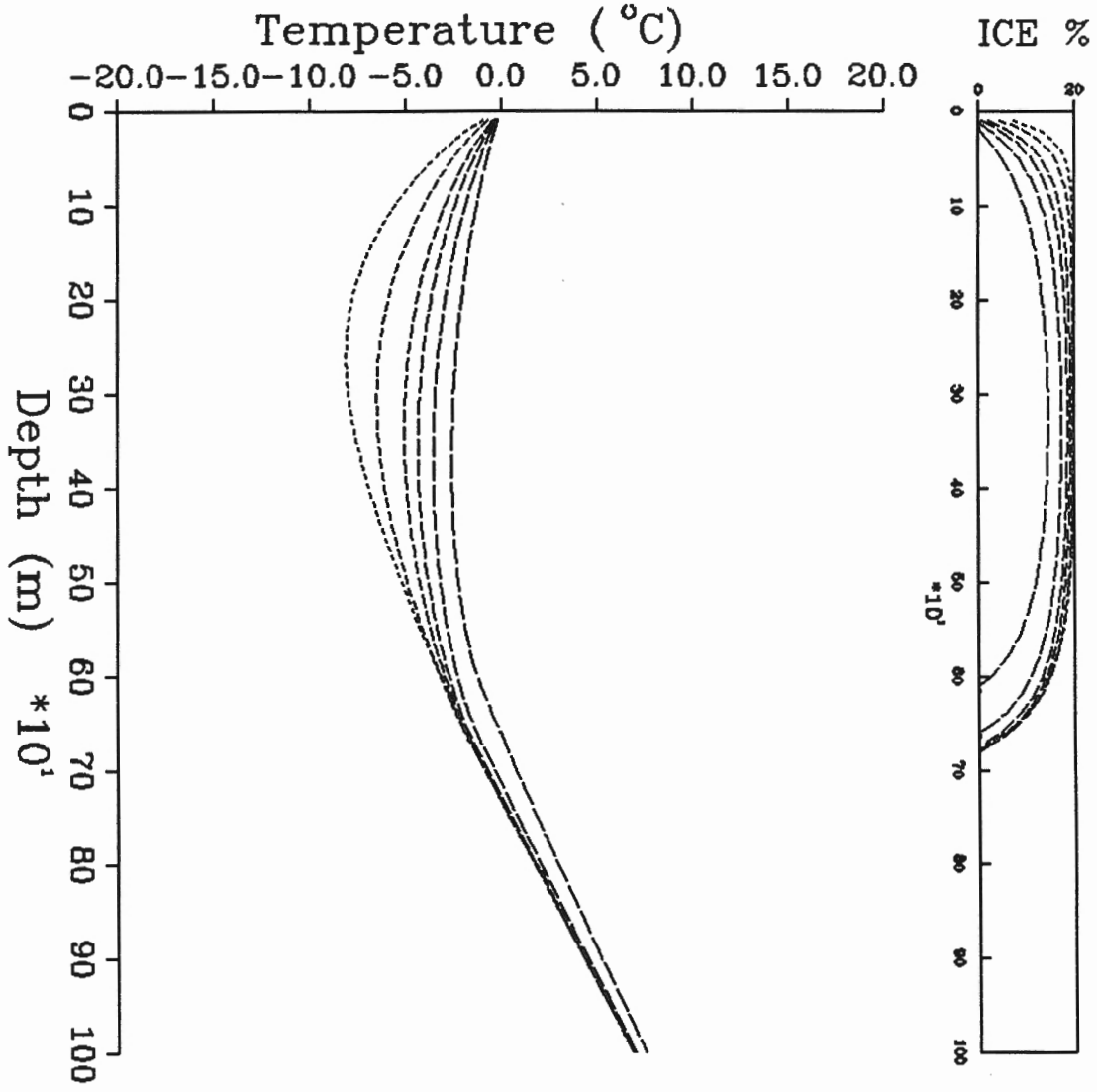

MEASURED DATA	0.00 C FOR 0.500 Ka	0.00 C FOR 1.000 Ka	0.00 C FOR 2.000 Ka
\TC\TDUM.DAT \LITH\LITH.DUM	To= -15.0 C Tf= -0.27 C n= 0.20 S= 5 ppt Ks= 2.00 W/mK Q= 40 W/m2 Ax= 0.7 DZ= 10 m	To= -15.0 C Tf= -0.27 C n= 0.20 S= 5 ppt Ks= 2.00 W/mK Q= 40 W/m2 Ax= 0.7 DZ= 10 m	To= -15.0 C Tf= -0.27 C n= 0.20 S= 5 ppt Ks= 2.00 W/mK Q= 40 W/m2 Ax= 0.7 DZ= 10 m
	OG1.DAT	OG2.DAT	OG3.DAT
	0.00 C FOR 3.000 Ka	0.00 C FOR 5.000 Ka	0.00 C FOR 10.000 Ka
	To= -15.0 C Tf= -0.27 C n= 0.20 S= 5 ppt Ks= 2.00 W/mK Q= 40 W/m2 Ax= 0.7 DZ= 10 m	To= -15.0 C Tf= -0.27 C n= 0.20 S= 5 ppt Ks= 2.00 W/mK Q= 40 W/m2 Ax= 0.7 DZ= 10 m	To= -15.0 C Tf= -0.27 C n= 0.20 S= 5 ppt Ks= 2.00 W/mK Q= 40 W/m2 Ax= 0.7 DZ= 10 m
	OG4.DAT	OG5.DAT	OG6.DAT

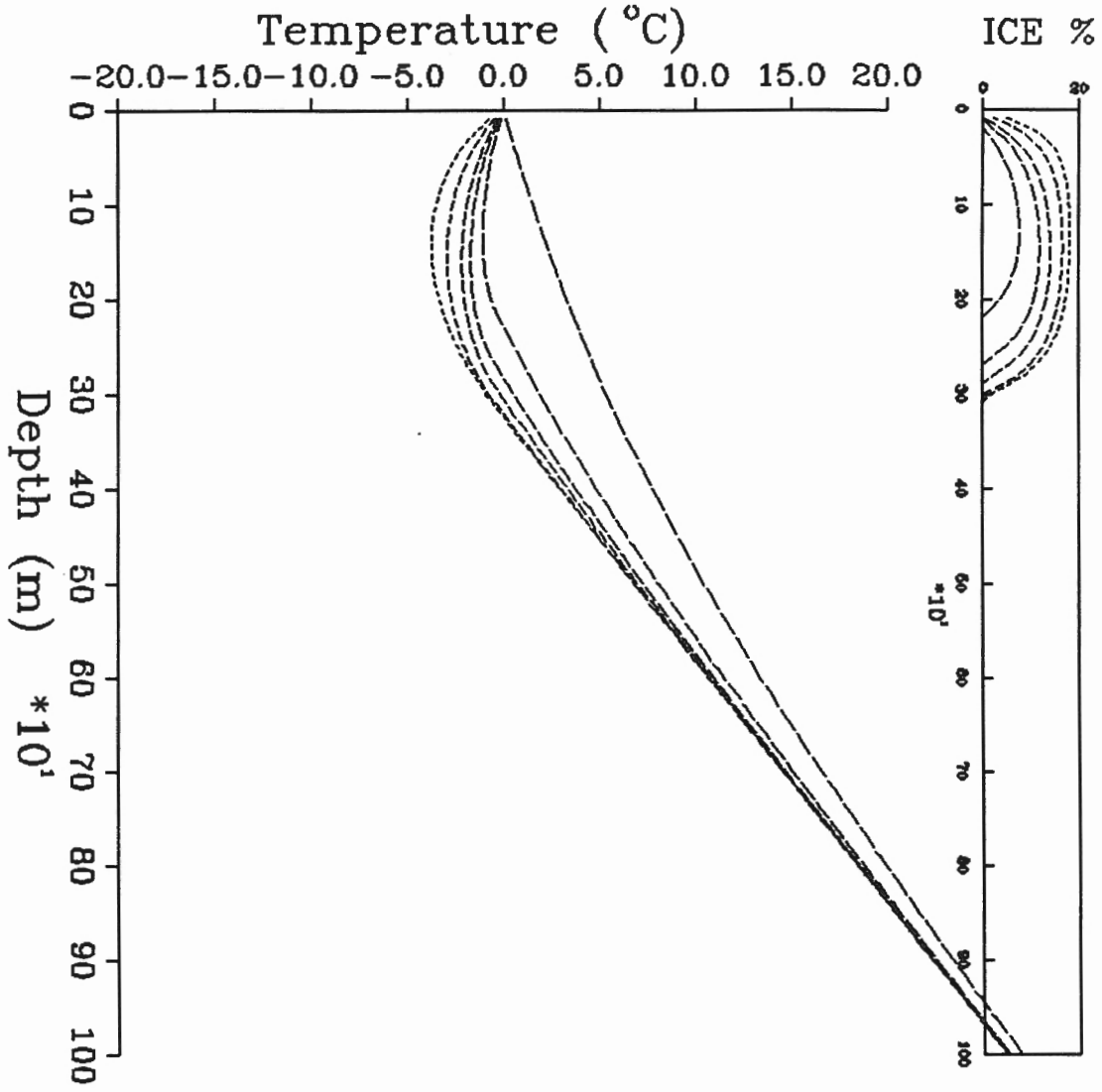

MEASURED DATA	0.00 C FOR 0.500 Ka	0.00 C FOR 1.000 Ka	0.00 C FOR 2.000 Ka
\TC\TDUM.DAT \LITH\LITH.DUM	To= −10.0 C Tf= −0.27 C n= 0.20 S= 5 ppt Ks= 2.00 W/mK Q= 60 W/m2 Ax= 0.7 DZ= 10 m	To= −10.0 C Tf= −0.27 C n= 0.20 S= 5 ppt Ks= 2.00 W/mK Q= 60 W/m2 Ax= 0.7 DZ= 10 m	To= −10.0 C Tf= −0.27 C n= 0.20 S= 5 ppt Ks= 2.00 W/mK Q= 60 W/m2 Ax= 0.7 DZ= 10 m
	OH1.DAT	OH2.DAT	OH3.DAT
	0.00 C FOR 3.000 Ka	0.00 C FOR 5.000 Ka	0.00 C FOR 10.000 Ka
	To= −10.0 C Tf= −0.27 C n= 0.20 S= 5 ppt Ks= 2.00 W/mK Q= 60 W/m2 Ax= 0.7 DZ= 10 m	To= −10.0 C Tf= −0.27 C n= 0.20 S= 5 ppt Ks= 2.00 W/mK Q= 60 W/m2 Ax= 0.7 DZ= 10 m	To= −10.0 C Tf= −0.27 C n= 0.20 S= 5 ppt Ks= 2.00 W/mK Q= 60 W/m2 Ax= 0.7 DZ= 10 m
	OH4.DAT	OH5.DAT	OH6.DAT

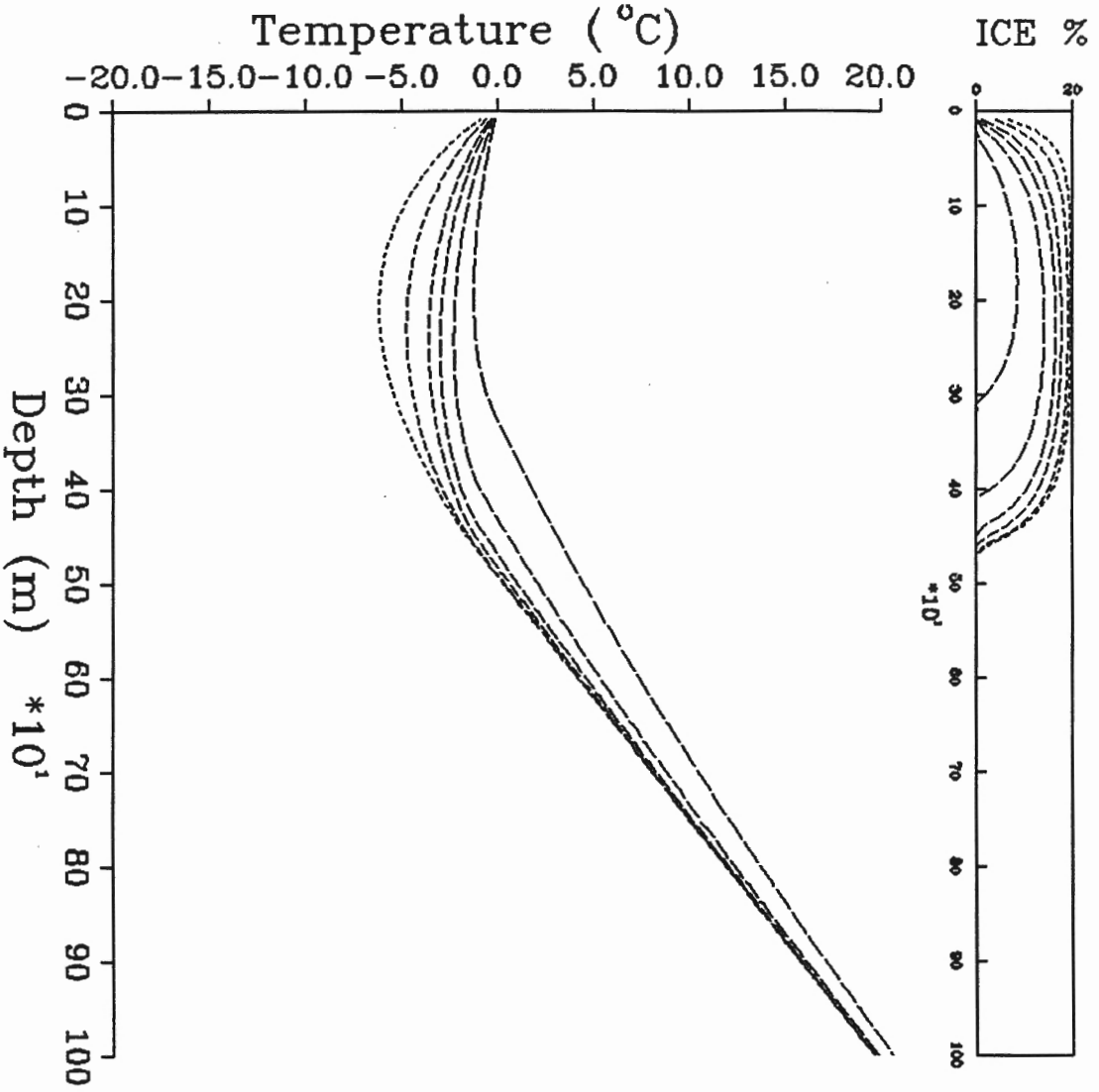

MEASURED DATA	0.00 C FOR 0.500 Ka	0.00 C FOR 1.000 Ka	0.00 C FOR 2.000 Ka
\TC\TDUM.DAT \LITH\LITH.DUM	To= -15.0 C Tf= -0.27 C n= 0.20 S= 5 ppt Ks= 2.00 W/mK Q= 60 W/m2 Ax= 0.7 DZ= 10 m	To= -15.0 C Tf= -0.27 C n= 0.20 S= 5 ppt Ks= 2.00 W/mK Q= 60 W/m2 Ax= 0.7 DZ= 10 m	To= -15.0 C Tf= -0.27 C n= 0.20 S= 5 ppt Ks= 2.00 W/mK Q= 60 W/m2 Ax= 0.7 DZ= 10 m
	OI1.DAT	OI2.DAT	OI3.DAT
	0.00 C FOR 3.000 Ka	0.00 C FOR 5.000 Ka	0.00 C FOR 10.000 Ka
	To= -15.0 C Tf= -0.27 C n= 0.20 S= 5 ppt Ks= 2.00 W/mK Q= 60 W/m2 Ax= 0.7 DZ= 10 m	To= -15.0 C Tf= -0.27 C n= 0.20 S= 5 ppt Ks= 2.00 W/mK Q= 60 W/m2 Ax= 0.7 DZ= 10 m	To= -15.0 C Tf= -0.27 C n= 0.20 S= 5 ppt Ks= 2.00 W/mK Q= 60 W/m2 Ax= 0.7 DZ= 10 m
	OI4.DAT	OI5.DAT	OI6.DAT

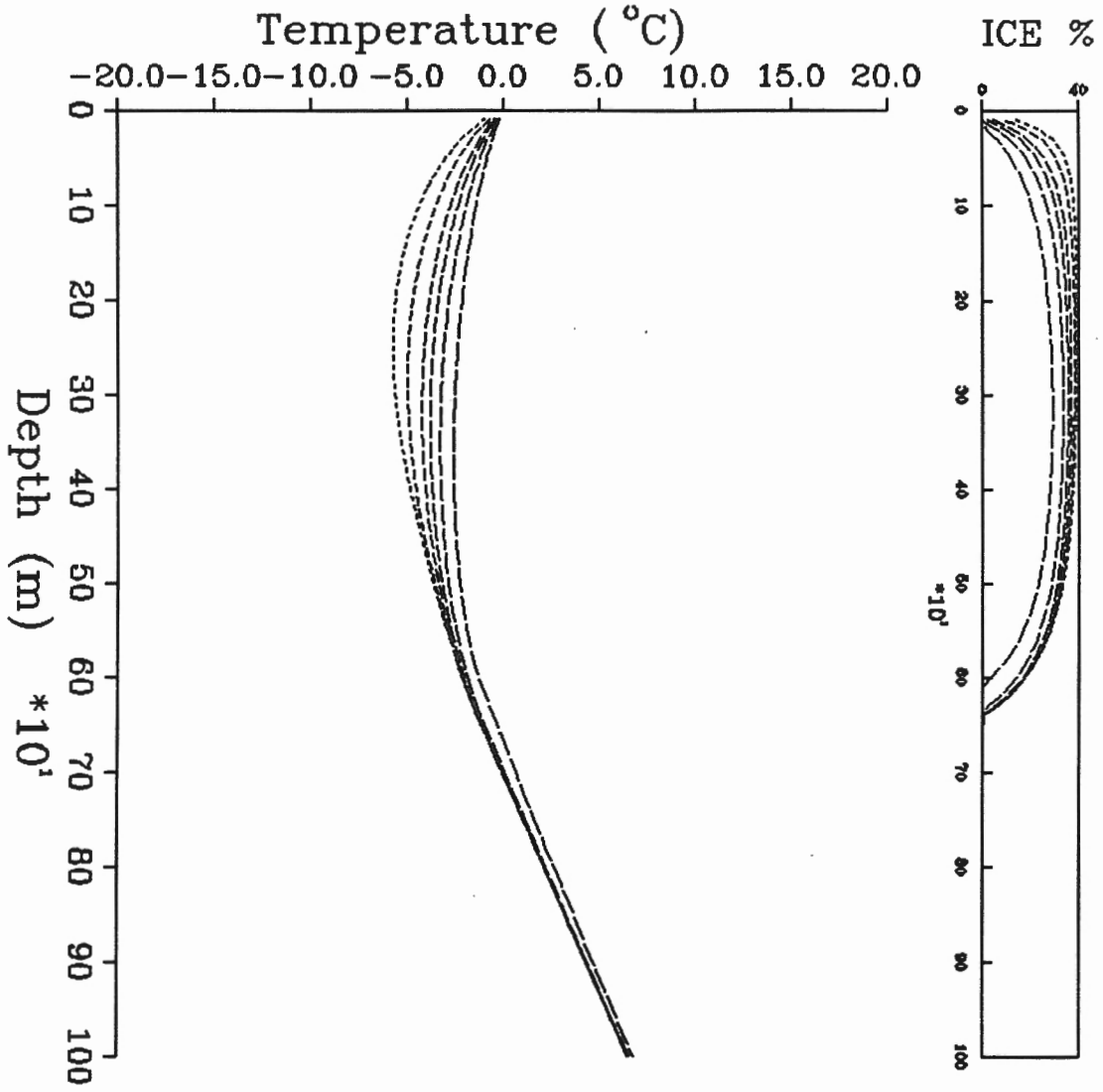

MEASURED DATA	0.00 C FOR 0.500 Ka	0.00 C FOR 1.000 Ka	0.00 C FOR 2.000 Ka
\TC\TDUM.DAT \LITH\LITH.DUM	To= −10.0 C Tf= −0.27 C n= 0.40 S= 5 ppt Ks= 4.00 W/mK Q= 40 W/m2 Ax= 0.7 DZ= 10 m	To= −10.0 C Tf= −0.27 C n= 0.40 S= 5 ppt Ks= 4.00 W/mK Q= 40 W/m2 Ax= 0.7 DZ= 10 m	To= −10.0 C Tf= −0.27 C n= 0.40 S= 5 ppt Ks= 4.00 W/mK Q= 40 W/m2 Ax= 0.7 DZ= 10 m
	OJ1.DAT	OJ2.DAT	OJ3.DAT
	0.00 C FOR 3.000 Ka	0.00 C FOR 5.000 Ka	0.00 C FOR 10.000 Ka
	To= −10.0 C Tf= −0.27 C n= 0.40 S= 5 ppt Ks= 4.00 W/mK Q= 40 W/m2 Ax= 0.7 DZ= 10 m	To= −10.0 C Tf= −0.27 C n= 0.40 S= 5 ppt Ks= 4.00 W/mK Q= 40 W/m2 Ax= 0.7 DZ= 10 m	To= −10.0 C Tf= −0.27 C n= 0.40 S= 5 ppt Ks= 4.00 W/mK Q= 40 W/m2 Ax= 0.7 DZ= 10 m
	OJ4.DAT	OJ5.DAT	OJ6.DAT

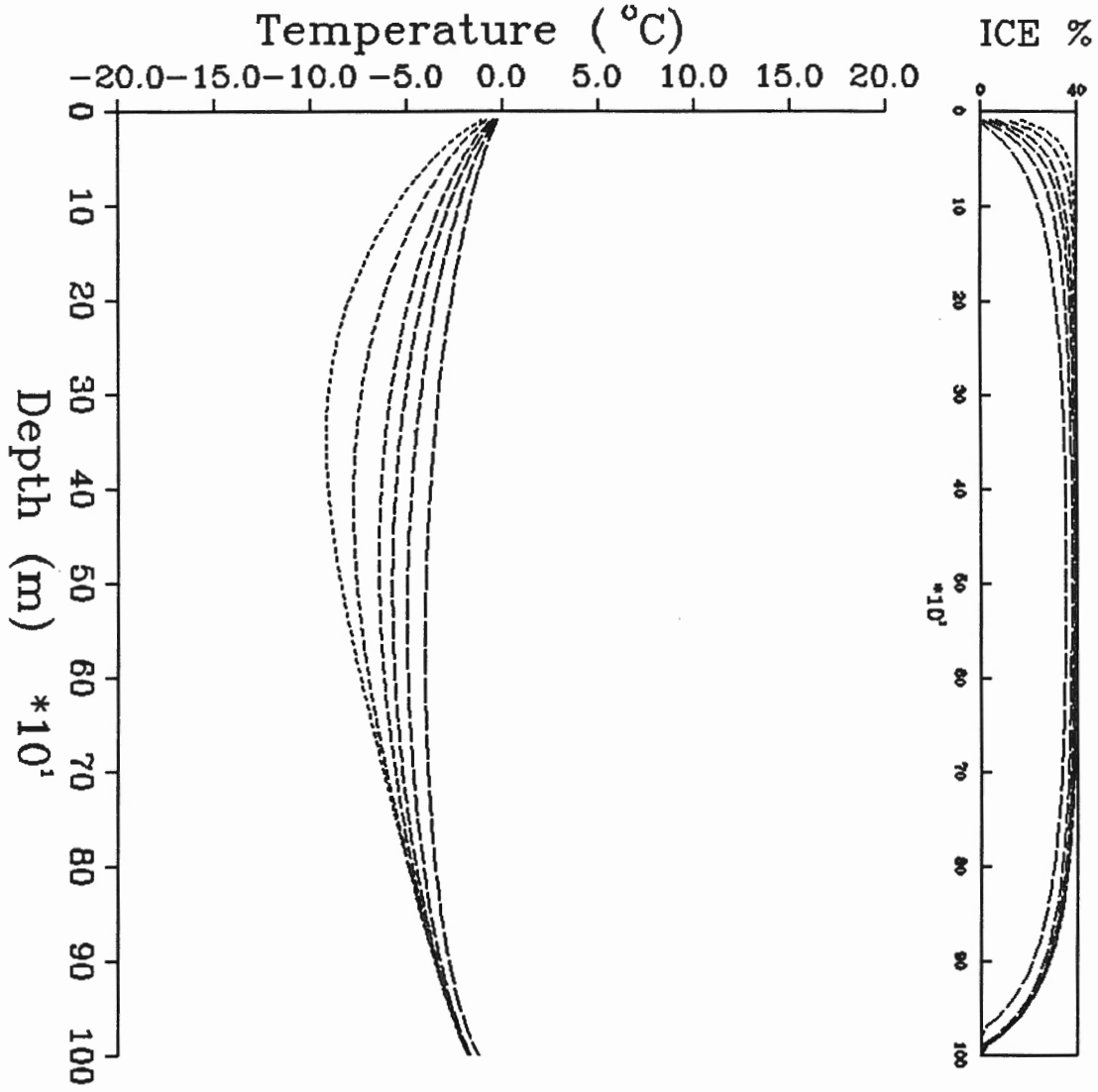

MEASURED DATA	0.00 C FOR 0.500 Ka	0.00 C FOR 1.000 Ka	0.00 C FOR 2.000 Ka
\TC\TDUM.DAT \LITH\LITH.DUM	To= -15.0 C Tf= -0.27 C n= 0.40 S= 5 ppt Ks= 4.00 W/mK Q= 40 W/m2 Ax= 0.7 DZ= 10 m	To= -15.0 C Tf= -0.27 C n= 0.40 S= 5 ppt Ks= 4.00 W/mK Q= 40 W/m2 Ax= 0.7 DZ= 10 m	To= -15.0 C Tf= -0.27 C n= 0.40 S= 5 ppt Ks= 4.00 W/mK Q= 40 W/m2 Ax= 0.7 DZ= 10 m
	OK1.DAT	OK2.DAT	OK3.DAT
	0.00 C FOR 3.000 Ka	0.00 C FOR 5.000 Ka	0.00 C FOR 10.000 Ka
	To= -15.0 C Tf= -0.27 C n= 0.40 S= 5 ppt Ks= 4.00 W/mK Q= 40 W/m2 Ax= 0.7 DZ= 10 m	To= -15.0 C Tf= -0.27 C n= 0.40 S= 5 ppt Ks= 4.00 W/mK Q= 40 W/m2 Ax= 0.7 DZ= 10 m	To= -15.0 C Tf= -0.27 C n= 0.40 S= 5 ppt Ks= 4.00 W/mK Q= 40 W/m2 Ax= 0.7 DZ= 10 m
	OK4.DAT	OK5.DAT	OK6.DAT

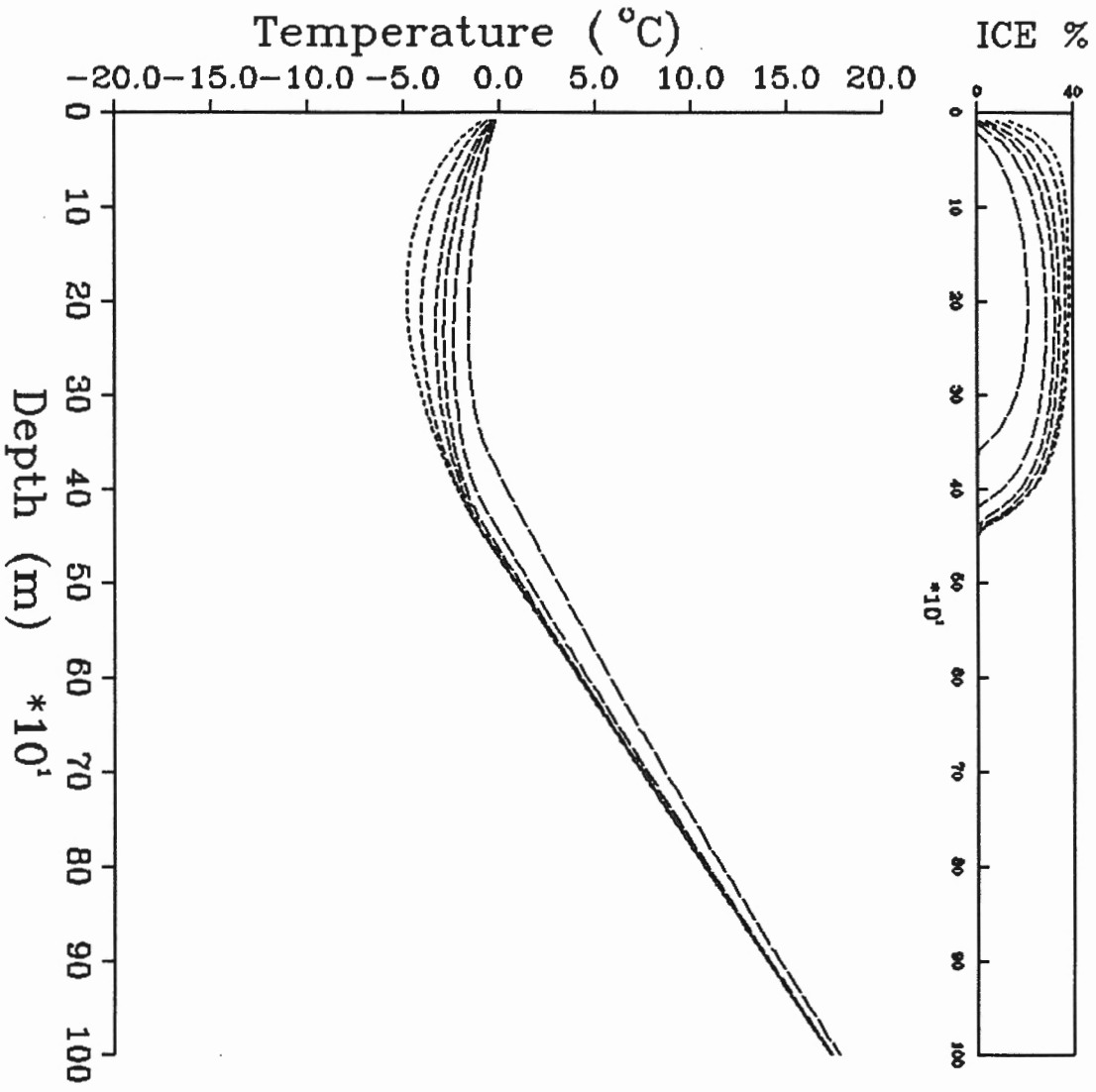

MEASURED DATA

\TC\TDUM.DAT
\LITH\LITH.DUM

0.00 C FOR 0.500 Ka

To= −10.0 C
Tf= −0.27 C
n= 0.40
S= 5 ppt
Ks= 4.00 W/mK
Q= 60 W/m2
Ax= 0.7
DZ= 10 m

OL1.DAT

0.00 C FOR 1.000 Ka

To= −10.0 C
Tf= −0.27 C
n= 0.40
S= 5 ppt
Ks= 4.00 W/mK
Q= 60 W/m2
Ax= 0.7
DZ= 10 m

OL2.DAT

0.00 C FOR 2.000 Ka

To= −10.0 C
Tf= −0.27 C
n= 0.40
S= 5 ppt
Ks= 4.00 W/mK
Q= 60 W/m2
Ax= 0.7
DZ= 10 m

OL3.DAT

0.00 C FOR 3.000 Ka

To= −10.0 C
Tf= −0.27 C
n= 0.40
S= 5 ppt
Ks= 4.00 W/mK
Q= 60 W/m2
Ax= 0.7
DZ= 10 m

OL4.DAT

0.00 C FOR 5.000 Ka

To= −10.0 C
Tf= −0.27 C
n= 0.40
S= 5 ppt
Ks= 4.00 W/mK
Q= 60 W/m2
Ax= 0.7
DZ= 10 m

OL5.DAT

0.00 C FOR 10.000 Ka

To= −10.0 C
Tf= −0.27 C
n= 0.40
S= 5 ppt
Ks= 4.00 W/mK
Q= 60 W/m2
Ax= 0.7
DZ= 10 m

OL6.DAT

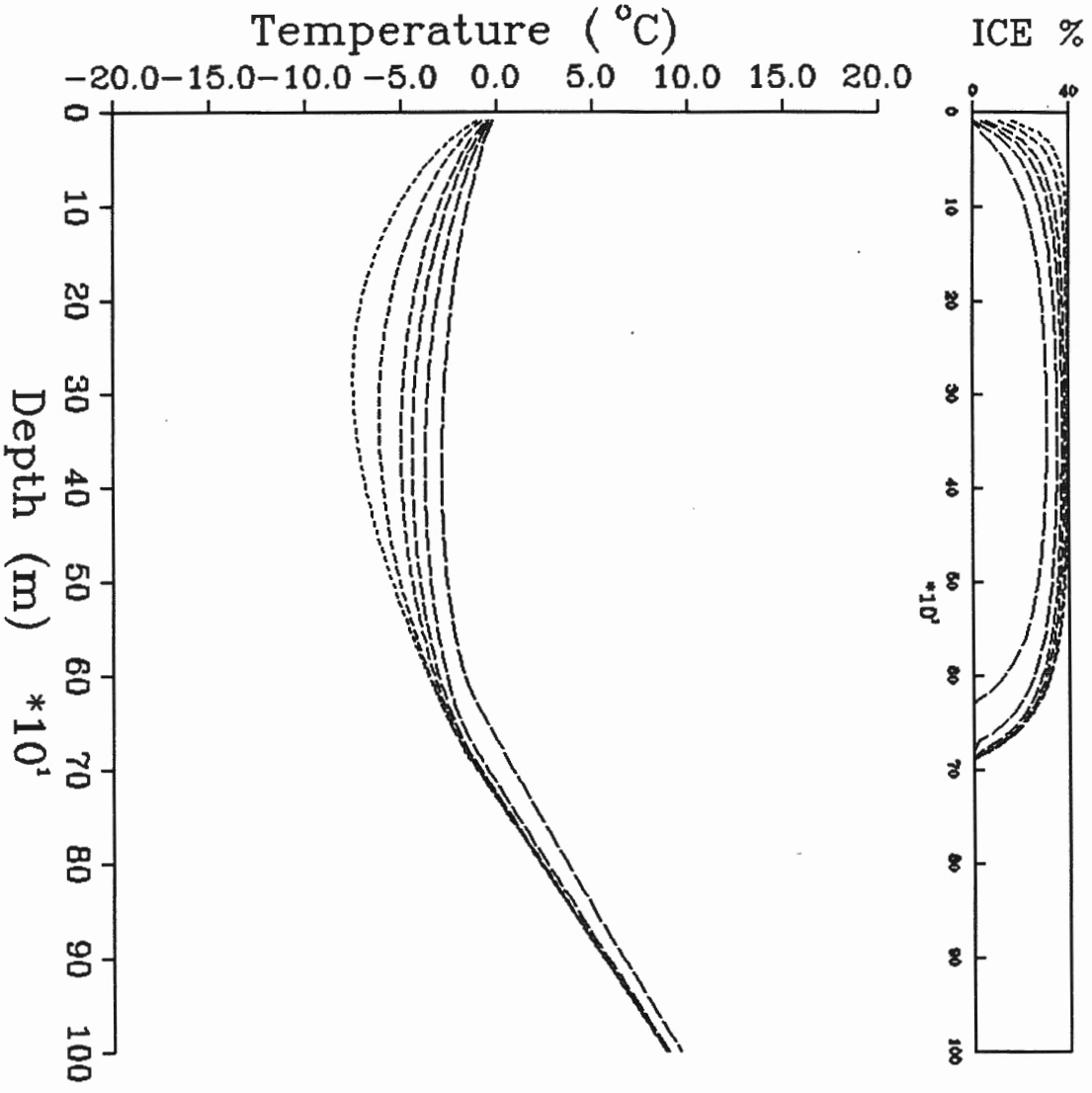

MEASURED DATA

\TC\TDUM.DAT
\LITH\LITH.DUM

0.00 C FOR 0.500 Ka	0.00 C FOR 1.000 Ka	0.00 C FOR 2.000 Ka
To= −15.0 C Tf= −0.27 C n= 0.40 S= 5 ppt Ks= 4.00 W/mK Q= 60 W/m2 Ax= 0.7 DZ= 10 m	To= −15.0 C Tf= −0.27 C n= 0.40 S= 5 ppt Ks= 4.00 W/mK Q= 60 W/m2 Ax= 0.7 DZ= 10 m	To= −15.0 C Tf= −0.27 C n= 0.40 S= 5 ppt Ks= 4.00 W/mK Q= 60 W/m2 Ax= 0.7 DZ= 10 m
OM1.DAT	OM2.DAT	OM3.DAT

0.00 C FOR 3.000 Ka	0.00 C FOR 5.000 Ka	0.00 C FOR 10.000 Ka
To= −15.0 C Tf= −0.27 C n= 0.40 S= 5 ppt Ks= 4.00 W/mK Q= 60 W/m2 Ax= 0.7 DZ= 10 m	To= −15.0 C Tf= −0.27 C n= 0.40 S= 5 ppt Ks= 4.00 W/mK Q= 60 W/m2 Ax= 0.7 DZ= 10 m	To= −15.0 C Tf= −0.27 C n= 0.40 S= 5 ppt Ks= 4.00 W/mK Q= 60 W/m2 Ax= 0.7 DZ= 10 m
OM4.DAT	OM5.DAT	OM6.DAT

APPENDIX C. Derived curves of permafrost growth during emergence.

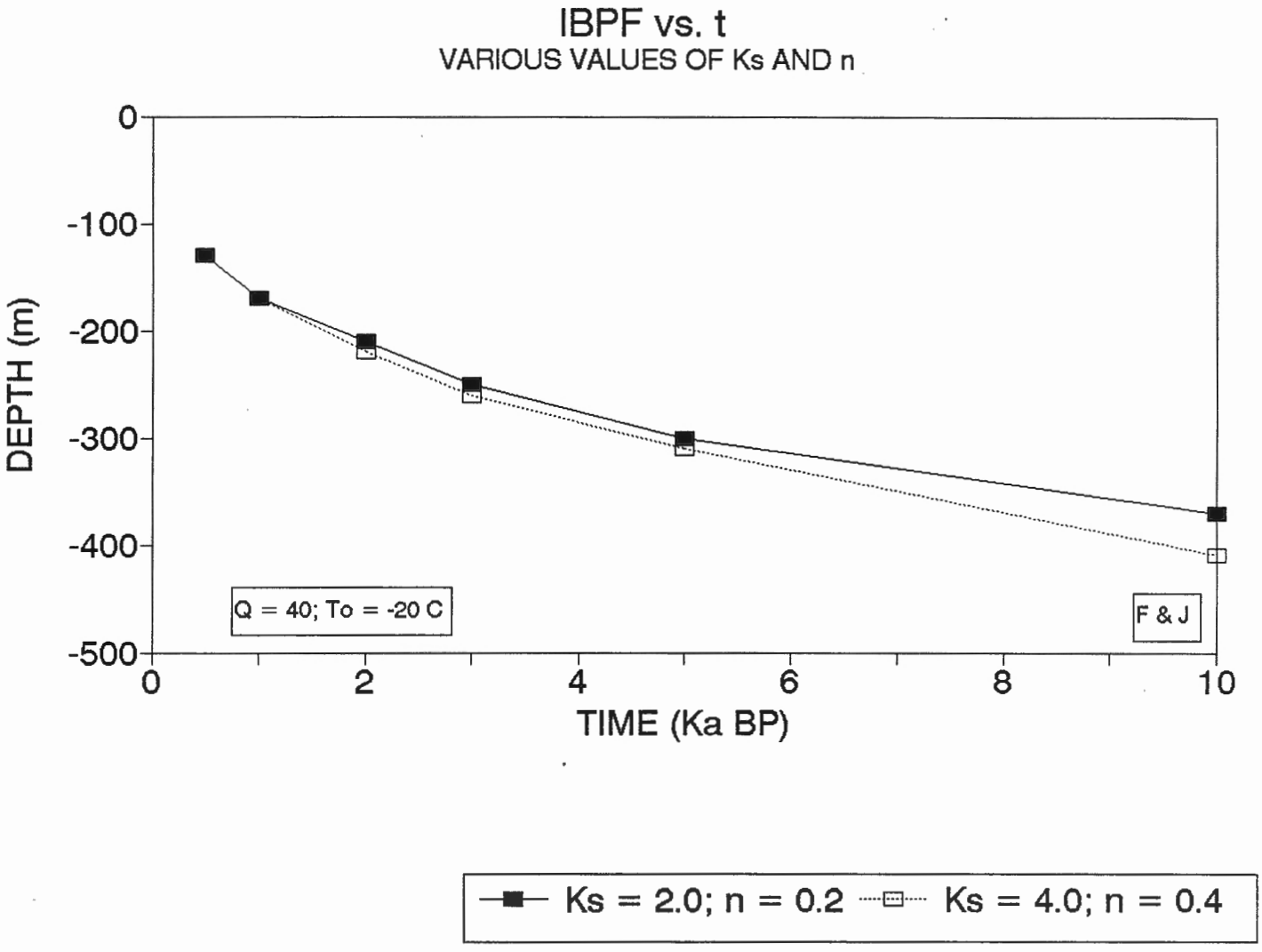
IBPF vs. t
VARIOUS VALUES OF Ks AND n
DEPTH (m)
0
-100
-200
-300
-400
-500
0
2
4
6
8
10
TIME (Ka BP)
Q = 40; To = -20 C
F & J
Ks = 2.0; n = 0.2
Ks = 4.0; n = 0.4

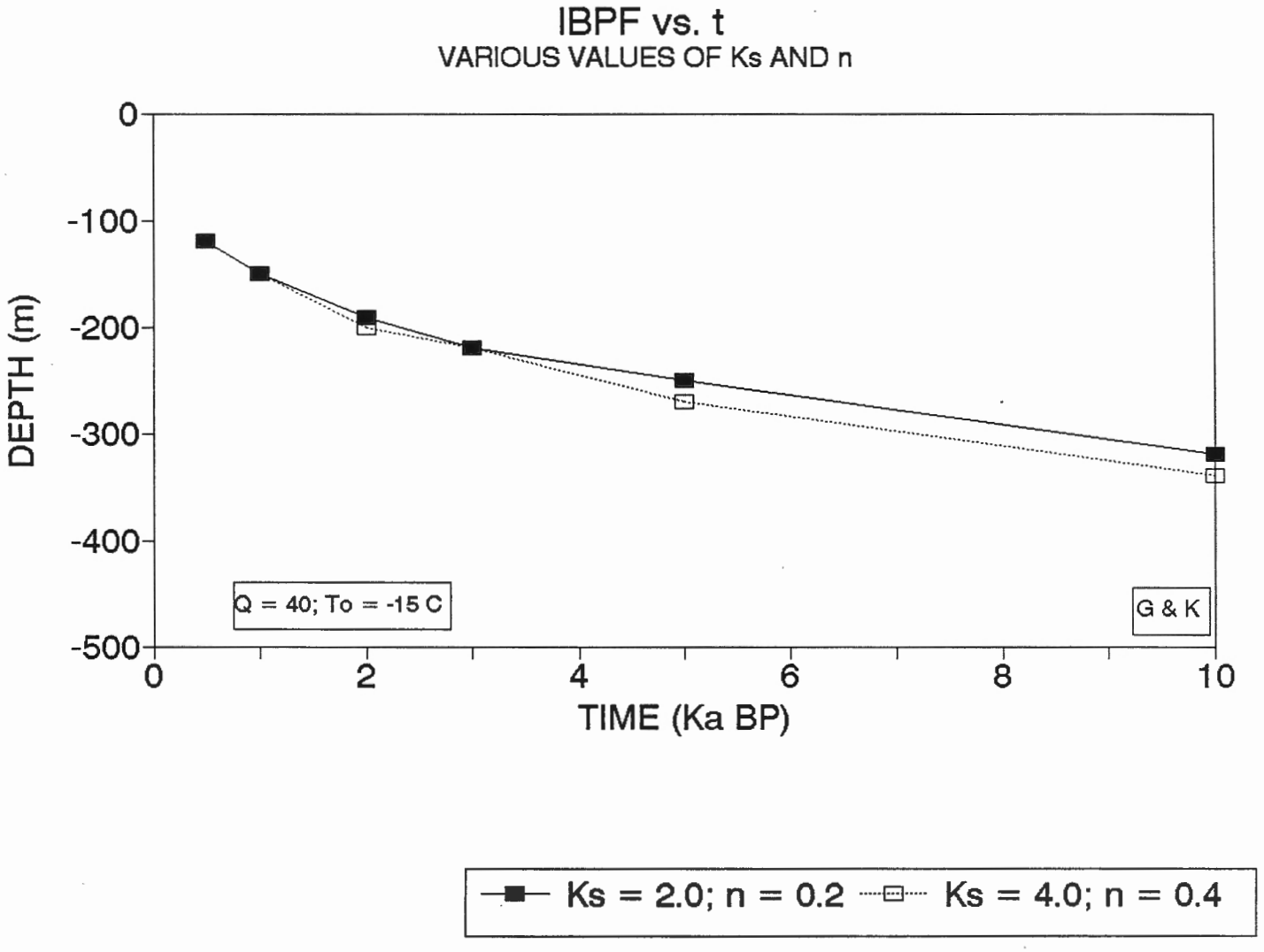
IBPF vs. t
VARIOUS VALUES OF Ks AND n
DEPTH (m)
0
-100
-200
-300
-400
-500
0
2
4
6
8
10
TIME (Ka BP)
Q = 40; To = -15 C
G & K
Ks = 2.0; n = 0.2
Ks = 4.0; n = 0.4

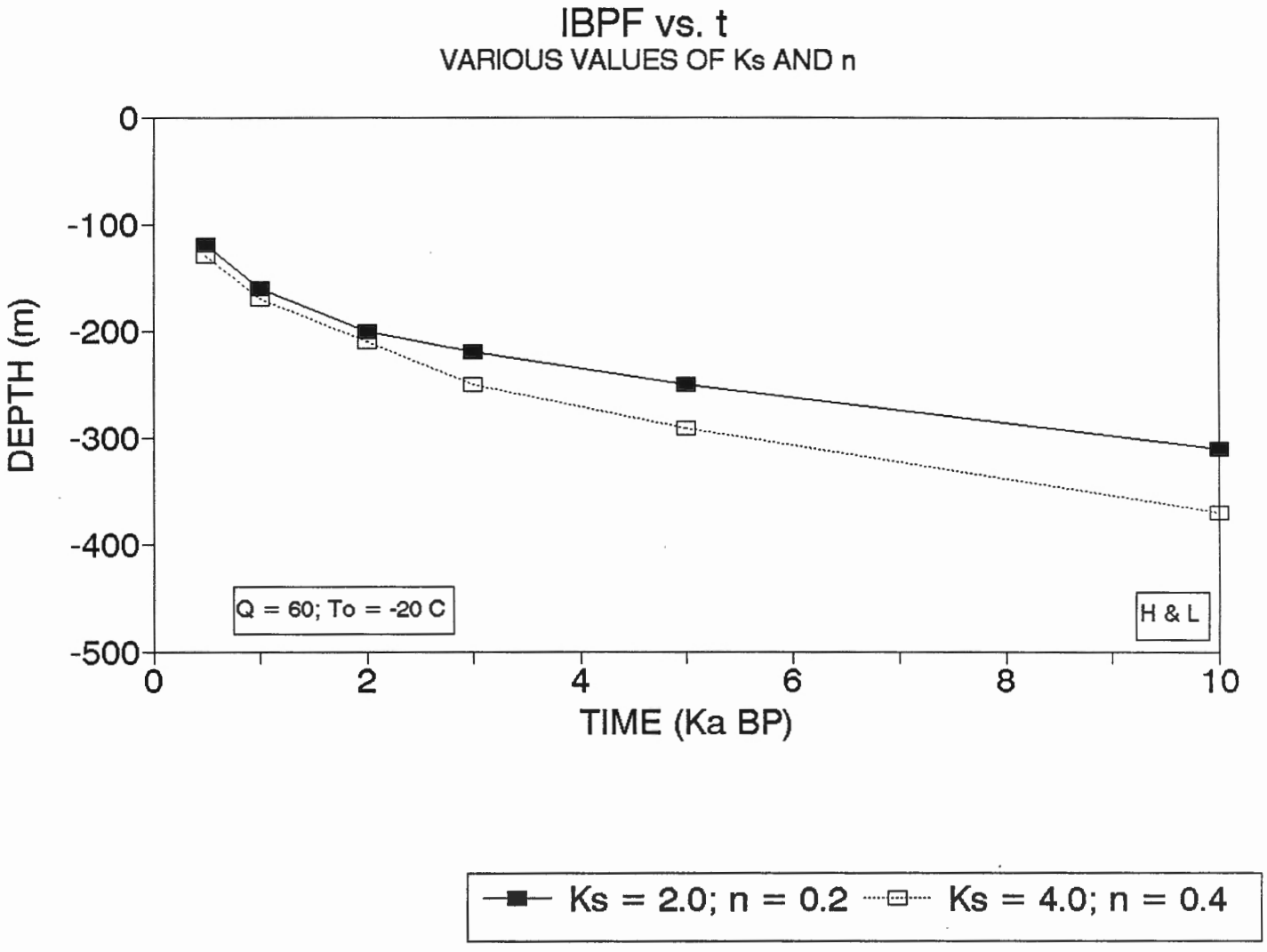
IBPF vs. t
VARIOUS VALUES OF Ks AND n
0
-100
-200
-300
-400
-500
DEPTH (m)
0
2
4
6
8
10
TIME (Ka BP)
Q = 60; To = -20 C
H & L
Ks = 2.0; n = 0.2
Ks = 4.0; n = 0.4

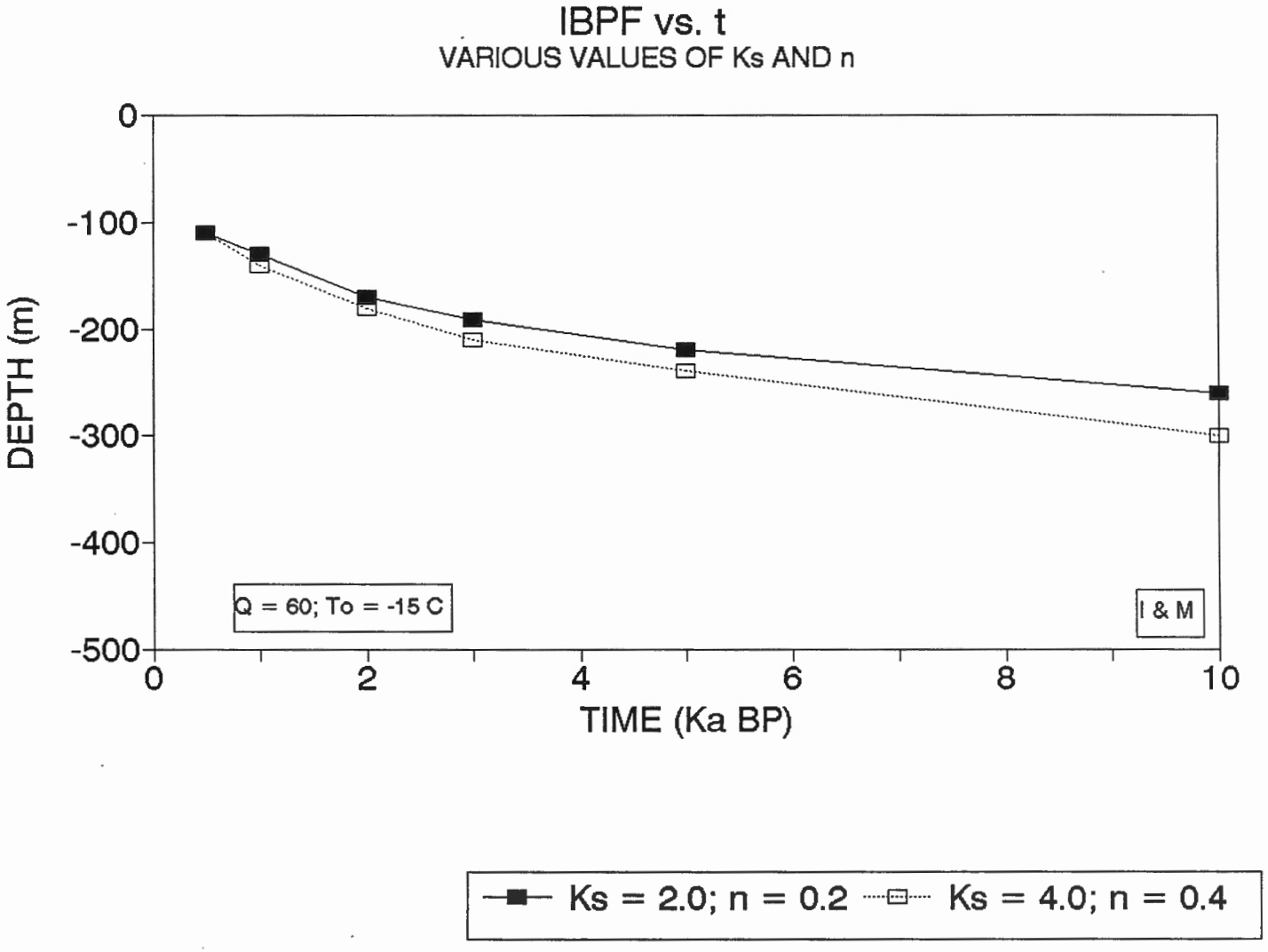
IBPF vs. t
VARIOUS VALUES OF Ks AND n
DEPTH (m)
0
-100
-200
-300
-400
-500
0
2
4
6
8
10
TIME (Ka BP)
Q = 60; To = -15 C
I & M
Ks = 2.0; n = 0.2
Ks = 4.0; n = 0.4

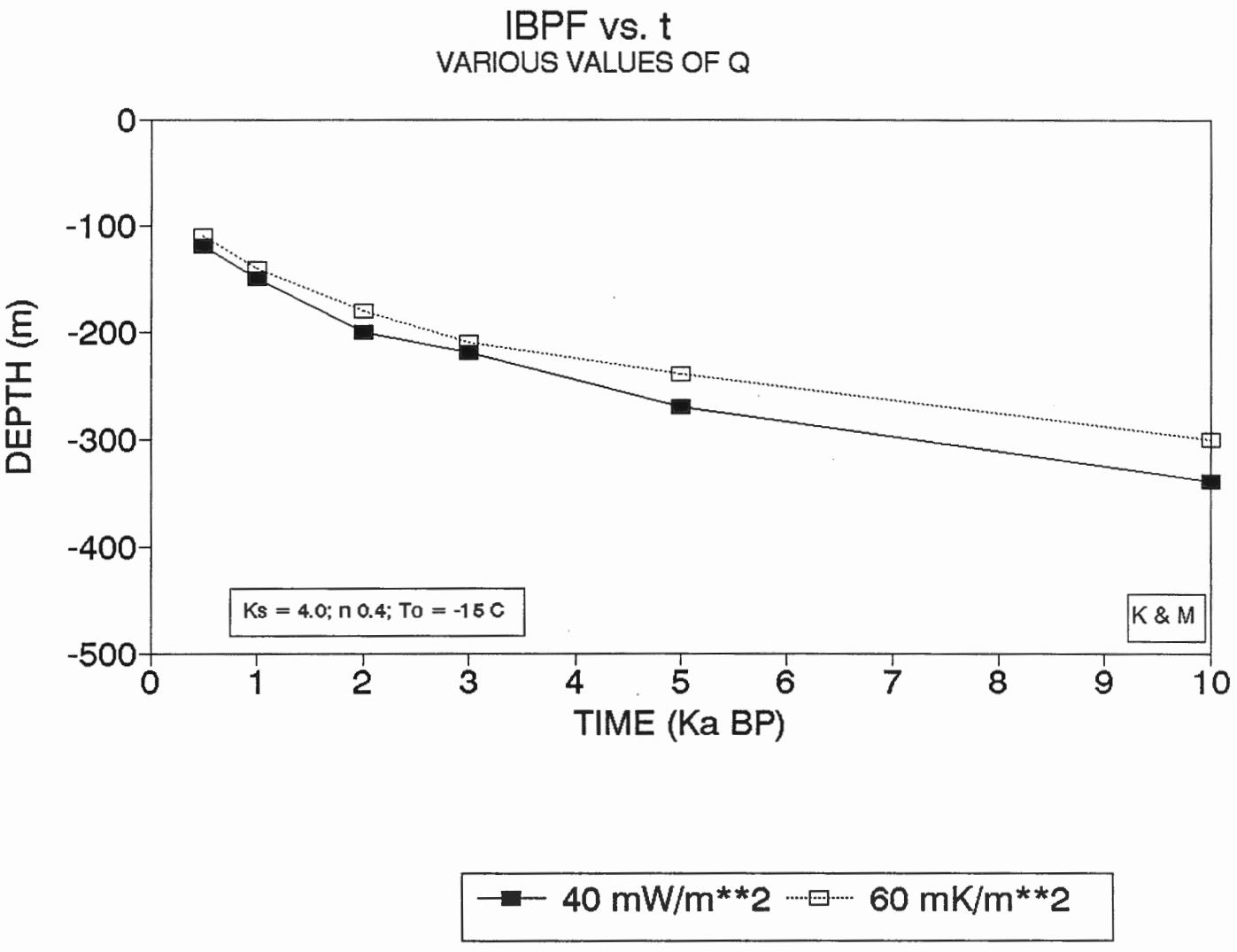
IBPF vs. t
VARIOUS VALUES OF Q
DEPTH (m)
0
-100
-200
-300
-400
-500
0
1
2
3
4
5
6
7
8
9
10
TIME (Ka BP)
Ks = 4.0; n 0.4; To = -1.5 C
K & M
40 mW/m**2
60 mK/m**2

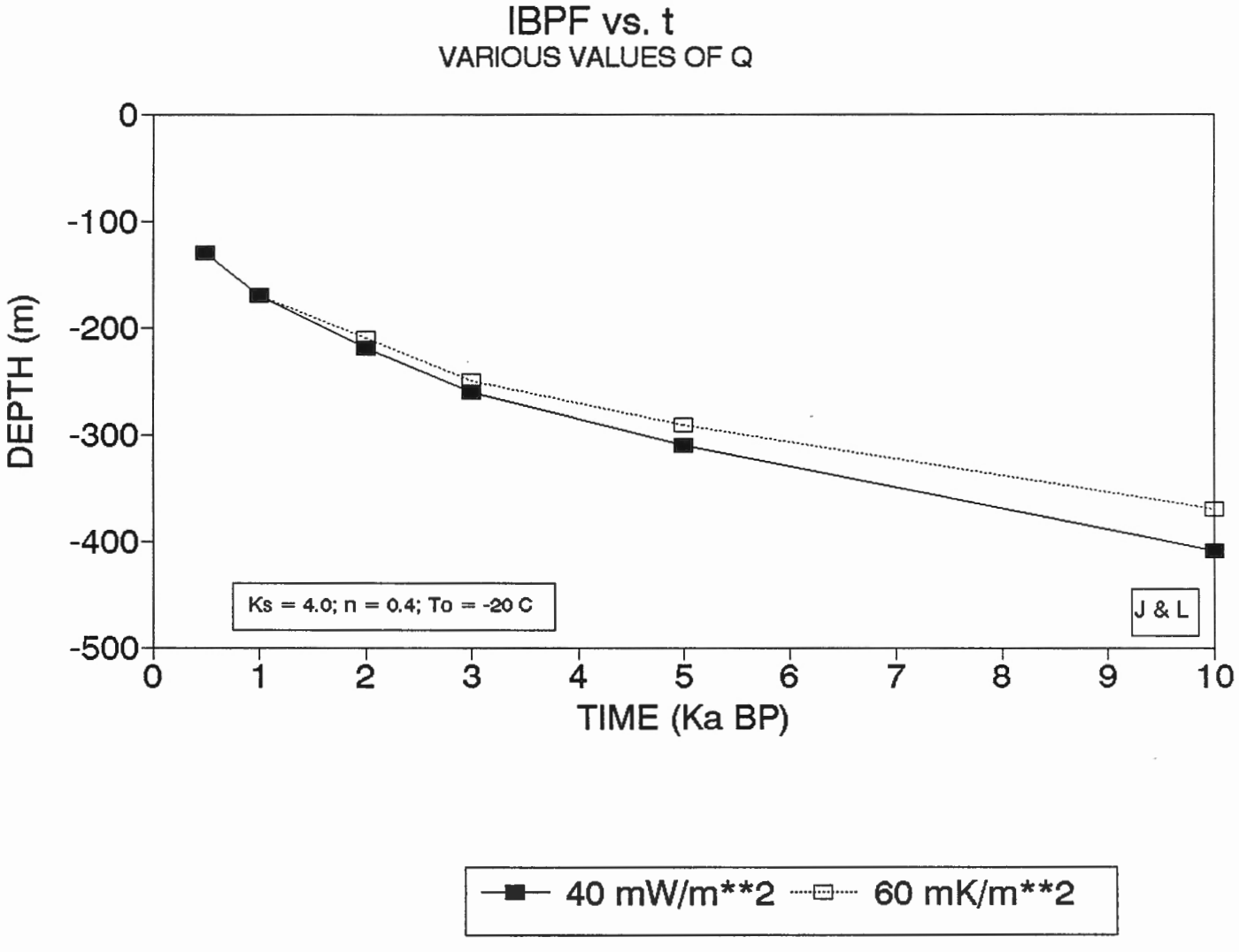
IBPF vs. t
VARIOUS VALUES OF Q
DEPTH (m)
0
-100
-200
-300
-400
-500
0
1
2
3
4
5
6
7
8
9
10
TIME (Ka BP)
Ks = 4.0; n = 0.4; To = -20 C
J & L
40 mW/m**2
60 mK/m**2

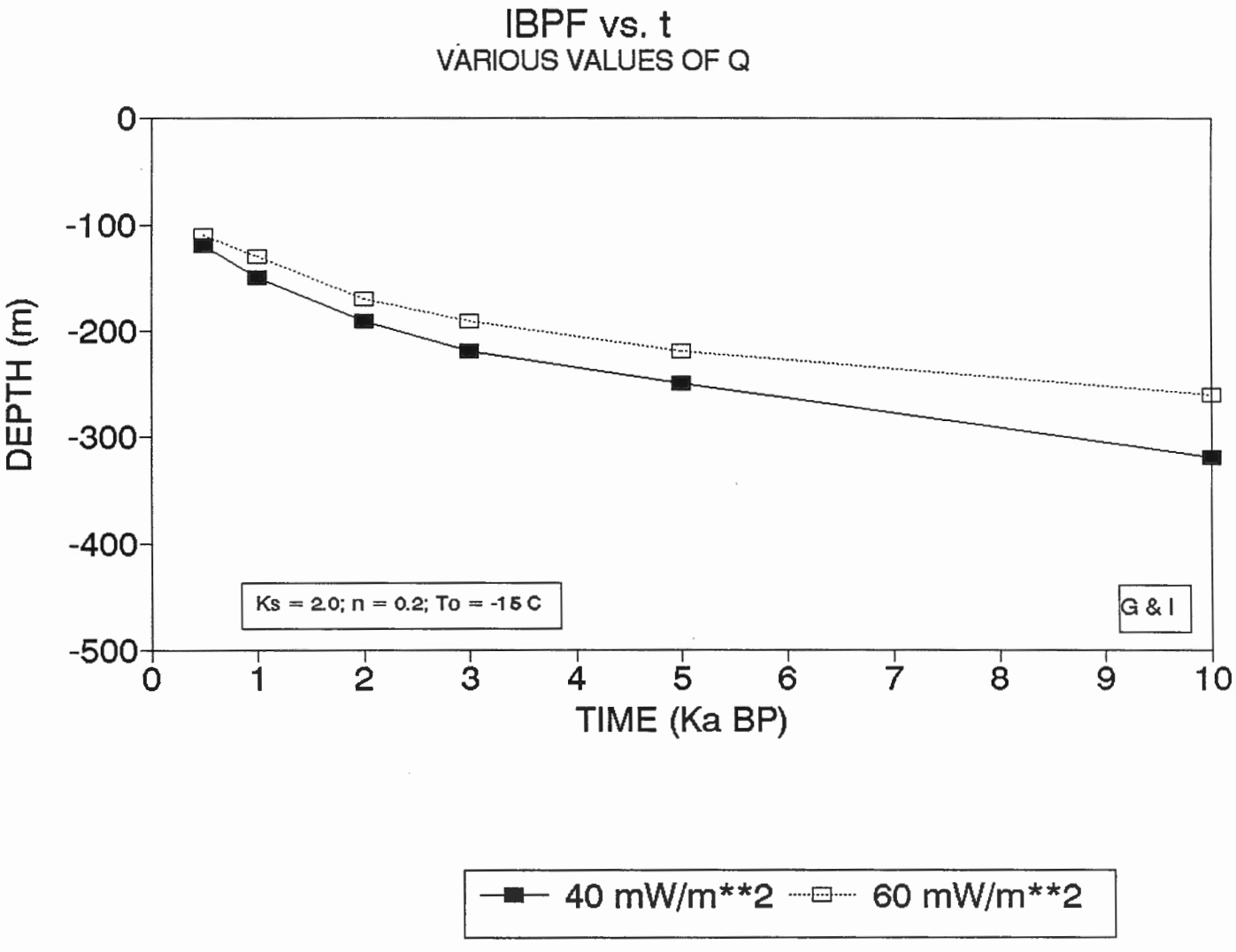
IBPF vs. t
VARIOUS VALUES OF Q
DEPTH (m)
0
-100
-200
-300
-400
-500
0
1
2
3
4
5
6
7
8
9
10
TIME (Ka BP)
Ks = 2.0; n = 0.2; To = -1.5 C
G & I
40 mW/m**2
60 mW/m**2

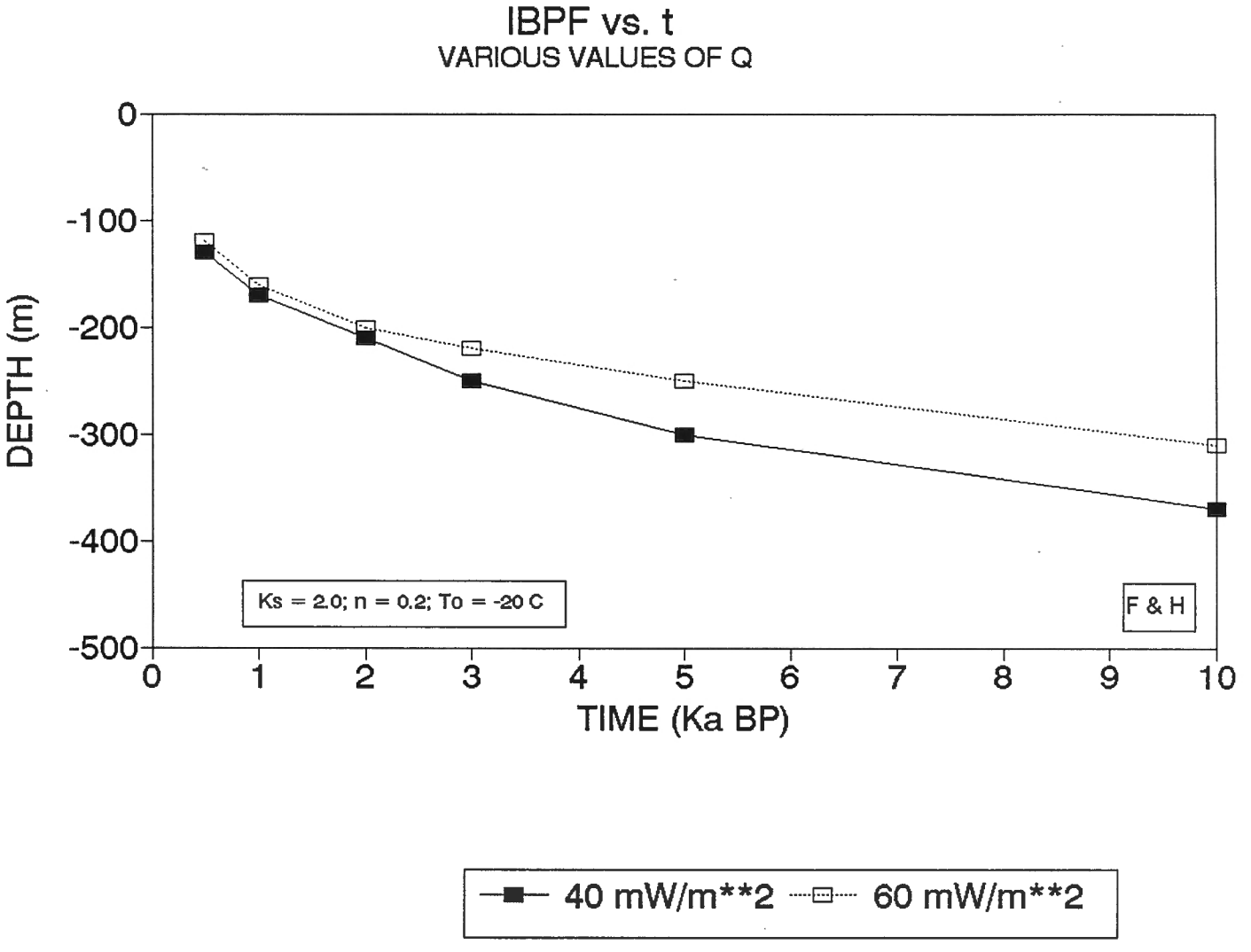
IBPF vs. t
VARIOUS VALUES OF Q
DEPTH (m)
0
-100
-200
-300
-400
-500
0
1
2
3
4
5
6
7
8
9
10
TIME (Ka BP)
Ks = 2.0; n = 0.2; To = -20 C
F & H
40 mW/m**2
60 mW/m**2

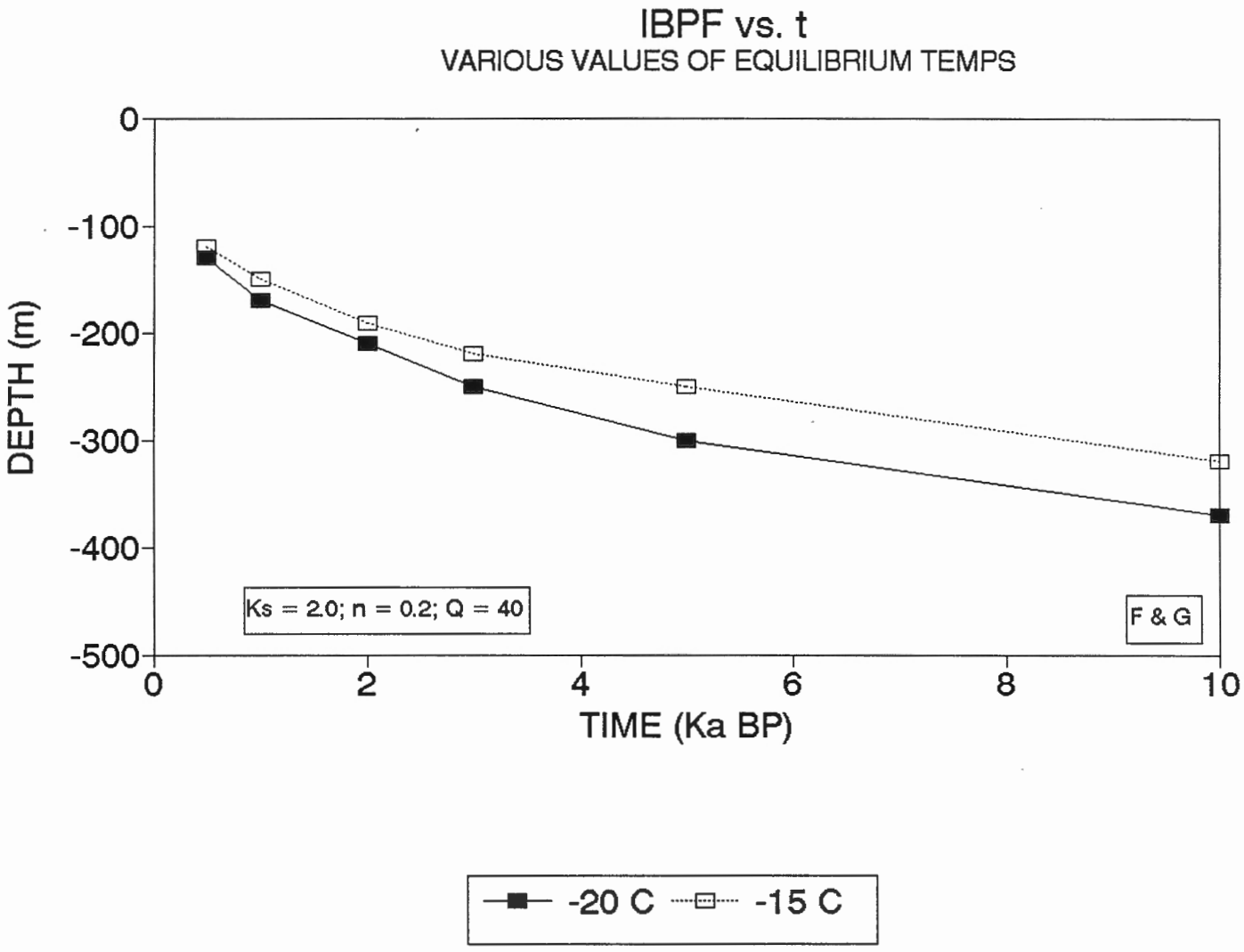
IBPF vs. t
VARIOUS VALUES OF EQUILIBRIUM TEMPS
DEPTH (m)
0
-100
-200
-300
-400
-500
0
2
4
6
8
10
TIME (Ka BP)
Ks = 2.0; n = 0.2; Q = 40
F & G
-20 C
-15 C

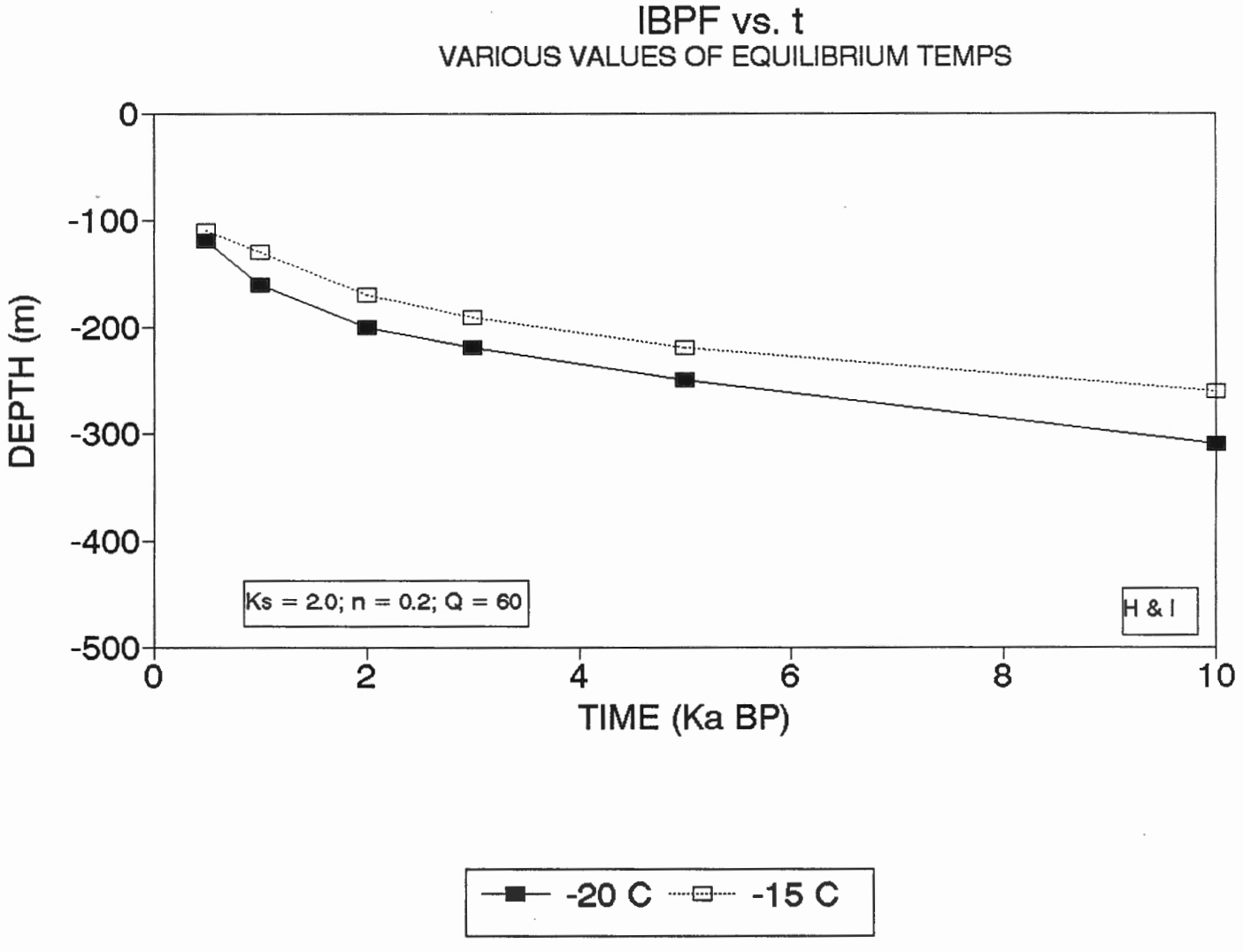
IBPF vs. t
VARIOUS VALUES OF EQUILIBRIUM TEMPS
DEPTH (m)
0
-100
-200
-300
-400
-500
0
2
4
6
8
10
TIME (Ka BP)
Ks = 2.0; n = 0.2; Q = 60
H & I
-20 C
-15 C

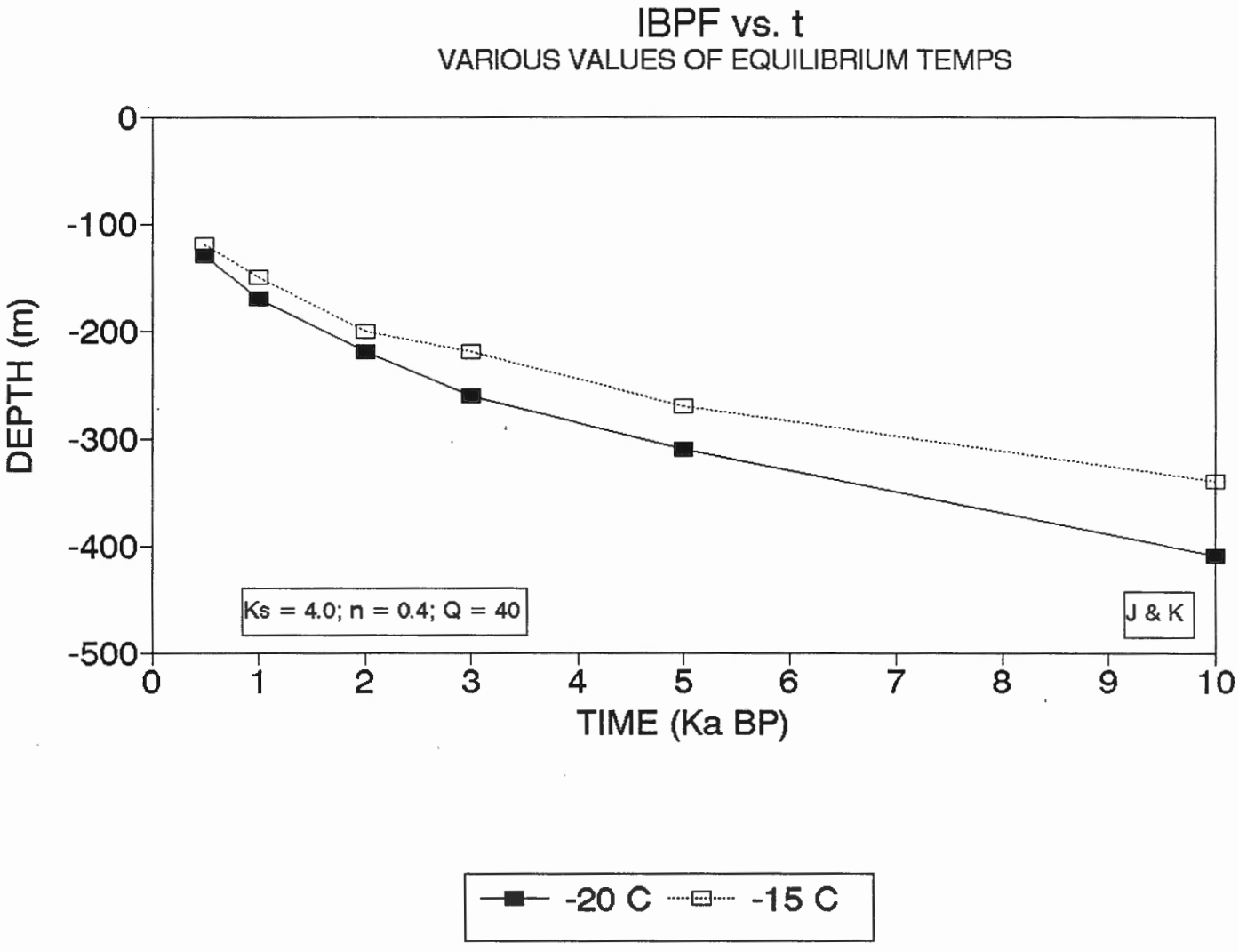
IBPF vs. t
VARIOUS VALUES OF EQUILIBRIUM TEMPS
DEPTH (m)
0
-100
-200
-300
-400
-500
0
1
2
3
4
5
6
7
8
9
10
TIME (Ka BP)
Ks = 4.0; n = 0.4; Q = 40
J & K
-20 C
-15 C

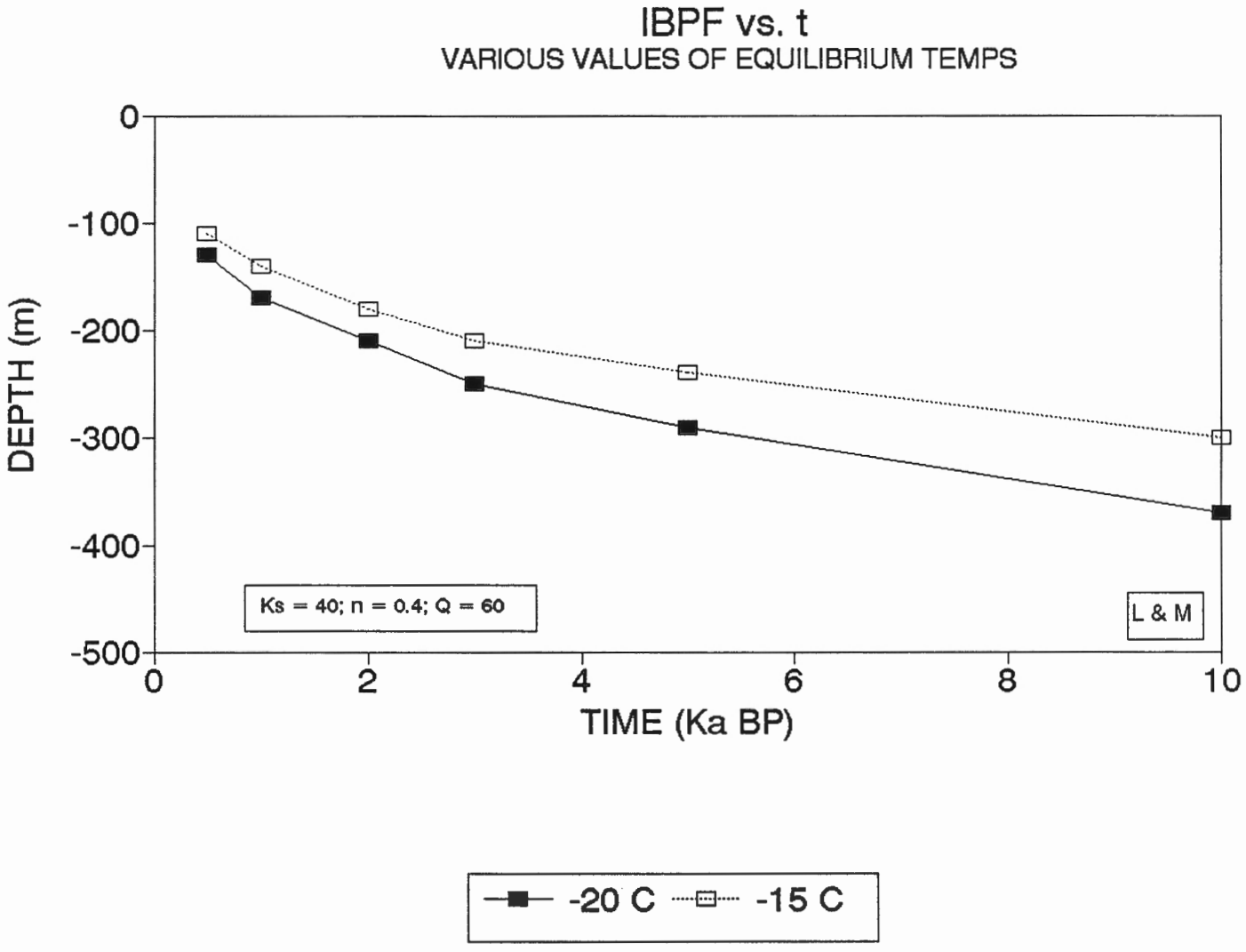
IBPF vs. t
VARIOUS VALUES OF EQUILIBRIUM TEMPS
DEPTH (m)
0
-100
-200
-300
-400
-500
0
2
4
6
8
10
TIME (Ka BP)
Ks = 40; n = 0.4; Q = 60
L & M
-20 C
-15 C

APPENDIX D. Derived curves of permafrost degradation following marine transgression.

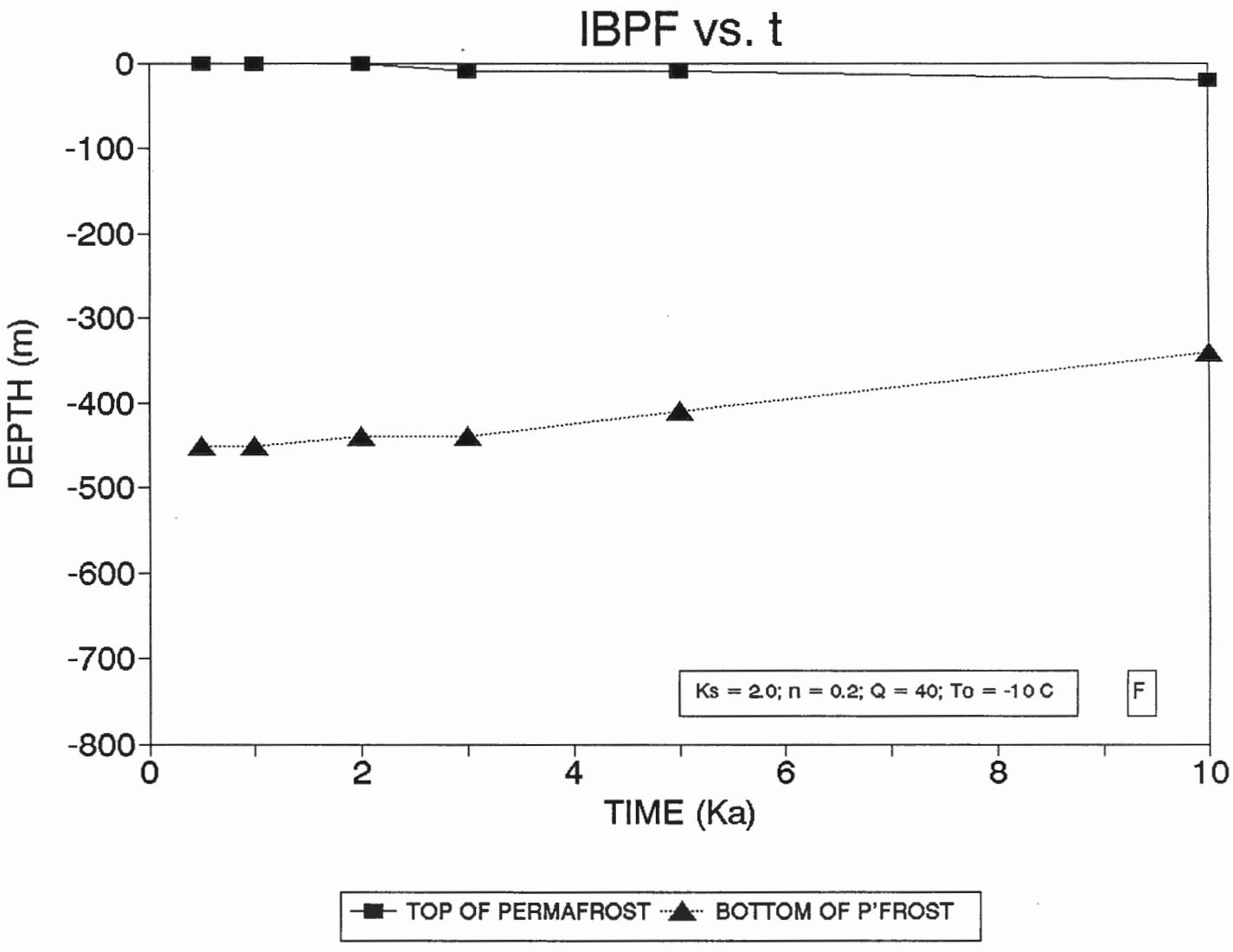
IBPF vs. t
0
-100
-200
-300
-400
-500
-600
-700
-800
DEPTH (m)
0
2
4
6
8
10
TIME (Ka)
Ks = 2.0; n = 0.2; Q = 40; To = -1.0 C
F
TOP OF PERMAFROST
BOTTOM OF P'FROST

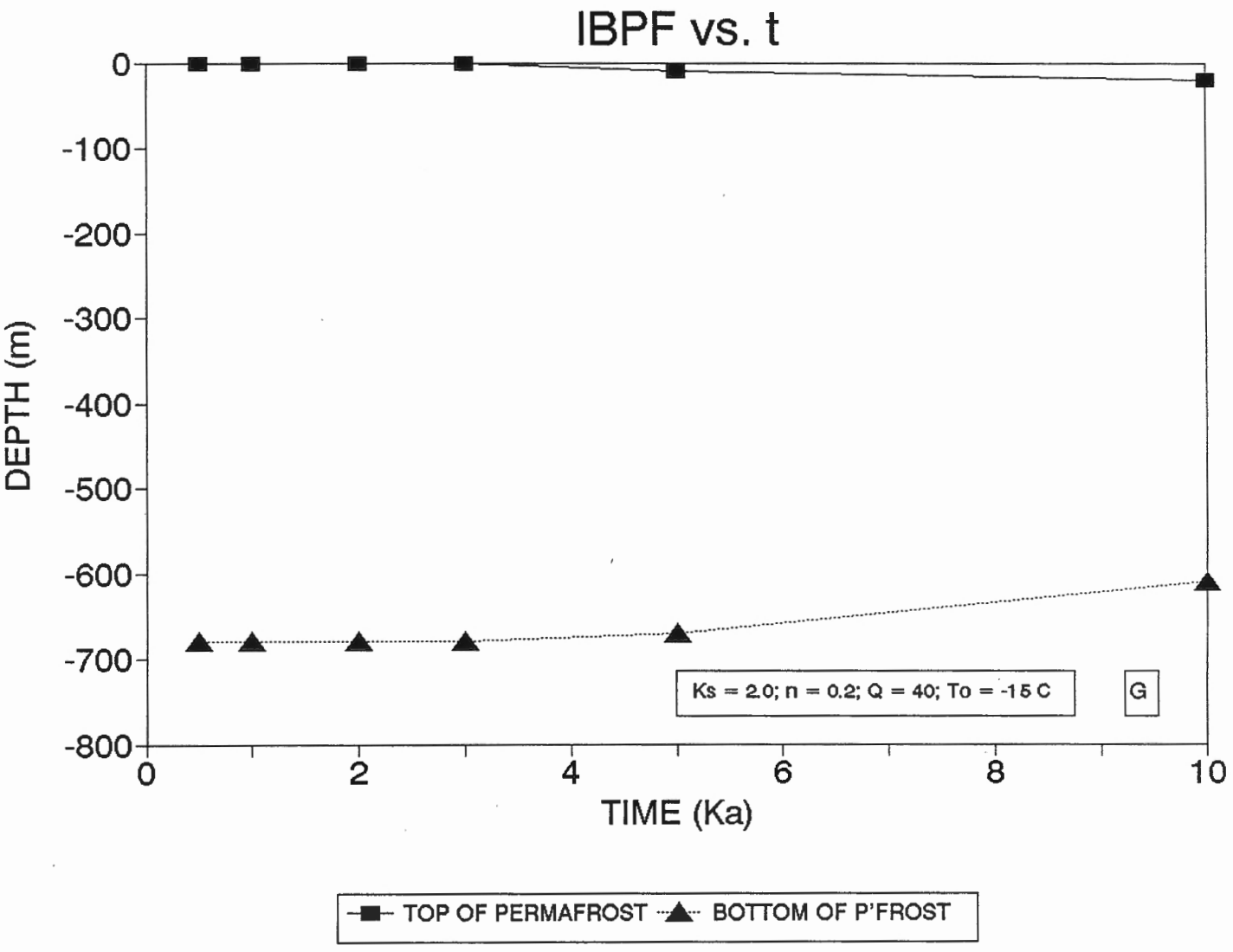
IBPF vs. t
0
-100
-200
-300
-400
-500
-600
-700
-800
DEPTH (m)
0
2
4
6
8
10
TIME (Ka)
Ks = 2.0; n = 0.2; Q = 40; To = -1.5 C
G
TOP OF PERMAFROST
BOTTOM OF P'FROST

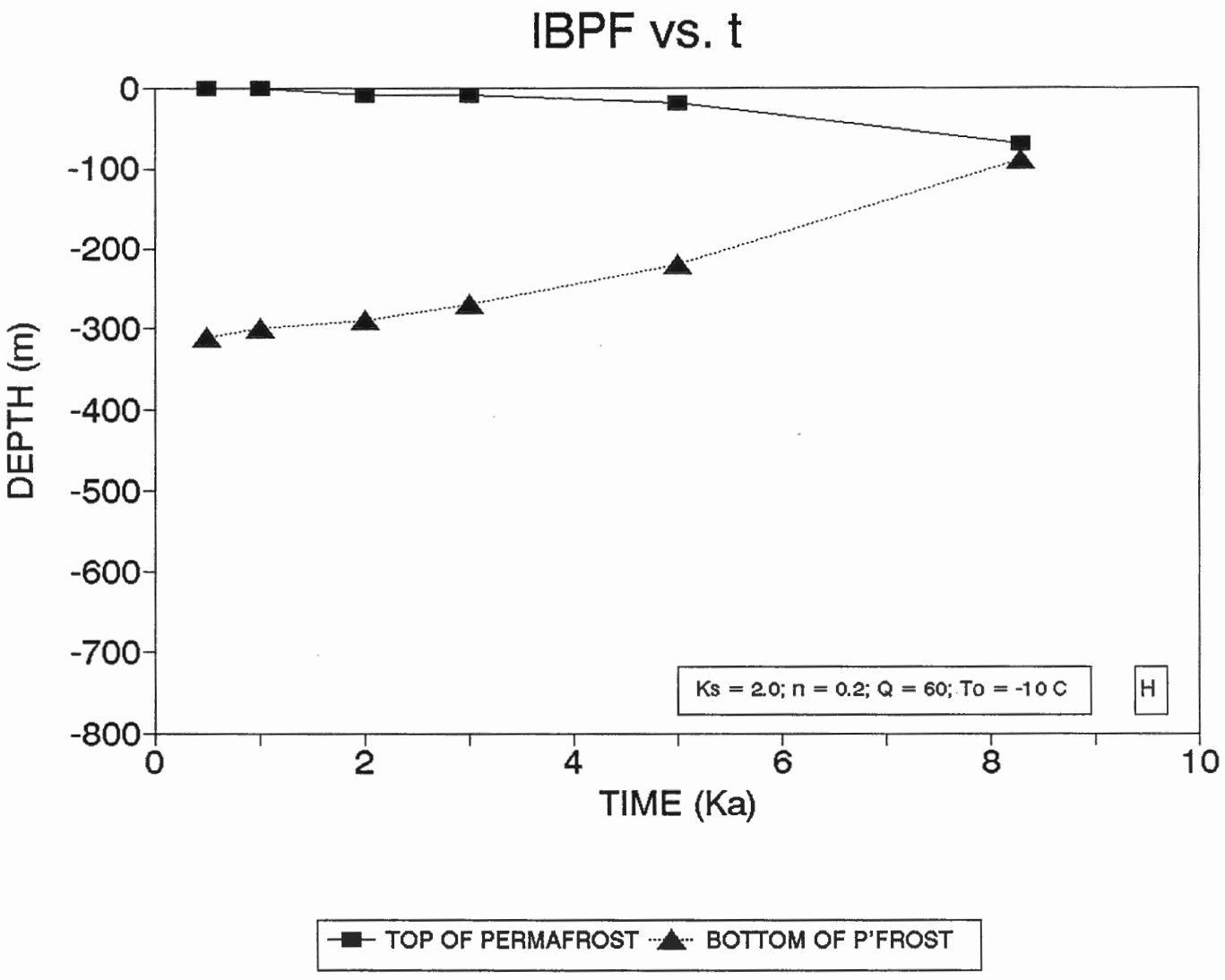
IBPF vs. t
0
-100
-200
-300
-400
-500
-600
-700
-800
DEPTH (m)
0
2
4
6
8
10
TIME (Ka)
Ks = 2.0; n = 0.2; Q = 60; To = -10 C
H
TOP OF PERMAFROST
BOTTOM OF P'FROST

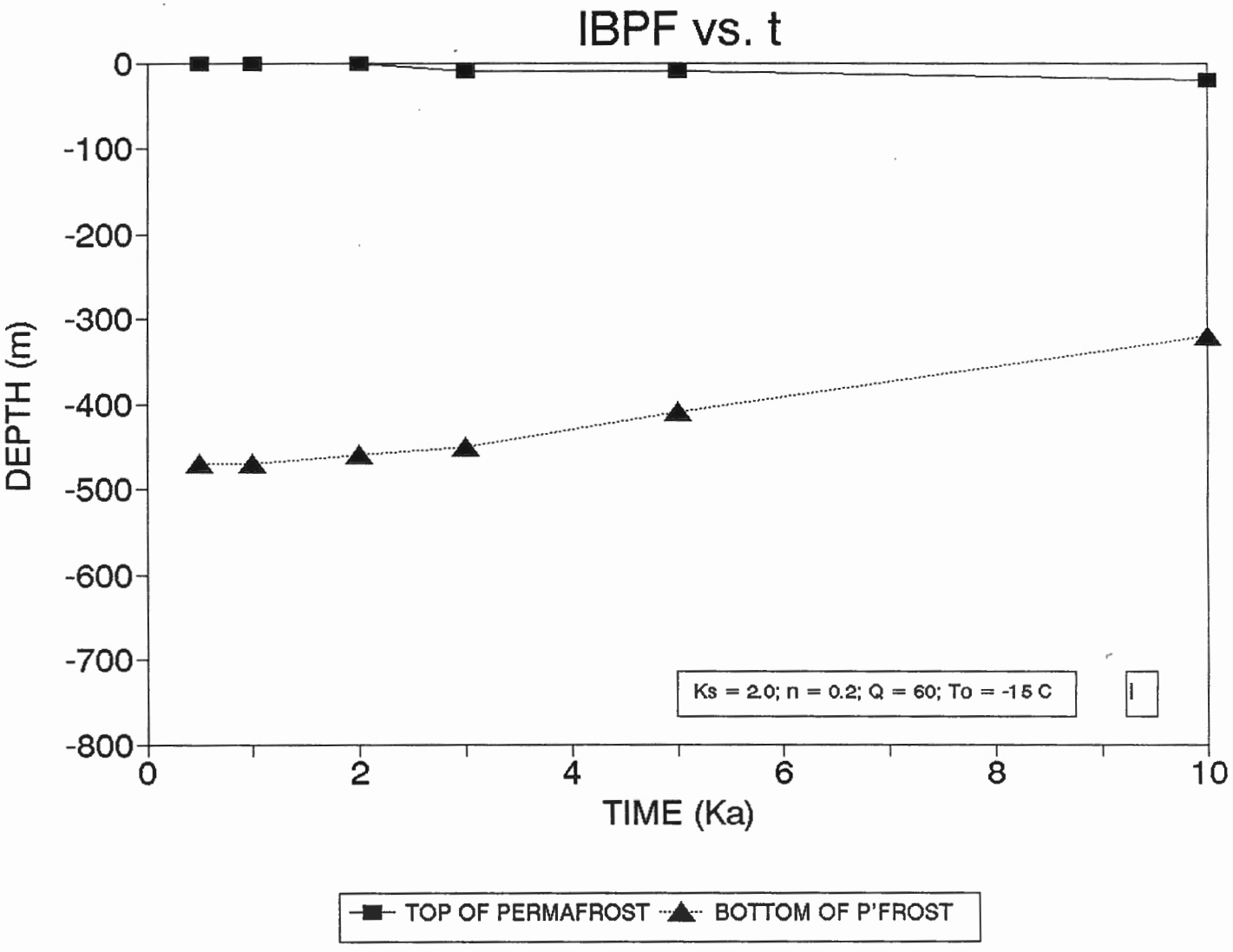
IBPF vs. t
0
-100
-200
-300
-400
-500
-600
-700
-800
DEPTH (m)
0
2
4
6
8
10
TIME (Ka)
Ks = 2.0; n = 0.2; Q = 60; To = -1.5 C
TOP OF PERMAFROST
BOTTOM OF P'FROST

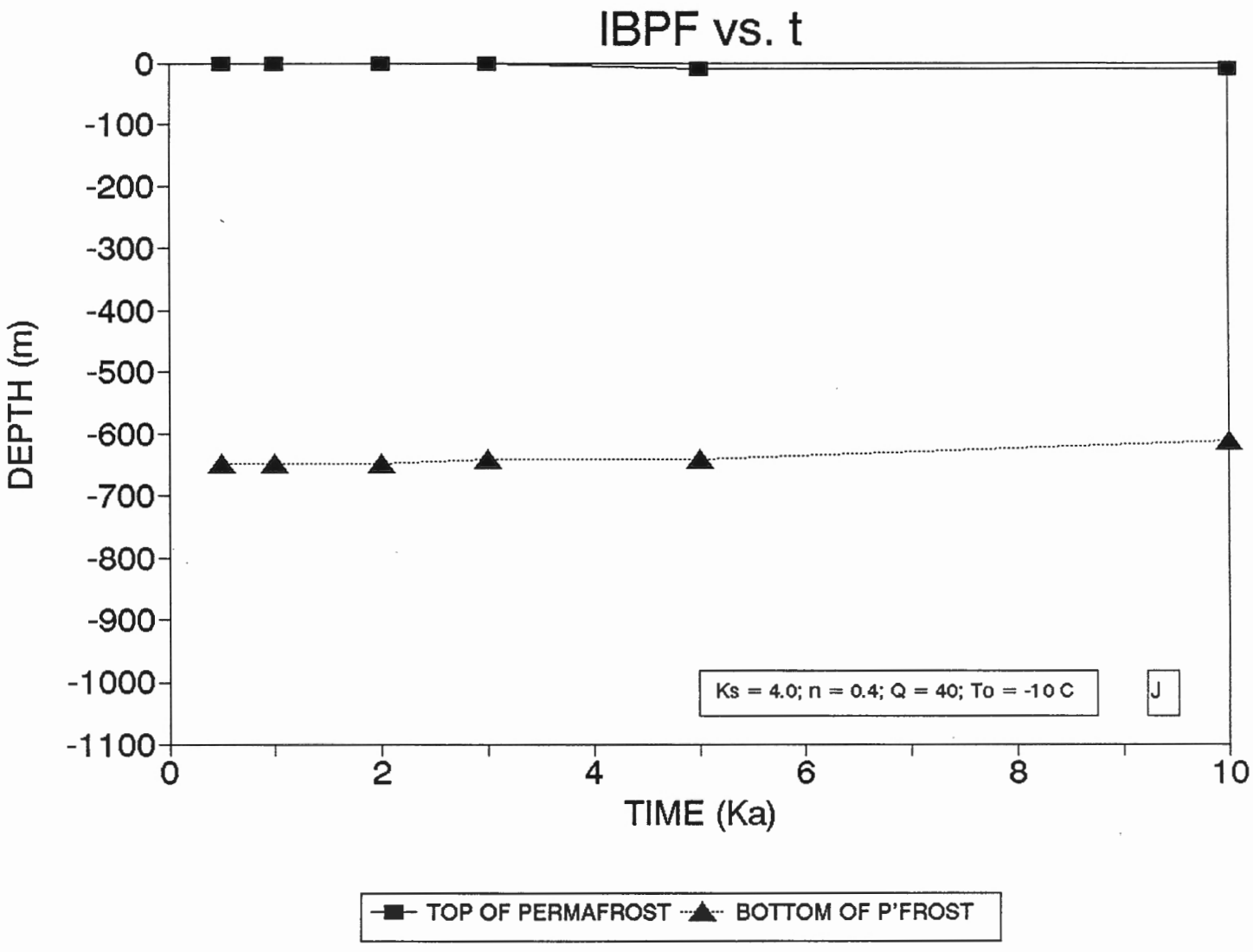
IBPF vs. t
DEPTH (m)
0
-100
-200
-300
-400
-500
-600
-700
-800
-900
-1000
-1100
0
2
4
6
8
10
TIME (Ka)
Ks = 4.0; n = 0.4; Q = 40; To = -10 C
J
TOP OF PERMAFROST
BOTTOM OF P'FROST

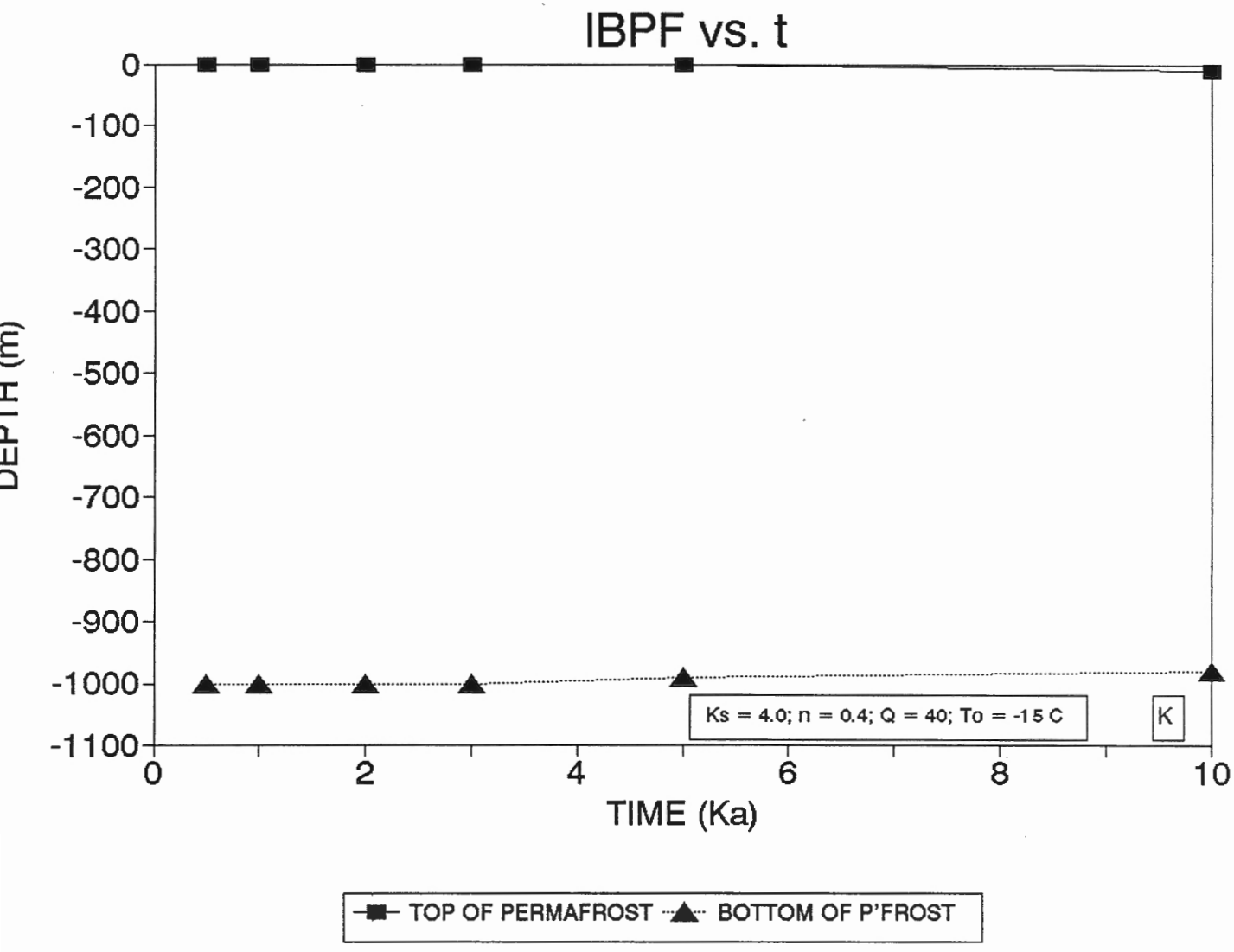
IBPF vs. t
0
-100
-200
-300
-400
-500
-600
-700
-800
-900
-1000
-1100
DEPTH (m)
0
2
4
6
8
10
TIME (Ka)
Ks = 4.0; n = 0.4; Q = 40; To = -1.5 C
K
TOP OF PERMAFROST
BOTTOM OF P'FROST

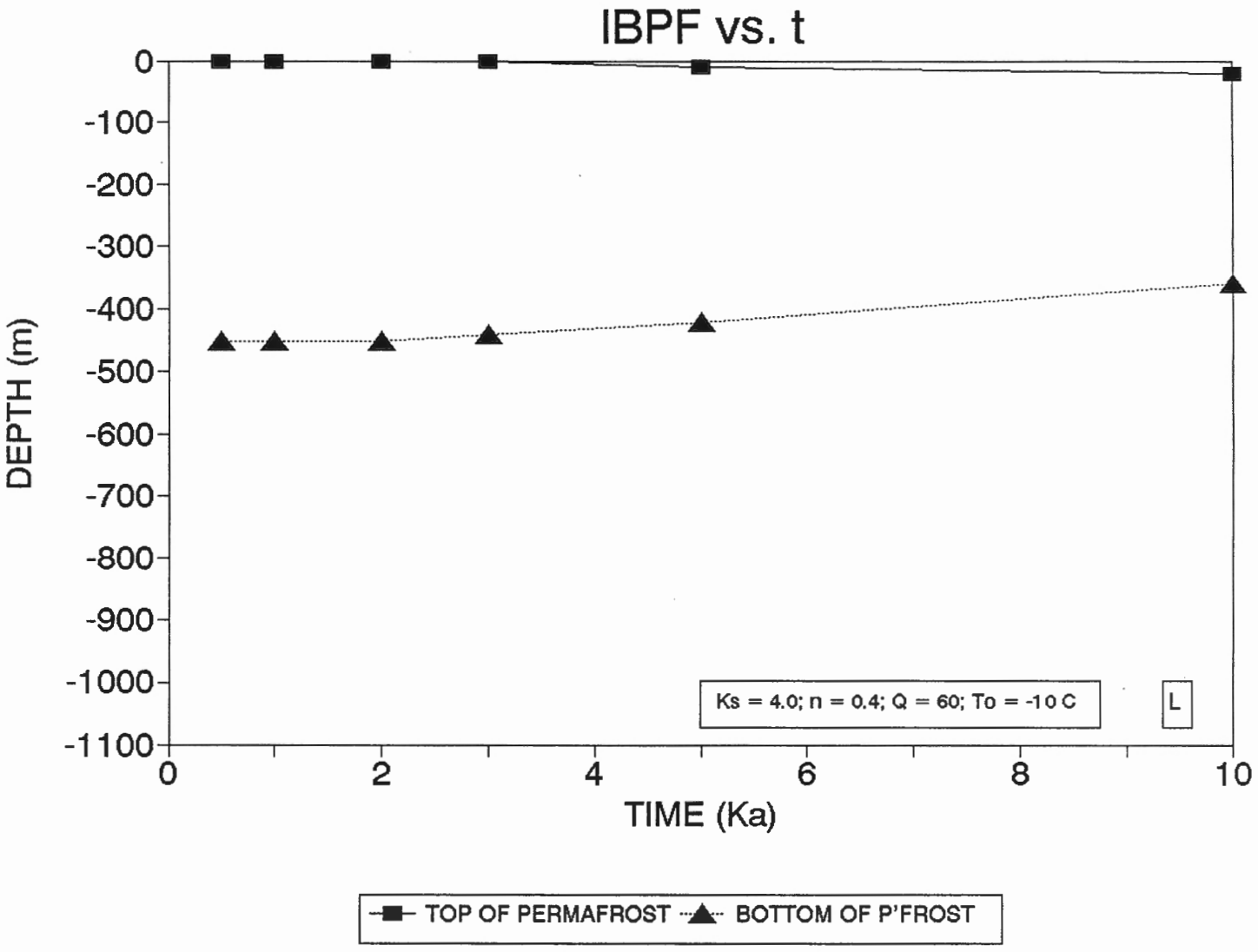
IBPF vs. t
0
-100
-200
-300
-400
-500
-600
-700
-800
-900
-1000
-1100
DEPTH (m)
0
2
4
6
8
10
TIME (Ka)
Ks = 4.0; n = 0.4; Q = 60; To = -10 C
L
TOP OF PERMAFROST
BOTTOM OF P'FROST

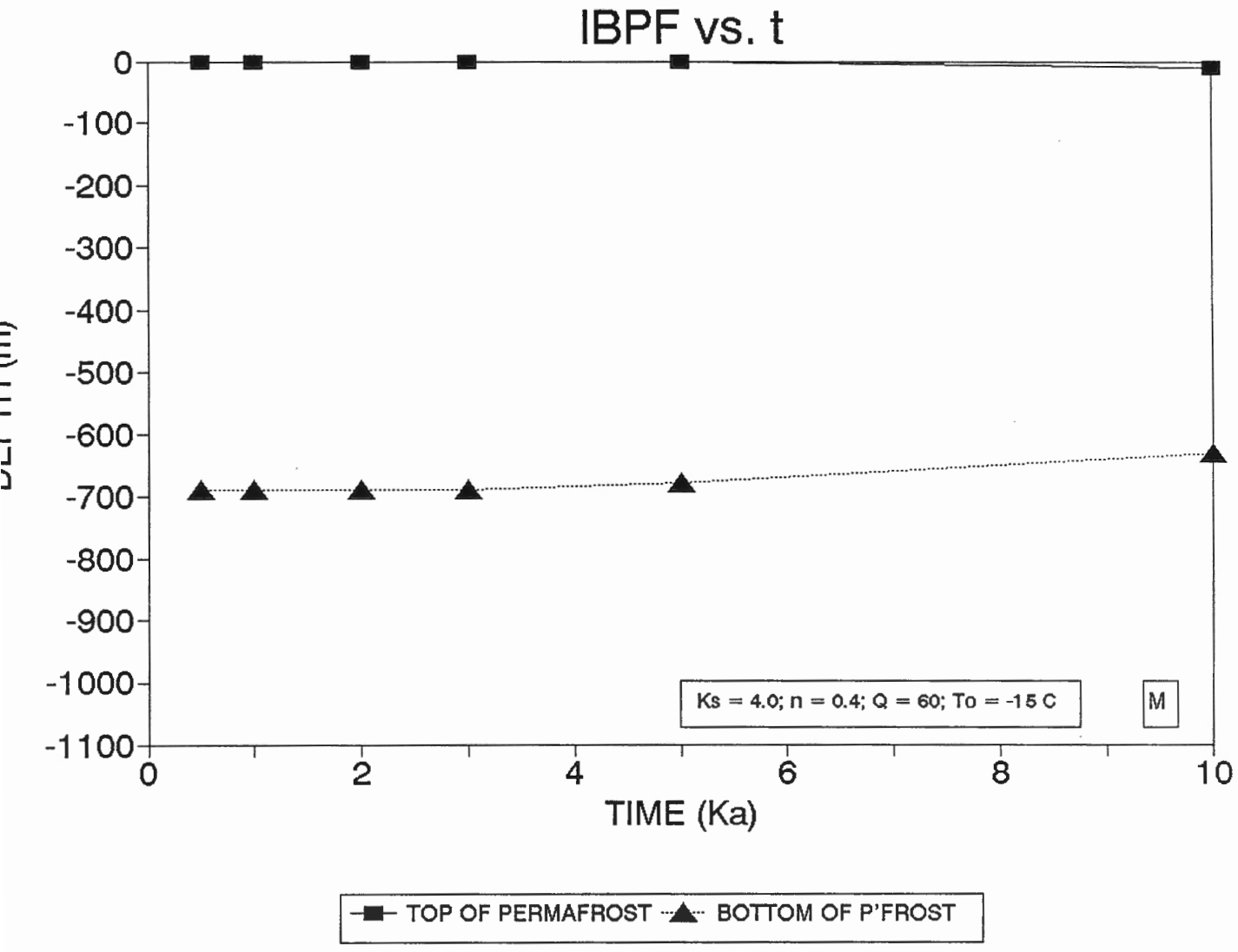
IBPF vs. t
0
-100
-200
-300
-400
-500
-600
-700
-800
-900
-1000
-1100
0
2
4
6
8
10
TIME (Ka)
Ks = 4.0; n = 0.4; Q = 60; To = -15 C
M
TOP OF PERMAFROST
BOTTOM OF P'FROST

APPENDIX E. Description of Outcalt's thermal diffusion equation
(a review written by Al Taylor)

Numeric mode

Outcalt (1985) uses a numerical implementation of the thermal diffusion equation to predict the general nature of temperature profiles noted in early observations of the deep permafrost of the Canadian Beaufort Shelf.

$$\frac{dT}{dt} = \frac{1}{C}\frac{d}{dz}\left\{ K \frac{dT}{dz} \right\} + f(L) \qquad (1)$$

T, t, z, K, C and L are the temperature, time, depth and thermal conductivity and volumetric sensible and latent heats, respectively. The method uses a one-dimensional finite difference technique, first to establish an equilibrium temperature profile consistent with the terrestrial heat flux and average thermal properties and then to generate subsurface temperature profiles according to a model of hypothesized past changes in surface temperatures. The program has been modified subsequently from the 1985 version to accommodate 420 depth nodes (e.g. 4 km at 10m increments), variable salinity (Wawrow, 1993) and a user-defined phase composition curve.

Constitutive relations

Physical properties of the ground are determined in the program as follows. The volume fraction occupied by pore space, X_p, is partitioned as

$$X_p = X_w + X_i \qquad (2)$$

where X_w and X_i are the volume fractions of liquid water and ice, respectively. The freezing point T_f based on salinity S (ppt) is

$$T_f = -54.11S/(1000-S) \qquad (3)$$

Thus

$$X_w = X_p \qquad T > T_f,$$

and

$$X_w = X_p * W$$
$$X_i = X_p - X_w \qquad T < T_f \qquad (4)$$

The phase composition curve W may be defined as simple exponential functions as in Outcalt (1985) or Nixon (1986), or as a functional relation derived from data. In this work, we assume

$$W = \exp[A_x(T - T_f)]$$

where A_x is 0.7, typical of silts (see Fig. E.1)
The average thermal conductivity K and volumetric heat capacity C at any depth node are calculated from the constitutive relations for the three material species, the dry solid component, water and ice (subscripts s, w and i, respectively).

$$K = K_s^{Xs} * K_w^{Xw} * K_i^{Xi} \qquad (5)$$

$$C = C_s * X_s + C_w * X_w + C_i * X_i + F \qquad (6)$$

F is the latent heat component of volumetric heat capacity.

$$F = 0; \qquad T > T_f,$$

$$F = X_w * L * A_x \qquad T < T_f \qquad (7)$$

The thermal diffusivity is

$$D = K/C \qquad (8)$$

The program was verified by comparision with modelled profiles for the Beaufort Shelf undertaken by Geo-engineering Ltd. (1990) using a recent version of Nixon's (1986) geothermal simulator. Also, the depth of phase change predicted by the program was compared with the Neumann theory (section 10.3 in Ingersoll et al., 1954). It is worth emphasizing here that model results for a particular problem are very sensitive to the shape of the phase composition curve that is employed (here A_x), since this governs the amount of latent heat that is active as temperatures change in time.

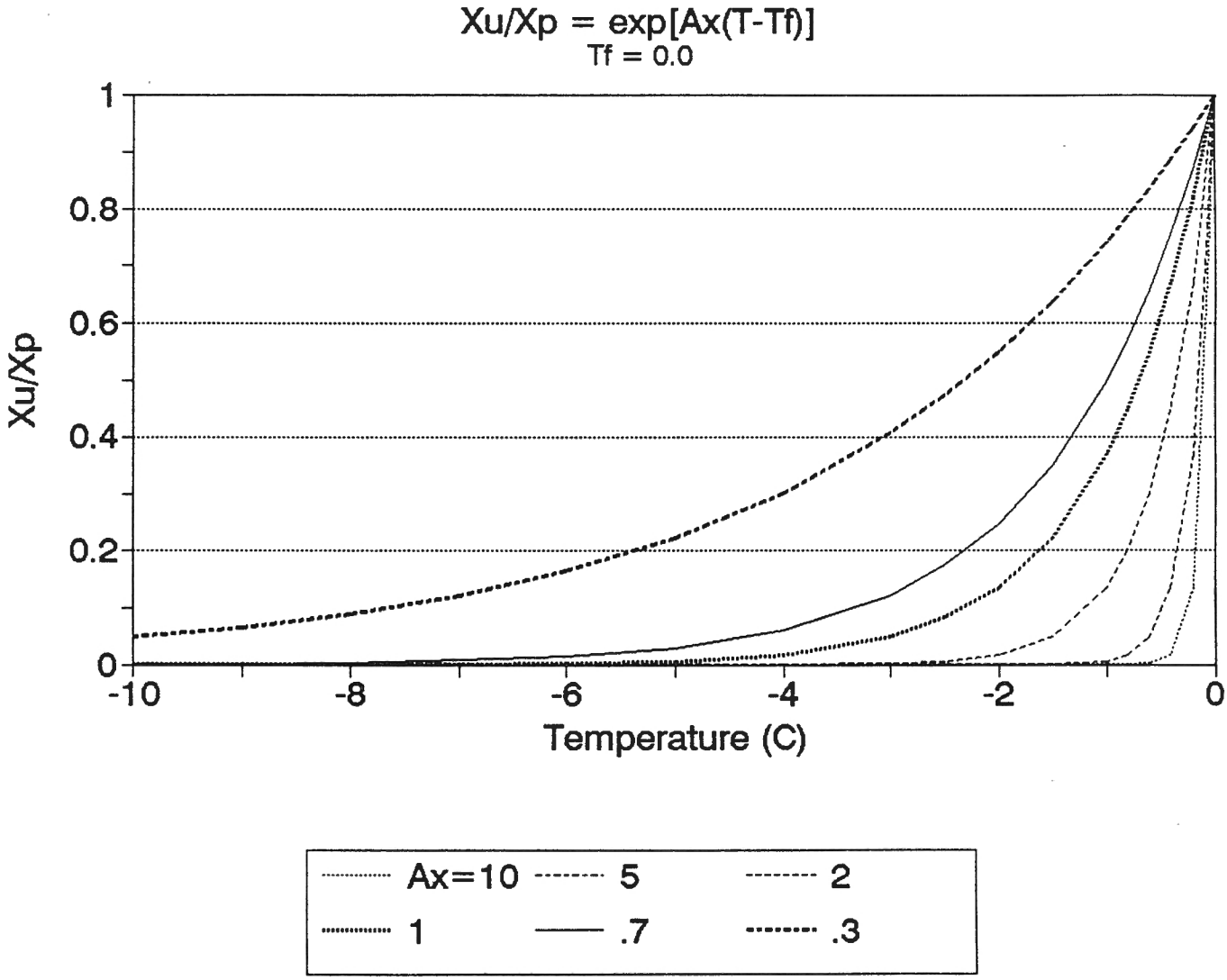

Fig E.1 Unfrozen water content curve for several values of A_x. A_x = 0.3 (typical of clays), A_x = 5 (typical of sands)